Inaugural dissertation

for

obtaining the doctoral degree

of the

Combined Faculty of Mathematics, Engineering and Natural Sciences

of the

Ruprecht - Karls - University

Heidelberg

presented by

Francesco Baccianti, M.Sc.

Born in: Florence, Italy

Oral examination: December 19th, 2022

1

Title:

Epstein-Barr virus infectious particles initiate B cell transformation and modulate cytokine response

Referees: Prof. Dr. Martin Muller

Prof. Dr. Dr. Henri-Jacques Delecluse

"Don't believe what your eyes are telling you. All they show is limitation. Look with your understanding. Find out what you already know and you will see the way to fly."

— **Richard Bach**, *Jonathan Livingston Seagull*

Table of Contents

4

Summary

The Epstein-Barr virus efficiently transforms primary B cells. In this thesis I show that this process starts immediately after cellular exposure to viral particles that activate STAT3 and p38/MK2, resulting in the expression of viral transforming genes. Indeed, virus binding to B cells led to activation of intracytoplasmic tyrosine kinases and of STAT3. Tegument proteins within the virion in turn activated the p38-MK2-ZFP36L1 pathway upon cellular entry, independently of the viral DNA. ZFP36L1 is a stress response protein that targets transcripts with an AU-rich 3'UTR and accordingly reduced IL-6 and TNFα transcription in infected cells. Expression of viral latent proteins after infection amplified the viral effects on p38 and MK2, but also on ZFP36L1, altogether resulting in a transitory and limited increase in IL-6 and TNFα transcription and secretion. However, cytokine release was much stronger in some individuals, which might have clinical consequences. p38 or STAT3 inactivation largely inhibited latent gene transcription without impeding infection itself, showing that proteins present in the virion influence events independent of virus entry. Thus, EBV virions are not merely vehicles that allow injection of the viral DNA into the nucleus, but manipulate cellular pathways to initiate transformation while modulating cytokine release.

Zusammenfasung

Das Epstein-Barr-Virus transformiert effizient primäre B-Zellen. Diese Arbeit zeigt, dass der Prozess der Transformation unmittelbar nach der Infektion der Zellen beginnt. Hierbei werden STAT3 und p38/MK2 aktiviert, was zur Expression von viralen Transformationsgenen führt. Die Bindung des Virus an B-Zellen führt zur Aktivierung von intrazytoplasmatischen Tyrosinkinasen und STAT3. Tegumentproteine innerhalb des Virions aktivieren ihrerseits den p38-MK2-ZFP36L1-Signalweg beim Eintritt in die Zelle, unabhängig vom Vorhandensein viraler DNA. ZFP36L1 ist ein Stressreaktionsprotein, das sich gegen Transkripte richtet, die eine AU-reiche 3'UTR tragen, wodurch die IL-6- und TNFα-Transkription in infizierten Zellen reduziert wird. Die postinfektiöse Expression latenter viraler Proteine verstärkt die viralen Effekte auf p38 und MK2, aber auch auf ZFP36L1, was insgesamt zu einem vorübergehenden und begrenzten Anstieg der IL-6- und TNFα-Transkription und -Sekretion führt. Diese Sekretion war in einigen Proben deutlich stärker ausgeprägt als in anderen und könnte klinische Bedeutung erlangen. Die Inaktivierung von p38 oder STAT3 hemmt weitgehend die Transkription latenter Gene, ohne dabei die Infektion selbst zu beeinträchtigen, was zeigt, dass im Virion vorhandene Proteine die Ereignisse unabhängig vom Viruseintritt beeinflussen. EBV-Virionen sind also nicht nur Vehikel, die die Injektion viraler DNA in den Zellkern ermöglichen, sondern sie manipulieren auch zelluläre Signalwege, um eine Transformation einzuleiten und gleichzeitig die Freisetzung von Zytokinen zu modulieren.

List of abbreviations

AD-HIES	Autosomal dominant hyper immunoglobulin E syndrome	HRP	Horseradish peroxidase
Amp	Ampicillin	HSV-1	Herpes simplex virus 1
ARE-BP	AU-rich element binding protein	IM	Infectious mononucleosis
ATP	Adenosine triphosphate	JAK	Janus kinase
BAC	Bacterial artificial chromosome	JNK	c-Jun N-terminal kinases
BART	BamHI-A rightward transcript	kbp	Kilobase pairs
BL	Burkitt lymphoma	kDa	Kilo dalton
Cam	Chloramphenicol	KO	Knockout
CLL	Chronic lymphoid leukaemia	KSHV	Kaposi sarcoma-associated herpesvirus
DABCO	1,4 Diazabicyclo[2.2.2]octane	LB	Luria–Bertani medium
DAPI	4′, 6-Diamidino-2-phenylindole dihydrochloride	LCL	Lymphoblastoid Cell Line
DDR	DNA damage response	LOF	Loss-of-function
DLBCL	Diffuse large B cell lymphoma	MAP2K	Mitogen-activated protein kinase kinase
DNA	Deoxyribonucleic acid	MAP3K	MAP kinase kinase kinase
EBER	Epstein–Barr virus–encoded small RNAs	MAPK	Mitogen-activated protein kinase
EBNA	Epstein–Barr nuclear antigen	MAPKAPK	MAP kinase-activated protein
EDTA	Ethylenediaminetetraacetic acid	MNK	MAPK interacting protein kinase
ELISA	Enzyme-linked Immunosorbent Assay	MSK	Mitogen and stress activated protein kinase
FBS	Fetal bovine serum	NES	Nuclear export signal
GC	Gastric carcinoma	NLS	Nuclear localization signal
GOF	Gain-of-function	NPC	Nasopharyngeal carcinoma
HCMV	Human cytomegalovirus	PAR-CLIP	Photoactivatable ribonucleoside-enhanced crosslinking and immunoprecipitation
HL	Hodgkin lymphoma	PBS	Phosphate-buffered saline
		PCR	Polymerase chain reaction

PIAS	Protein inhibitor of activated
PTLD	Post-transplant lymphoproliferative disorders
PTP	Protein tyrosine phosphatase
RBP	RNA binding protein
RIPA	Radioimmunoprecipitation assay
RNA	Ribonucleic acid
ROS	Reactive oxygen species
SDS	Sodium dodecyl sulfate
SOCS	Suppressor of cytokine signaling
SSC	Saline-sodium citrate
STAT	Signal transducer and activator of transcription
TBS	Tris-buffered saline
TCL	T-cell lymphoma
TPA	12-O-tetradecanoylphorbol-13-acetate
Tris	tris(hydroxymethyl)aminomethane
VLP	Virus-like particles
VZV	Varicella zoster virus

1. Introduction

1.1 The Epstein-Barr virus

1.1.1 Virion and genome structure

Epstein-Barr virus (EBV) was first discovered in 1964 by Epstein, Barr and Achong in a cultured sample of Burkitt lymphoma cells (1). It belongs to the *Herpesviridae* family, subfamily *Gammaherpesvirinae*, genus *Lymphocryptovirus*. It is the only virus in the *Lymphocryptovirus* genus known to infect human beings, with the other viruses infecting Old World and New World monkeys (2). As suggested by the genus name, these viruses prevalently infect lymphocytes, specifically B lymphocytes, where they establish life-long latent infection (3). In humans, EBV has also been described to infect epithelial cells, T- and NK-cells, as well as smooth muscle cells (4). Over time, EBV has been identified as the etiological agent for several malignancies, both of solid tissues and of the blood, as well as one of the pathogens responsible for infectious mononucleosis (5). Recent epidemiological studies have confirmed EBV involvement in multiple sclerosis development (6–9), and a link to other autoimmune conditions has also been suggested (10).

1.1.1.1 Structure and composition of EBV viral particles

Viruses belonging to the *Herpesviridae* family are characterized by a common architecture, with a membranous envelope containing a structurally defined proteic capsid in which the DNA is contained. Between the envelope and the capsid, a layer of loosely associated proteins called tegument is present. The envelope is characterized by the presence of glycoproteins, which mediate the interaction with the cell receptors and subsequent fusion.

The capsid

The structure of EBV capsid has been resolved by cryo-electron microscopy in the past few years (11–13). The capsid is characterized by an icosahedral symmetry with a diameter of approximately 125 nm. Each capsid is formed by a total of 161 capsomers (150 hexamers, 11 pentons) and a portal complex at one of the vertexes. Hexamers and pentamers are formed by the major capsid protein (MCP, BcLF1 in EBV) and form the main structure of the capsid, with

pentons positioned at each vertex of the icosahedron, except the one occupied by the portal complex, a cylindrical structure formed by 12 copies of BBRF1, and hexamers forming the rest of the structure. Hexamers and pentamers are interconnected by a network of triplexes formed by a dimer of the protein BDLF1 (Ta) and a monomeric BORF1 (Tc). The whole surface of the capsid is decorated with proteins that can interact with the different structural components of the capsid and that are involved in the various steps of capsid maturation and DNA packaging. The small capsid protein (SCP, BFRF3 in EBV) is the main protein decorating the capsid and it is present in a total of 6 copies for each hexamer, one per vertex. Two other important proteins that are present on the capsid surface are BGLF1 and BVRF1. These two proteins, together with the tegument protein BPLF1, form the capsid-associated tegument complex (CATC), a structure that binds to the triplex adjacent to each penton, forming altogether a star-shaped density that extends from the top of the penton to the adjacent triplexes and exons. Interestingly, Li and colleagues have identified that only 20% of the penton vertices are actually occupied by the CATC (12). This probably correlates to its function of both stabilizing the capsid and increasing the intra-capsid pressure which is required for the efficient ejection of the genome into the nucleus.
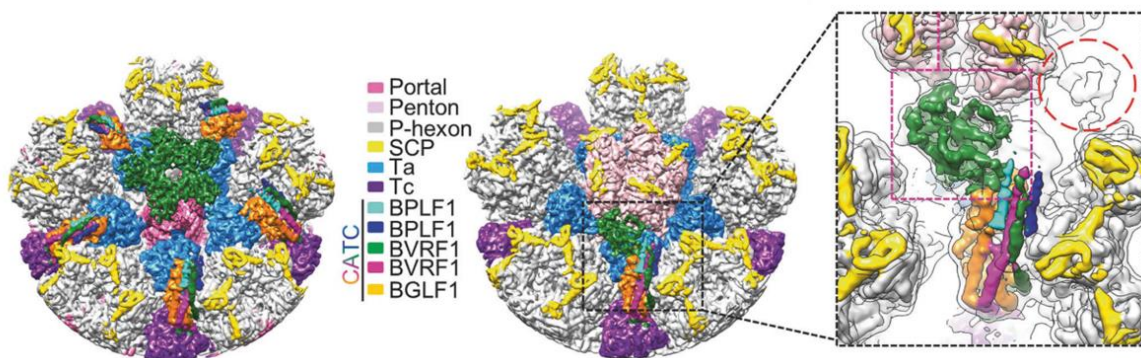
Figure 1.1: 3D structure of EBV capsid. 3D reconstruction of the portal region (left) and an adjacent penton (right) as obtained by high-resolution cryoEM. Single proteins or protein complexes are colour-coded as indicated in the legend. Adapted from Z. Li, et al., CryoEM structure of the tegumented capsid of Epstein-Barr virus. *Cell Res*. **30**, 873–884 (2020).

The tegument

The tegument is composed of proteins produced during the lytic phase that gets incorporated into the virion and that serve several functions during the infection process (14). Mass spectrometry analysis of fully formed EBV particles performed by Johannesen, Luftig and colleagues identified the components of the tegument (15). The analysis revealed the presence

of 13 viral proteins, plus additional host proteins such as actin, tubulin, cofilin, and HSP-70. The identified EBV proteins were: BNRF1 (MTP, major tegument protein,), BPLF1 (LTP, large tegument protein), BOLF1 (LTPBP, LTP-binding protein), BGLF4, BBLF1 (MyrP, myristoylated protein), BGLF2 (MyrPBP, MyrP-binding protein), BSRF1 (PalmP, palmitoylated protein), BKRF4, BRRF2, BLRF2, BVRF1, and BGLF1 (See Table 1). Functional studies of the identified tegument proteins have revealed that they can participate in the virus production step, as shown for BGLF2 and BOLF1 (16), or be essential in the infection process, as shown for example for BNRF1 (17, 18). However, the function of many tegument proteins has not been fully described, especially because they can play different roles during the productive phase of lytic replication or during the early stages of infection.

The envelope

The membranous envelope that surrounds and delimits the viral particle is characterized by the presence of several glycoproteins. EBV encodes for a total of 13 glycosylated proteins, 11 of which have been detected in enveloped viral particles (15). The glycoproteins detected in the viral particles and present in the envelope are: BLLF1a/b (gp350/220), BKRF2 (gL, gp25), BXLF2 (gH, gp85), BZLF2 (gp42), BALF4 (gB, gp110), BILF2 (gp78), BDLF3 (gp150), BBRF3 (gM), BLRF1 (gN), BMRF2, and BDLF2. BLLF1, BKRF2, BXLF2, BZLF2, and BALF4 are all involved in EBV's ability to bind and enter into target cells and define EBV tropism towards epithelial cells or B cells (19). BDLF3 has been recently associated with the ability of EBV to escape immune surveillance by downregulating antigen presentation via MHC class I, class II, and CD1d (20, 21). BBRF3 and BLRF1 form a complex which is required for the proper enveloping of newly formed viral particles and interacts with the host protein p32 in the process (22). BDLF2, originally described as a tegument protein, has been later identified as a type II glycosylated protein interacting with BMRF2 (23), and with BMRF2 possibly involved in infection of epithelial cells (24).

1.1.1.2 EBV genome structure

EBV is a double-strand DNA virus (class I of the Baltimore classification) with a genome length of approximately 172 kbp, with different strains and viral isolates differing slightly in the total length (25). The EBV genome exists in two conformations: during latency, it is present in a circular form associated to the host genome, known as an episome (26); during lytic

reactivation it becomes linearized to allow for replication and gets incorporated as such in the viral capsid (27). Replication during these two stages is controlled by three different origins of replication, one used for maintenance of the circular genome during latency, called oriP (28), and two selectively used for the amplification of the genome during lytic reactivation, called oriLyt (27). Like other members of the *Herpesviridae* family, EBV contains terminal repeats (TRs) at the two extremities of the linearized genome (29) which are essential for both the
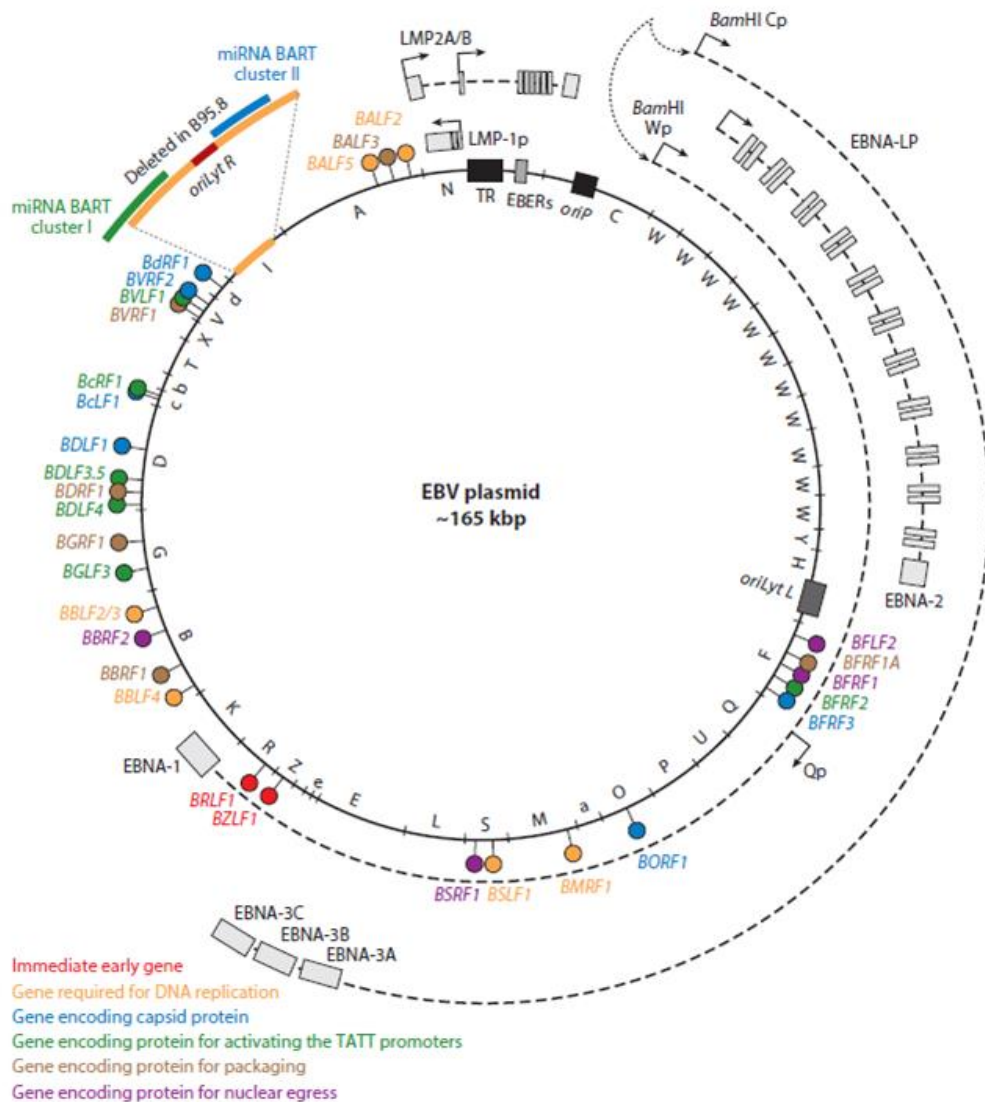
Figure 1.2: The EBV genome organization. Transcriptional units, origins of replication, and terminal repeats are indicated. Latent transcripts are reported on the outside, with exons marked as grey rectangles. Promoters for these transcripts are also reported. Coloured lollipops identify different groups of lytic genes as reported in the legend. The letters on the inside refer to the original *BamHI* restriction fragments used to generate the assembly. Adapted from Y. F. Chiu, B. Sugden, Epstein-Barr Virus: The Path from Latent to Productive Infection. *Annu. Rev. Virol*. **3**, 359–372 (2016).

circularization of the incoming viral genome upon entry in the host cell (30) as well as the encapsidation of the genome during viral particle production (31). Additional repeated regions are present in the genome.

1.1.2 EBV life cycle

1.1.2.1 Viral entry

B cells

EBV interacts with the cell membrane of the target cell through different glycoproteins. Each glycoprotein plays a role at a specific stage of the binding/fusion process. In B cells, gp350/gp220 interacts with CD21 (CR2) promoting the initial binding of the virus to the target cell. The binding is followed by the interaction of the trimer gH/gL/gp42 with HLA class II via gp42. This interaction promotes the conformational change that is required to reduce the distance between the viral envelope and the cell plasma membrane (from open to closed conformation). The now proximal membranes are then fused after the activation of gB, triggered probably by the conformational change in the gH/gL/gp42/HLA complex (24, 32, 33).

Binding of EBV particles to the CD21 protein on the cell membrane induces EBV internalization in a clathrin-independent manner and promotes the co-capping of the B cell receptor (34, 35). The human CD21 is a transmembrane glycoprotein containing 15 or 16 stretches of 60 amino acids, each called short consensus repeats (SCRs), that together form the extracellular domain. Even if most of the SCRs have unknown functions, SCR1 and SCR2 have been described as essential for gp350/gp220 and CD3d binding to CD21 (36–40). CD21 is anchored to the membrane through a short transmembrane domain (24 amino acids) and protrudes in the cytoplasm with a cytoplasmic tail 34 amino acids long (41). Due to the limited cytoplasmic domain of CD21, this membrane protein has been largely considered able to regulate B cell activation through interaction with other membranous proteins, such as CD19 (42). However, already Balbo *et al.* described how pep34, a peptide corresponding to the cytoplasmic domain of CD21, could prevent the proliferation of B cells exposed either to EBV or C3d, possibly disrupting the formation of the signaling complex (43). The ability of CD21 to induce a signaling cascade independently of CD19 has been extensively investigated by the

group of R. Frade (44–47). In the context of EBV infection, the role played by the cytoplasmic tail is not fully clarified. An earlier report from Carel *et al.* showed that the cytoplasmic tail of CD21 is essential for EBV infection (38), while a more recent analysis performed by Arredouani *et al.* showed that it is dispensable, with latency being established (48). The different results could be explained considering the different cellular systems employed for the analysis, with the former transfecting a CD21 mutant lacking the cytoplasmic tail in two non-B cell lines, and the latter using two pre-B-cell acute lymphoblastic leukemia cell lines. For this reason, the role played by the cytoplasmic tail of CD21 in the events that follow virus binding has still to be determined.

As previously mentioned, EBV establishes several interactions on the cell surface of B cells during the early stages of infection. In addition to binding to CD21, gp350/220 is able to bind to CD35 (49), while the complex gH/gL/gp42 interacts with MHC class II (50, 51). CD35 has been shown to bind to gp350/220 and allow cell infection when co-expressed together with MHC class II (49). The interaction between gp350/220 and CD35 involved the same domain of gp350/220 that is responsible for the binding to CD21, while multiple domains are mediating the binding for CD35. This was proven experimentally by using mutant variants of CD35 lacking different portions of the extracellular domain. These mutants were all able to allow binding but were not able to sustain infection. Another substantial difference that the authors highlighted was that the kinetic of infection was different when mediated by CD21 and when mediated by CD35. Infection through binding to CD35 was indeed significantly slower, with a delay in the detection of EBV infection up to 18 hours, and more sensitive to a reduction in the temperature.

Epithelial cells

Infection of epithelial cells occurs in a different manner than what is described for B cells. Indeed, infection does not require the expression of CD21, which in the nasopharynx is limited to tonsil epithelium (52). Binding and entry into epithelial cells, therefore, require a different set of glycoproteins, which includes the gH/gL complex, BMRF2, and gp110. gH/gL can interact with integrin αvβ5, αvβ6 or αvβ8 on the surface of epithelial cells (53, 54) via the integrin-binding KGD motif (55), although recent evidence has shown that an αv knockout in epithelial cells did not affect viral infection (56). More recently, a new interaction partner for

16

gH/gL has been identified, the Ephrin receptor A2 (EphA2) (56, 57). Silencing or knockout of EphA2 impaired the infection of epithelial cells, proving that EphA2 is indeed the receptor required for EBV infection of epithelial cells. Another factor which has been shown to play a role during the infection of nasopharyngeal epithelial cells and to interact with gH/gL is the nonmuscle myosin heavy chain IIA (NMHC-IIA), a protein normally located in the cytoplasm (58). Xiong and colleagues discovered that when cultured under certain conditions, immortalized nasopharyngeal epithelial cells form spheroid-like aggregates that could be infected by EBV with higher efficiency compared to cells cultured as a monolayer. Interestingly, these cells express NMHC-IIA on the cell surface. The authors discovered that NMHC-IIA on the cell membrane interacts with the gH/gL complex, supporting EBV infection. Indeed, when NMHC-IIA was knocked down via siRNA, the infection rate was significantly affected.

BMRF2, a multispan membrane protein, binds to two integrins, α3β1 and α5β1, via the RGD motif located in one of its extra-cellular loops (59, 60). This protein was shown to be required to sustain EBV infection in epithelial cells by allowing binding and fusion, and no effect was shown when B cells were considered (61).

In epithelial cells, gB plays an additional role besides that of the fusion protein by interacting with the cellular protein neuropilin 1 (NRP1) (62). This interaction is mediated by aa 23-88 and aa 428-431 of gB, with both domains being essential for the binding. Binding of gB to NRP1 results in the activation of the epidermal growth factor receptor (EGFR) signaling pathway, which induces AKT and ERK. Additional pathways could be activated upon gB interaction with NRP1, given that it acts as a co-receptor for receptor tyrosine kinases (RTKs) (63).

Additional mechanisms have been identified for the infection of epithelial cells that rely on cell-to-cell interactions. The first to be described was the cell-mediated transfer infection, in which EBV loaded B cells showed to be a viable mean to transfer and infect epithelial cells (64–66). The mechanism of infection was defined *in vitro* using a model of polarized epithelial cells, and it was shown that transfer infection required the establishment of interaction between CD11b on B cells and CD44v3 on the basolateral membrane of epithelial cells, as well as the interaction of gH with cellular integrins and fibronectin on the receiving cells (65). Another

process described for the infection of epithelial cells is the so-called in-cell infection, where EBV infected B cells form cell-in-cell structures that allow for the efficient infection of
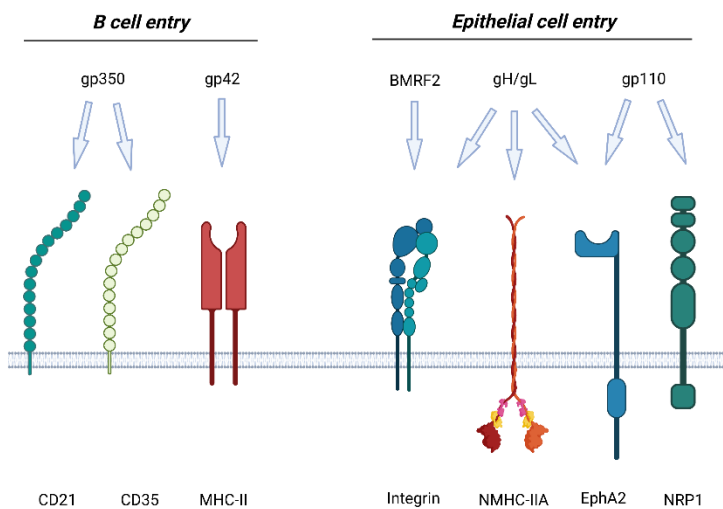
Figure 1.3: Cellular proteins involved in EBV infection of B cells and epithelial cells. Modified from J. Chen, R. Longnecker, Epithelial cell infection by Epstein-Barr virus. *FEMS Microbiol. Rev.* **43**, 674–683 (2019). Created with BioRender.com.

otherwise non-susceptible epithelial cells (67).

1.1.2.2 Latency

EBV life can be distinguished into a latent, non-productive phase, and a lytic and productive cycle during which new viral particles are released. Under physiological conditions, EBV infects resting naïve B cells (68, 69) and establishes life-long lasting latent infection in resting memory B cells, which eventually do express only a few viral genes (70–72). *In vitro*, however, EBV establishes a latent infection that is able to immortalize the infected B cells, generating lymphoblastic cell lines (LCL), and which is defined by the expression of all latency-associated genes (73–75). Several different latency programs have been identified and EBV-related malignancies have been characterised based on these latency programs. Each latency program is defined by the set of viral proteins being expressed, with only the non-coding RNAs EBERs and BARTs being expressed throughout all the stages (see Table 2, for a summary of latent protein function see Table 3).

Latent protein expression begins with the expression of EBNA2 and EBNA-LP, driven from the W promoter (76–79) and then by the C promoter shortly after infection (80, 81). Initial expression from the W promoter is regulated by the host transcription factor BSAP/PAX5 (82, 83). EBNA2 is then responsible for inducing the expression of the other latent genes from the

C promoter, which drives the expression of EBNA3A, 3B, and 3C, as well as EBNA1 (81, 84, 85). EBNA2 is also responsible for the expression of LMP1 and LMP2, although EBNA2-independent expression has been described for both genes (86, 87). The EBV-encoded miRNAs (BARTs), as well as EBERs, are regulated by different promoters, and only BHRF1 expression begins from the C promoter (88). It has been shown, both at early time points during natural infection and *in vitro* during the generation of LCLs, that a latency stage, called IIb, precedes type III latency and it is characterized by the lack of expression of LMP1 and LMP2 proteins while EBNAs and non-coding RNAs are being expressed (89–91) (reviewed in (92)). After latency III, once the cell has reached the germinal center, it switches to latency IIa, characterized by the expression of EBNA1, which is regulated at this stage by the Q promoter, LMP1 and LMP2, and noncoding RNA (25). Latency program I and 0 are limited to the duplicating and resting memory B cells, respectively (25). During latency 0 only the non-coding RNA EBERs and BARTs are expressed, while maintenance of EBV episomes during cell duplication is ensured by the Qp-driven (76, 93, 94) expression of EBNA1 (70, 72).

1.1.2.3 Lytic replication

Expression of lytic genes occurs at two different stages during the EBV life cycle. During a so-called pre-latent stage, which follows shortly after the expression of the first latent genes, the partial activation of the EBV lytic cascade has been detected, although no viral particle is produced at this point (95–102). Several lines of evidence have shown that this abortive step is required for transformation, with genes involved in immune evasion (99) and cell survival (103) being expressed. This initial lytic phase is induced independently of BZLF1 activity, but rather as the result of leaky expression due to the lack of methylation on the viral genome (102).

In healthy carriers, EBV lytic reactivation and production of viral particles occur only in plasma cells (33). The current hypothesis is that resting memory B cells, upon engagement of the B cell receptor, become activated and begin differentiating into plasma cells. The plasma cell differentiation program, via the transcription factors XBP1 and BLIMP1, induces the expression of BZLF1, therefore promoting the activation of the lytic cycle (29, 30, 31). By promoting the downregulation of the B cell receptor and the secretion of complement, the lytic cycle fosters the differentiation into plasma cells (32). In pathological conditions, such as the case of nasopharyngeal carcinoma (104), EBV reactivation is a characteristic of the disease

and can contribute to oncogenesis via different mechanisms (reviewed in (105)). *In vitro*, LCLs generated with some viral strains have shown the ability to spontaneously undergo lytic replication (106). Induction of lytic replication can also be obtained by treating LCL with sodium butyrate combined with TPA (107) or by B cell receptor crosslinking (108). Other stimuli have also been described to reactivate lytic replication in latently infected B cells, both *in vitro* and *in vivo* (109).

Activation of the lytic cascade results in the expression of nearly all the EBV transcription units (110). Lytic genes have been classified into immediate early (IE), early (E), and late (L) based on the timing of their expression. Two immediate early genes, BZLF1 and BRLF1, act as transactivators and are responsible for inducing all other lytic genes. BZLF1 is a transcription factor similar to human AP-1 and CREB (111, 112) and binds to BZLF1-responsive elements (ZRE) located in the promoters of viral and human genes and induces their expression (113, 114). Interestingly, BZLF1 specifically binds to methylated CpGs, which are abundant in lytic gene promoters of latently infected cells (115–117). BZLF1 also binds to oriP during lytic viral DNA synthesis (118). BRLF1 acts as a transcriptional factor and co-factor, either by directly binding to BRLF-responsive elements (RRE) or by interacting with other transcriptional factors, inducing the expression of the genes downstream (119–122). Induction of BZLF1 and BRLF1 results in the expression of early genes, among which the components of the DNA replication complex: BALF5 (core DNA polymerase); BALF2 (single strand DNA binding protein); BMRF1 (processivity factor); BSLF1 (primase complex), BBLF2/3/4 (helicase complex), and BKRF3 (uracil DNA glycosylase) (118, 123–125). Viral genome replication occurs by a combination of semiconservative and rolling circle amplification which results in the formation of concatemers (126, 127). This amplified viral DNA is then used as a template by the viral preinitiation complex (vPIC) for the expression of late lytic genes, among which
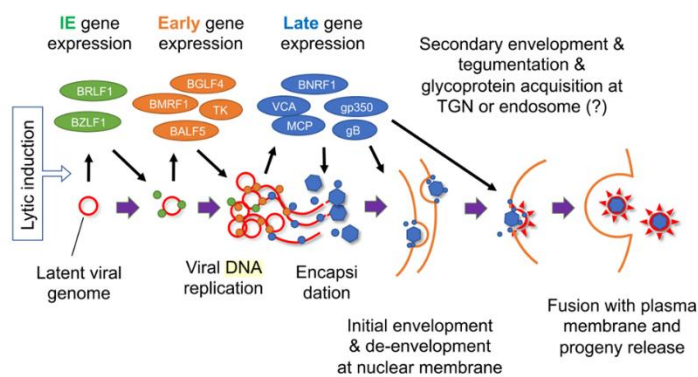
Figure 1.4: Lytic replication cycle in human B cells. Adapted from T. Murata, et al., Molecular Basis of Epstein-Barr Virus Latency Establishment and Lytic Reactivation. *Viruses* **13**, 2344 (2021).

many structural genes required for viral particle production (128–134). Single copies of viral DNA are then cleaved by a terminase complex within the terminal repeats (31, 135). Viral DNA is then loaded into nucleocapsids which will be transfer to the trans-Golgi network. Here they will acquire both tegument and envelope before being released by the cell (109).

1.1.3 Immune response against EBV

In the majority of cases, EBV infection occurs without the development of symptoms. Due to the asymptomatic course of the infection, the immune response against EBV has been studied mainly through the lenses of some of the pathologies associated with EBV infection. Infectious mononucleosis (IM) and various other primary immunodeficiencies have given the opportunity to understand the role played by the innate and adaptive immune response against EBV (reviewed in (136–138)). Infectious mononucleosis is normally detected in adolescents and young adults and it manifests with pharyngitis, cervical lymph node enlargement, fatigue, and fever (139). Several explanations have been proposed as to why EBV infection has a higher probability to manifest as infectious mononucleosis with increasing age (140), and some studies have identified genetic variants in the human leukocyte antigens (141, 142) and TLRs (143) associated with IM. During symptomatic infection, an expansion of NKG2A+ natural killer cells (NKG2A+ NK), natural killer T cells (NKT), γδ T cells, and CD8+ αβ T cells has been observed (144–146). The different populations have been described to preferentially target EBV-infected cells based on their latent/lytic expression pattern. Anti-EBV CD8+ αβ T cells preferentially target lytically replicating cells (147, 148). EBV-specific CD8+ T cells can increase up to 5 or 10 times in absolute number (136, 149) and become more than 50% of the overall CD8+ T cell population (136, 149–151). NK cells also respond to lytic antigens (144, 152), while both NKT cells and γδ T cells respond to the expression of latent genes, with NKT cells targeting type II latently infected B cells (153, 154) and γδ T cells type I latently infected B cells, respectively (146, 155). Both depletion and adoptive transfer experiments in animal models confirmed the importance of these subpopulations in controlling EBV infection and its tumorigenic potential (156). In addition to peripheral immune cells, the NKG2A+ CD54+ NK cells resident in the tonsils also play an important role in controlling EBV infection by releasing interferon γ and engaging through NKp44 (157, 158). Finally, the broad activation of CD8+ T cells, as well as that of the other immune cells, results in high levels of proinflammatory and immunomodulatory cytokines in the blood of IM patients (159–163) (reviewed in (164)).

The innate and cell-mediated adaptive response is complemented by the humoral response, with antibodies being secreted after infection and remaining detectable in most cases for the rest of a person's life (25, 165). Initial response results in the secretion of IgM against the viral capsid antigen (VCA) and early antigen (EA), which fades a few weeks after. The IgG response is delayed and initially directed against the total VCA protein and, shortly after, the small capsid protein (VCA p18). IgG antibodies targeting the EBNA proteins, mainly EBNA1, only arise several weeks post-infection, during the convalescence period, and slowly increase over time. IgG against VCA p18 and EBNA proteins are then found at stable levels for the rest of life and can increase during lytic reactivation or in case of chronic infection.

1.2 The signal transducer and activator of transcription 3

1.2.1 Overview of the JAK-STAT signaling cascade

1.2.1.1 The JAK protein family

The Janus kinase (JAK) family consists of four different proteins which act as non-receptor tyrosine protein kinases, mediating the transduction of the signal initiated by the membrane receptors. The four JAKs identified are JAK1, JAK2, JAK3, and TYK2. They present a conserved structure formed by the N-terminal FERM domain, an SH2 domain, the pseudokinase domain, and the kinase domain at the C-terminus. The FERM domain and the SH2 domain together are responsible for the interaction with the proximal box1/2 of the cytoplasmic tail of the cellular receptor (166–168). The pseudokinase domain, a peculiarity of JAK proteins, has structural homology with the kinase domain at the C-terminus but misses the catalytic domain (169). It has been described to play a critical role in modulating the activity of the true kinase domain and in its absence the kinase domain becomes constitutively active (169–171). The kinase domain contains the two conserved tyrosine residues which are essential for JAKs activation (172).

1.2.1.2 The STAT protein family

The signal transducer and activator of transcription (STAT) is a class of transcriptional factors that mediate multiple intracellular signaling pathways. Identified in the 90s as the transcriptional factors downstream of the interferon pathway activation, STAT proteins have been identified as the final step in the signaling cascade activated by more than 35 cellular receptors for cytokines, chemokines, and growth factors (173). This class comprises 7 members which are involved in many basic cellular functions: STAT1, STAT2, STAT3, STAT4, STAT5a, STAT5b, and STAT6. The seven members share a common structure with characterized domains and conserved functions (172):

- An N-terminal domain (NTD) which promotes dimerization, interaction with the PIAS co-activator protein family, and regulates nuclear translocation.
- A coiled-coil domain which regulates the import/export to and from the nucleus and is involved in the binding to other transcription factors.

23

- A DNA-binding domain which is responsible for binding to the regulatory sequence located in the target gene. It also regulates the import/export to and from the nucleus.

- An SH2 domain which recognizes the phosphotyrosine motifs located in the cytoplasmic tail of cytokine receptors. The SH2 domain is also involved in the formation of homo- or heterodimers upon phosphorylation. The DNA-binding domain and the SH2 domain are linked by the linking domain.

- A transactivation domain (TAD) which contains tyrosine and serine residues essential for the phosphorylation-mediated regulation of STAT transcriptional activity (174). The domain is also responsible for the interaction with other regulators of transcription (175).

1.2.1.3 The JAK-STAT signaling cascade

The JAK-STAT signaling cascade can be distinguished into canonical and non-canonical pathways. The canonical pathway requires the binding of a ligand to one of the JAK-STAT associated receptors. The binding of the ligand to the receptor induces its dimerization which results in the phosphorylation of the receptor-bound JAKs. Phosphorylated JAKs are now active and can phosphorylate the tyrosine residues in the cytoplasmic tail of the receptor they are associated to. The phosphorylated tail is recognized by STATs which are then phosphorylated by JAKs. Phosphorylated STAT proteins detach from the tail of the receptor and form homo- or heterodimers which then translocate to the nucleus. Here they can act as transcriptional factors (172).

The noncanonical JAK-STAT pathway collectively includes all the alternative ways in which the activation of JAK and STAT differs from the events described for the canonical pathway. This includes, but is not limited to, kinase-independent JAK activity, activity by non-phosphorylated STAT proteins, and JAK-independent phosphorylation of STAT (reviewed in (172, 176)).

Due to the importance that the JAK-STAT pathway has in many aspects of cell biology, several positive and negative regulators modulate its activation and function. Three families of proteins have been described to act as negative regulators of JAK-STAT activation: the protein inhibitor of activated STAT (PIAS) family, the Suppressors of Cytokine Signaling (SOCS) and the cytokine-inducible SH2 protein (CIS) families, and protein tyrosine phosphatase (PTP) family.

Proteins belonging to the PIAS family act by blocking the DNA-binding ability of the STAT dimers, recruiting other negative regulators or inducing SUMOylation of STAT complexes. SOCS proteins are induced by STAT activation and act at the level of the receptor preventing JAK kinase activity or the recruitment of STAT. Finally, phosphatases bind to phosphorylated residues via their SH2 domain and dephosphorylate them, blocking the signaling cascade (172, 177).
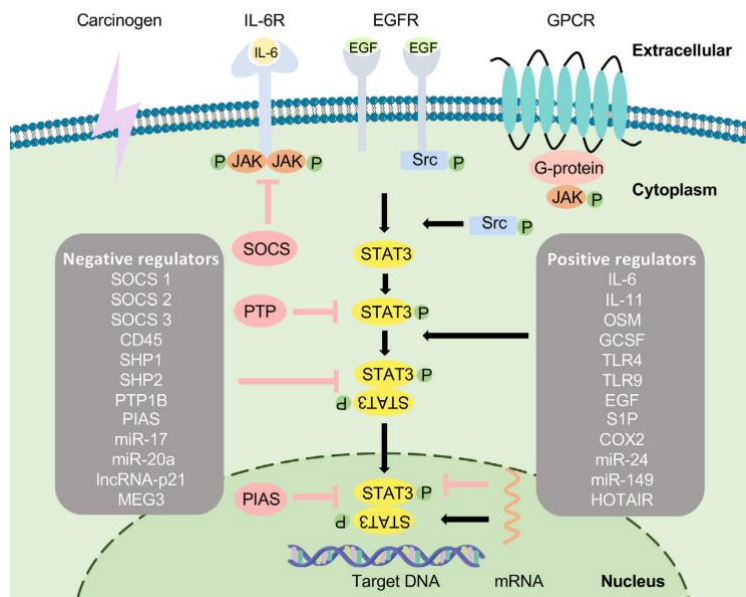
Figure 1.5: STAT3 signaling cascade. Both canonical and noncanonical pathways are indicated. Positive and negative regulators are listed. Adapted from H.-Q. Wang, et al., STAT3 pathway in cancers: Past, present, and future. *MedComm* **3**, e124 (2022).

1.2.2 STAT3: general characteristics and functions

Originally identified in 1994 (178, 179), STAT3 is one of the most studied members of the STAT family. Located on chromosome 17q21, it is highly conserved between different species, with only one amino acid difference between mouse and human (180). The main transcript, STAT3α, contains 24 exons and a second isoform, STAT3β, is generated from an alternative splicing acceptor in exon 23, resulting in the replacement of the last 55 amino acids with a sequence of 7 amino acids specific to STAT3β. Due to this substitution, STAT3β is characterized by the absence of the S727 phosphorylation site (181–183). Additional variants have been identified, although little is known about their functions (184, 185). STAT3α and STAT3β have been shown to play different functions (186) and to be different in terms of specificity of DNA-binding and transcription activity (187). A germline knockout of both

STAT3α and STAT3β resulted in the death of the embryo, a unicum among STAT proteins (188). The lack of STAT3α also resulted in the death of the animals shortly after birth (186), while mice lacking STAT3β were viable and fertile, although presenting hyperactivation of the inflammatory cascade (186, 189).
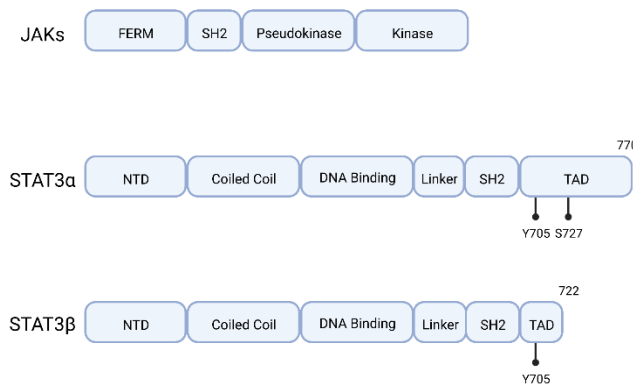
Figure 1.6: Structure of a general JAK kinase and of the two STAT3 isoforms. The lollipops indicate phosphorylation sites important for activation of STAT3. Created with BioRender.com.

Under physiological conditions, STAT3 activation can be induced by a plethora of stimuli, including the IL-6 receptor family. Activation is mainly mediated by JAKs, which are responsible for the phosphorylation of tyrosine 705. However, other factors have been shown to induce STAT3 Y705 phosphorylation without requiring the activation of JAKs. This includes the epidermal growth factor receptor (EGFR) kinase (187, 190) and the spleen tyrosine kinase (SYK) (191–193). Phosphorylation at Y705 is normally associated with the formation of homodimers, although in certain conditions STAT3 can also interact with STAT1, STAT5a, STAT5b and STAT4 (194). After activation, STAT3 translocates to the nucleus, where it binds to the consensus sequence $CCT(N)_3GAA$ in the promoter of the target gene, although binding to non-canonical motifs has also been described (180, 195). Unphosphorylated STAT3 can also shuttle between the cytoplasm and the nucleus, where it can bind to other factors and regulate the transcription of genes which do not carry the conventional STAT3 binding site (196–199). STAT3α phosphorylation at serine 727, which can be carried out by several cellular kinases, improves transcriptional activation of certain STAT3 targets (200–202). In addition, STAT3 S727 can also prevent STAT3 Y705 phosphorylation (203).

Despite its primary localization in the cytoplasm and in the nucleus, STAT3 has been detected also in the mitochondria and in the endoplasmic reticulum. In the mitochondria, STAT3 has been shown to foster the activity of complex I and II of the electron transport chain, bind to regulatory elements of mitochondrial DNA and modulate mitochondrial gene expression, and

regulate the mitochondrial permeability transition pore (204–207). Phosphorylation at serine 727 was thought to be required for STAT3 activity in the mitochondria, with no involvement by Y705 (204, 208). More recent work from Peron *et al.* identified a new role for Y705 in the mitochondrial import of STAT3, while confirming the previously described role of S727 in the transcriptional activation of mDNA (209). In the endoplasmic reticulum, STAT3 phosphorylated at S727 regulates ER Ca^{2+} fluxes and apoptosis by interacting with IP3R3 and promoting its proteasomal-dependent degradation, which in turn modulates the mitochondrial Ca^{2+} uptake (210).

Given the broad spectrum of activity in which STAT3 is involved, it is not surprising that STAT3 dysregulation has been described in several pathologies. Increased STAT3 activity is present in more than 70% of human cancers (211, 212). This is often the result of the hyperactivation of upstream tyrosine kinases, the activity of oncoproteins like BCR-ABL (213), and the inactivation of negative regulators. In lymphoid malignancies, activating mutations of STAT3 have also been identified (214–216). The constitutively activated STAT3 acts as an oncogene (reviewed in (217–220)), promoting tumour development and/or progression (221–227), resistance to treatment (228, 229), and immune regulation and evasion (reviewed in (230, 231)).

1.2.3 STAT3 and immunity

Some of the functions that STAT3 performs in the context of the immune response have been identified by studying the immune disorders associated with loss- or gain-of-function of STAT3.

One example of a condition caused by the loss-of-function (LOF) of STAT3 is the autosomal dominant hyper immunoglobulin E syndrome (AD-HIES), also known as Job's syndrome. This condition can be caused by mutation of different regulatory genes, among which STAT3 (232). STAT3-HIES is characterized by frequent bacterial infections of the skin and lungs, as well as fungal infection of the oral cavity, hyperactive innate immune pro-inflammatory response, abnormalities of the bone and connective tissue, and increased serum levels of IgE and reduced memory B cells (232–235). One of the major contributors to the development of the clinical manifestations of AD-HIES is the lack of STAT3-dependent IL-17 secretion by CD4+ T cells which is required to generate a proper antibacterial response (236, 237). Loss-of-function of

STAT3 is also responsible for the reduced expression of IL-22 that causes an impairment in the epithelial barrier function (236–238), and for the reduced activity of memory CD8+ T cells, resulting in recurrent EBV and VZV infections (239).

Gain-of-function (GOF) mutations in STAT3 affect mainly conserved residues different from those identified in HIES and are clinically associated with autoimmune conditions such as type I diabetes and solid organ autoimmunity (240–242). The clinical manifestation of the disease is probably due to an increased DNA binding activity of STAT3 (240) and dysregulation of other STAT signaling pathways (240–242). Patients carrying GOF mutations of STAT3 are also characterized by a reduction in several immune cell compartments, including regulatory T cells, plasmacytoid dendritic cells, natural killers, Th17 helper T cells, and class-switched B cells (241).

As described in the previous sections, both LOF and GOF mutations in STAT3 affect the B cell response. Naïve B cells from AD-HIES patients showed partial alterations in the response to IL-10 and IL21 stimulation, two known modulators of B cell proliferation, class-switching, and differentiation, and failed to activate the program required to differentiate into plasma cells (235, 243, 244). The importance of IL-21 in the STAT3-mediated regulation of naïve B cell differentiation into plasma cells has been also confirmed by using conditional knockout mice lacking *Stat3* in the CD19+ B cell population (245). The authors showed that these mice present fewer germinal centers and fewer post-GC cells, probably because of an increased apoptotic rate. Using a similar model, Kane and colleagues (246) were also able to show that IgG class switching is only moderately affected by STAT3 deficiency and that the absence of STAT3 drives an aberrant switching towards the IgE phenotype. Moreover, the affinity maturation process required to generate high-affinity antibodies was significantly affected by the lack of STAT3, although the somatic hypermutation process was not affected, as shown by the similar mutation rate between wild type CD19+ naïve B cells and their STAT3 knockout counterpart.

Activation of the immune response as a result of the presence of a pathogen or of tissue damage induces inflammation. One of the peculiarities of STAT3 is that, based on the tissue, the cell type, and the activatory stimuli, STAT3 can either promote or suppress inflammation. When STAT3 activation is mediated by IL-6 in secondary lymphoid tissues, it supports T and B cells proliferation and survival, and promotes differentiation of Th17 T cells and follicular helper T

cells, while limiting the formation of Foxp3+ regulatory T cells (247). On the other hand, the IL-10-mediated activation of STAT3 has a completely opposite effect, promoting the resolution of inflammation by inducing differentiation of CD4+ T cells into regulatory T cells (248), suppressing the T helper 1 (Th1)-mediated response (249), and regulating apoptosis of B cells (250).

1.2.4 Role of STAT3 during infections

As detailed in the previous section, STAT3 can play both pro- and anti-inflammatory roles depending on the activating pathway. The activatory stimuli that are elicited during an infection can induce high levels of STAT3 activation. Many viruses have developed ways of benefiting from these high levels of STAT3 activation which result in the upregulation of pro-survival and pro-proliferation genes (reviewed in (251–253)). In many cases, viruses are fostering STAT3 activation either directly, by promoting the activation of pathways which result in STAT3 expression and phosphorylation, or by targeting STAT3 negative regulators. This is true for example for several Herpesviruses, such as HCMV, KSHV, VZV, and EBV itself. HCMV and KSHV can induce STAT3 activation by increasing IL-6 secretion (254) or via viral homologues of IL-6 and IL-10 (255–257). VZV has also been shown to induce STAT3 activation, even though a mechanism has not been elucidated yet (258). In addition, STAT3 inhibition using resveratrol was able to reduce VZV infection (259). EBV infection is also linked to STAT3 activation through many different mechanisms. Phosphorylation of STAT3 occurs early after EBV infection of primary B cells (260), similarly to endothelial cells infected with KSHV (261). In the context of the early events regulating transformation, STAT3 activation is important for the modulation of the DNA damage response and progression through the cell cycle. STAT3 activation induces a caspase-activation cascade involving caspase 9 and caspase 7 which results in the cleavage of claspin. The lack of claspin impairs the ATR-mediated phosphorylation of Chk1 and, therefore, the activation of the intra-S phase checkpoint in response to the viral-induced replication stress, allowing cell cycle progression (262, 263). *In vitro,* latently infected primary B cells and EBV positive nasopharyngeal carcinoma cell lines control STAT3 phosphorylation via the viral protein LMP1. Several signaling pathways have been involved in the LMP1-mediated activation of STAT3, highlighting a self-sustaining positive feedback loop involving IL-6 (264) and EGFR (265, 266). Together with LMP1, EBNA2 has also been shown to regulate STAT3 activity by

increasing STAT3 DNA binding capacity (267). In latently infected cells, STAT3 activation level was shown to be important for the maintenance of latency via PCBP2 (268–270). In lytically replicating cells, BGLF2 was able to reduce STAT3 activation by blocking Tyk2 phosphorylation, therefore promoting lytic reactivation instead of latency (271).
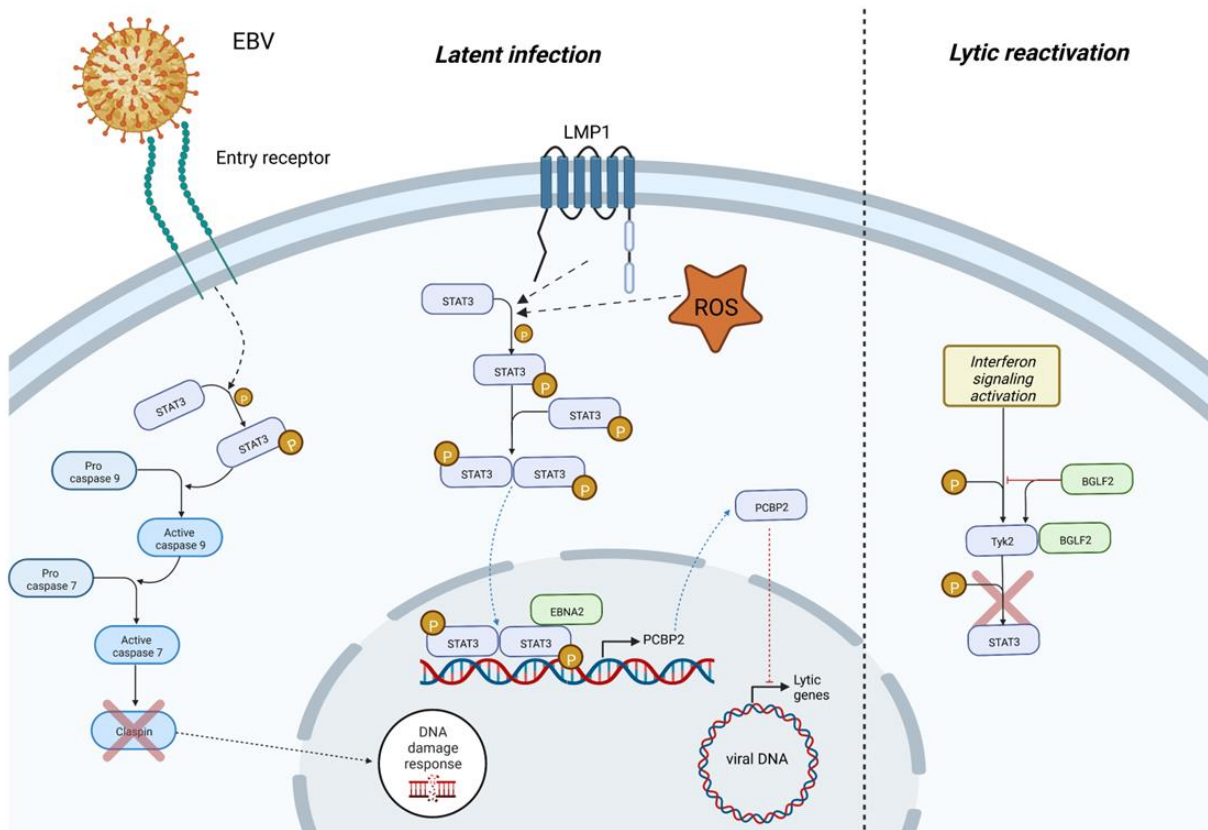
Figure 1.7: STAT3 in EBV infected cells. Different mechanisms of STAT3 activation during EBV latent infection with downstream effects are reported. Inactivation of STAT3 mediated by BGLF2 during lytic replication is also visualized (right). Created with BioRender.com.

1.3 The p38-MK2 signaling pathway

1.3.1 Overview of the signaling cascade

1.3.1.1 General aspects

Mitogen activated protein kinase (MAPK) signaling cascades are highly evolutionary conserved pathways used by cells to respond to a very broad variety of extracellular stimuli. In mammals, three major branches of the MAPK family have been identified: ERK1/2, p38, and JNK.

p38α was initially reported in 1994 by four independent studies that looked at the response to several stimuli including lipopolysaccharide (LPS), heat shock, and osmotic stress (272–274). p38α, encoded by the gene MAPK14 located on chromosome 6p21, has several isoforms with unclarified functions. In addition, three more proteins with high homology with p38α have also been identified: p38β, p38γ, and p38δ (275). The high homology between the different p38 kinases results from a shared ancestor from which the different genes originated following duplication events (276). As shown by animal models, despite their high structural similarity, the p38 kinases differ in their tissue distribution and their functions, although with some overlap (reviewed in (277)).

1.3.1.2 Signaling cascade: activation and regulation

Activation of the pathway

The canonical pathway of p38 activation is similar to other mitogen activated protein kinases (MAPKs) and requires the activation of MAPK kinase kinase (MAP3Ks) which in turn activates the MAPK kinase (MAP2Ks). MAP2Ks are then responsible for phosphorylating and activating MAPKs, among which p38 itself. Different MAP3Ks have been shown to be able to induce the downstream activation of p38, with some of them shared with other MAPKs, mainly JNKs. The great variety of MAP3Ks which are able to induce the downstream activation of the p38 signaling means that the pathway can be activated in response to several stimuli. MKK3 and MKK6 are the two main MAP2K kinases that can specifically phosphorylate p38 (278), although MKK4, which preferentially acts on JNKs kinases, can also activate p38α (279). Activation of p38 occurs by phosphorylation of the threonine 180 and tyrosine 182 residues located in the Thr-Gly-Tyr motif of the activation loop in the C-terminus (280). While in the

absence of phosphorylation the protein has a low affinity for ATP, upon dual phosphorylation the induced change in the 3D structure allows for a more open conformation that improves substrate recognition and docking which, in turn, improves ATP binding (281, 282).

Two additional non-canonical mechanisms are responsible for the activation of p38 without the involvement of both MAP3Ks and MAP2Ks. The first is mediated by TGF-Beta Activated Kinase 1 (MAP3K7) Binding Protein 1 (TAB1), which can cause p38 activation either via the canonical pathway or by inducing its autophosphorylation (283). The second mechanism is mediated by ZAP70 and requires T cell receptor activation (284). ZAP70-mediated phosphorylation occurs on tyrosine 323 of p38α and p38β and is sufficient to induce p38 autophosphorylation on Thr180. This monophosphorylation still maintains some kinase activity, although with different substrate specificity (285). Interestingly, several autoimmune disease animal models carrying a Y323F mutation in p38α and p38β showed a reduction in the level of autoimmunity and inflammation (286–288).
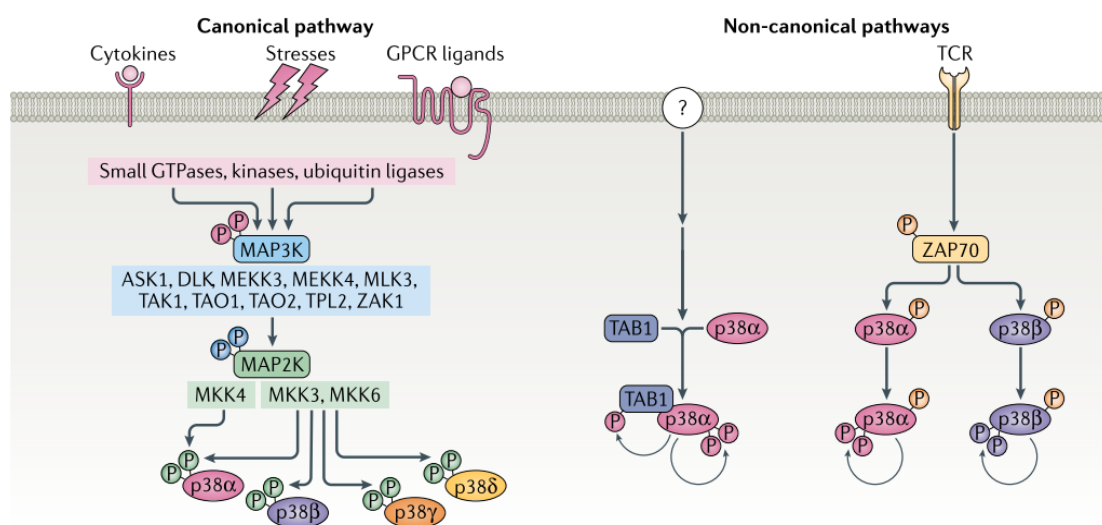
Figure 1.8: p38 signaling cascade. Both canonical and noncanonical pathways are indicated. Adapted from B. Canovas, A. R. Nebreda, Diversity and versatility of p38 kinase signalling in health and disease. *Nat. Rev. Mol. Cell Biol.* **22**, 346–366 (2021).

Regulation of the pathway

Due to the many functions performed by p38, several layers of control ensure that p38 activity is maintained at the required levels. Several phosphatases have been described to directly dephosphorylate the p38 activation loop, with some, like DUSP1, being induced directly by

p38 to generate a negative feedback loop. This is important for the expression of pro-inflammatory genes (289), as well as for the regulation of stress-induced cell death (290, 291). Direct regulation of p38 phosphorylation status is one of the several mechanisms adopted by the cell to control the activity of the pathway. Other post-transcriptional modifications such as acetylation of Lys53 (292), which promotes ATP binding, or methylation (293, 294) have also been shown to play a role. In addition, binding to other proteins, including scaffold proteins and importins, helps localise p38 to a specific cell compartment and integrate it with other signaling pathways (275).

1.3.1.3 Downstream targets of p38

Due to the great versatility of the p38 signaling pathway, it is not surprising that p38 kinases have been described to phosphorylate more than 100 substrates (reviewed in (295, 296)) which are involved in a variety of functions: transcriptional factors, chromatin binding proteins, RNA binding proteins, kinases, and structural proteins. Some of the main downstream targets of p38 are kinases themselves and are responsible for further amplifying the signaling cascade (reviewed in (297)):

- The MAPK-activated protein (MAPKAP) kinase family members MK2, MK3 and MK5 (273, 274, 298–300).
- The mitogen- and stress-activated protein kinase (MSK) 1 and 2, that regulate transcriptional factors and are involved in chromatin remodelling (301, 302).
- The MAP kinase-interacting serine/threonine-protein kinase (MNK) 1 and 2, which regulate protein synthesis by phosphorylating the eukaryotic initiation factor-4e (eIF-4E) (303, 304).

MAPK-activated protein kinase 2

MK2, together with MK3, plays a pivotal role in amplifying the signal induced by p38 activation, extending the target pool that can be regulated and controlled by the pathway. Structurally, MK2 contains a proline-rich domain at the N-terminus, the kinase domain and a nuclear export signal (NES) and a nuclear localisation signal (NLS) at the C-terminus (305). Two isoforms of MK2 exist, with one presenting a longer N-terminus domain due to the usage of a different translation initiation site (306).

MK2 activation, which can be mediated only by p38 (273, 274), occurs via phosphorylation of two residues located in the kinase domain (T220 and S272) and one located in the C-terminus (T334) (307, 308). In its unphosphorylated form, MK2 resides in the nucleus. Once p38 activation has occurred, p38 interacts with the NLS of MK2 via its catalytic domain, resulting in the phosphorylation of MK2 (309). p38 binding to the NLS masks it and causes the exposure of the NES, allowing for MK2 to be exported to the cytoplasm via Exportin 1-dependent mechanism (307, 308, 310). In the cytoplasm, the inactivation of MK2 is mediated by the E3 ligase Mdm2 which induces proteasome-dependent degradation (311).

Several proteins have been identified as targets of activated MK2. Among them, are proteins involved in cell cycle regulation, RNA stability, DNA repair, cytoskeleton remodelling, chromatin remodelling, gene expression, and cellular response to stress (reviewed in (297, 312)). One of the most studied functions of MK2 is the regulation of RNA binding proteins, in particular of the adenine/uridine(AU)-rich elements binding protein (ARE-BP) class. These proteins are principally involved in the regulation of mRNA transport, localization, and degradation, providing a platform for the rapid switching on/off of translation. ARE BPs bind to specific sequences in the mRNA, formed by stretches of adenines and uridines, which are mainly located in the 3´UTR of the target mRNA (312, 313). In this group of proteins, MK2 regulates the ZFP36 protein family, Human antigen R (HuR), and AU-rich element RNA-binding protein 1 (AUF1). In all three cases, MK2-mediated phosphorylation of these proteins modifies the proteins' ability to bind to their target as well as cellular localization. Interestingly, if ZFP36 family members and AUF1 play a negative role in promoting mRNA destabilisation via a combination of decapping and deadenylation, HuR is instead able to promote mRNA translation (313). Overall, the activation of the p38-MK2 axis favours the expression of the ARE-containing transcripts by inhibiting the activity of ZFP36 and AUF1 while promoting HuR relocalization to the cytoplasm (312).

The ZFP36 protein family will be covered in detail in section 1.4.

1.3.2 p38-MK2 and immunity

The p38α -MK2 axis plays a central role in regulating the immune response and inflammation. However, its role is ambiguous since it can promote and suppress inflammation depending on the activatory stimuli and the cell type. p38 ability to control cytokine release is an example of

this duality. p38α can regulate cytokine secretion via different means. It can act directly, by phosphorylating transcription factors or regulating mRNA translation, or indirectly via one of the downstream kinases. In the case of the two pro-inflammatory cytokines IL-6 and TNFα, p38α promotes their release by phosphorylating the transcription factor MEF2C (314, 315) or by activating MK2 and MK3 as described in the previous section. At the same time, by activating MSK1 and MSK2, can induce the phosphorylation of CREB and, therefore, the expression of anti-inflammatory factors such as *IL10* (316). Not only p38 affects the secretion of proinflammatory cytokines, but also their function. For example, the efficacy of the TNFα-induced cell death is also regulated by MK2, which phosphorylates the kinase RIPK1, preventing the induction of apoptosis (317–319).

In addition to controlling the release of soluble factors and their downstream signaling, p38 can also modulate the adaptive immune response. For example, Gurusamy and colleagues showed that, in the context of antitumoral T cell-mediated response, p38 inactivation was able to improve the T cell expansion, stemness, and genomic stability (320). This is also true for cytotoxic T cells, where blocking the p38 cascade stabilises IFNAR1, improving their viability (321). On contrary, inhibition of p38 during V(D)J- or class switch recombination in T and B cells has a detrimental effect on the cells' fitness and survival (322). In B cells, p38 activation was also shown to be important for both CD40-induced proliferation (323) and B cell survival and proliferation upon B cell receptor activation and germinal center formation (324, 325).
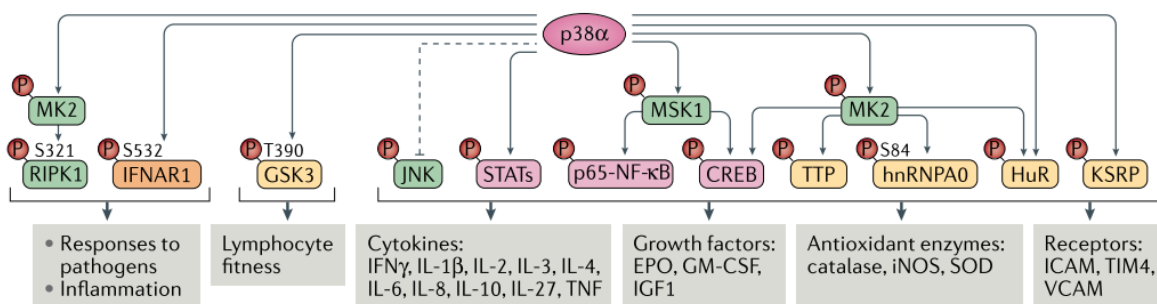
Figure 1.9: Downstream targets of the p38 pathway that are involved in the regulation of the immune response. Adapted from B. Canovas, A. R. Nebreda, Diversity and versatility of p38 kinase signalling in health and disease. *Nat. Rev. Mol. Cell Biol.* **22**, 346–366 (2021).

1.3.3 Role of p38-MK2 during infections

Due to the many functions that p38 can have, the role it plays in the context of viral infections can be either pro- or anti-viral and many viruses have developed ways to induce or suppress p38 activation in order to promote infection and viral replication (326, 327). Almost all the members of the *Herpesviridae* family that are known to be pathogenic in humans have been described to induce activation of the p38 pathway through different mechanisms during their life cycle. HSV-1 infection, for example, was shown to induce p38 activation via the upstream regulator MKK4/SEK1 (328, 329) or by inducing the production of reactive oxygen species (ROS) (330). In the case of HCMV, it regulates p38 induction differently depending on whether it occurs during the early or late stages of infection (331). On the contrary, for VZV the entrance of the virus inside the target cell and the release of tegument proteins in the cytoplasm are not sufficient to induce the activation of the p38 pathway, but *de novo* expression of viral genes is required (332). In the context of KSHV infection, the Kaposin B protein can induce p38 and MK2 activation, which results in the stabilization of cytokine mRNAs (333). Indeed, Kaposin B-mediated activation of the p38/MK2 pathway induces the MK2-HSP27-p115RhoGEF-RhoA signaling axis causing the disruption of the P-body network, which is involved in mRNA degradation (334, 335). Interestingly, both ZFP36 and ZFP36L1 are known to be important components of P bodies and are involved in the processing of the target mRNA (336).

In latently EBV-infected cells, p38 is an important regulator of the transition between latency and lytic replication due to its ability to regulate autophagy (337–339). In addition, the EBV latent membrane protein 1 (LMP1), which is expressed during latency, activates p38 signaling predominantly via its C-terminal activating region 2 (CTAR2) in a TRAF6/IRAK dependent manner and upregulates IL-6, IL-8 and IL-10 expression (340–343). LMP1-mediated activation of p38 is also establishing a positive feedback loop that increases the expression of LMP1 itself (344).

1.4 The ZFP36 protein family

1.4.1 General overview

RNA binding proteins (RBPs) constitute a regulatory network that is involved in the maintenance of cell homeostasis. RBPs can perform their function by interacting both with the target RNA, through an RNA binding domain, and with other proteins which are involved in the network (345, 346).

In humans, one of the families of RBPs is the ZFP36 family, which includes ZFP36 (also known as TTP), ZFP36L1 (also known as BRF1) and ZFP36L2 (also known as BRF2). The proteins belonging to this family are characterized by the presence of a tandem zinc-finger domain (TZF), a region of the protein spanning 64 amino acids which is responsible for binding the single strand mRNA via the two CCCH zinc fingers. Due to the type of interactions that are responsible for the binding of the zinc fingers to the ARE sequences and their limited secondary sequence, the protein backbone is very important to determine ZFP36 family members´ specificity in the recognition of the target sequences (347, 348). This is probably one of the reasons why there is high evolutionary conservation of the TZF across the different eukaryotic species (349).

Another highly conserved domain within eukaryotes is the C-terminal domain. This domain has been shown to interact with NOT1, an important component of the deadenylase CCR4-NOT1 complex (350, 351). In human ZFP36 the N-terminal region also contains the ability to interact with the CCR4-NOT1 complex, in particular with CCR4, as well as with proteins involved in decapping, such as Dcp1a/Dcp2, and the exosome component Rrp4 (352).

Besides the two highly conserved regions containing the TZF and NOT1-binding domains, there is little conservation in the amino acid sequence either between family members in the same species and between species. Two exceptions that show some level of conservation are the nuclear export sequences that have been identified in the different ZFP36 family members, both in mammals and in *D. melanogaster* (353, 354), and the phosphorylation sites that are important for the functional regulation of these proteins.

Despite a similar structure and ability to bind to the adenylate-uridylate-rich elements (AREs) in the 3' UTR of target mRNAs, the function and the binding ability of the three components of the ZFP36 family are not completely overlapping and could be differently modulated based on the cell type and the timing of the response (349, 355, 356). In recent years, several studies aimed at identifying ZFP36 targets at a global scale have been performed and suggested that ZFP36 binds preferentially to the UUAUUUAUU or UAUUUAU motifs present in the 3´UTR of the mRNA (357–359). PAR-CLIP experiments showed that ZFP36 can also bind to the AU-rich elements present in the introns, even though much fewer binding sites have been described outside the 3´UTR (358, 360). This preference can probably be explained by the fact that ZFP36 exerts its function mainly in the cytoplasm on mature mRNA. Indeed, ZFP36 mediates the degradation of the target mRNAs in cytoplasmic complexes called stress granules and processing bodies (361–364).

Phosphorylation plays a pivotal role in the regulation of ZFP36 activity. Several kinases have been described to be targeting it: p38, ERK, JNK, and AKT (365, 366). The p38 pathway, via the activation of MK2, regulates ZFP36 ability to promote mRNA degradation (367, 368). MK2 phosphorylates ZFP36 at Ser60 and Ser186 (corresponding to Ser52 and Ser178 in mouse) (369). The phosphorylation at these two serine residues increases ZFP36 stability and promotes the interaction with the adaptor protein 14-3-3 (367). According to Clement and colleagues, the phosphorylation of ZFP36 results in its inability to recruit the Ccr4-Caf1-Not and Pan2-Pan3 deadenylase complexes while still maintaining the binding to the target mRNA. The binding to the adapter protein 14-3-3 that follows ZFP36 phosphorylation inversely correlates with the recruitment of these complexes and could directly inhibit their recruitment.

Since phosphorylation plays a pivotal role in the regulation of ZFP36 activity, two phosphatases, DUSP-1 and the protein phosphatase 2A (PP2A), are mainly responsible for the regulation of its activation status. DUSP-1, which is normally expressed at very low levels in unstimulated cells, is induced by the same stimuli that activate the p38 MAPK cascade. By dephosphorylating p38, as well as other MAPK, DUSP-1 generates a negative feedback loop that can result in the termination of the inflammatory response (370, 371). Bone marrow-derived macrophages in a murine model of *Dusp1-/-* showed a much stronger response to LPS stimulation as measured via the secretion of several inflammatory cytokines. However, this increase could be reversed by introducing a mutation at Ser52 and Ser178 of ZFP36, indicating

that DUSP-1 plays a role in the regulation of ZFP36 activity by targeting p38 for dephosphorylation (372). PP2A, on the contrary, acts directly on ZFP36 and it is responsible for the dephosphorylation of Ser52 and Ser178 (373). The knock-down of *Pp2a* in a mouse alveolar macrophage cell line (MHS cell line) resulted in increased phosphorylation of p38 MAPK, MK2 and ZFP36, as well as an increased interaction of ZFP36 with 14-3-3 and increased expression of TNFα mRNA (373).

Other mechanisms are involved in the regulation of ZFP36 ability to target mRNAs for degradation. Competition between ZFP36 and HuR for the binding of the AU rich elements in the 3´ UTR of target mRNAs has been shown to be modulated by the p38-MK2 axis. HuR, an ARE-binding protein able to promote transcript stabilisation and translation initiation, was enriched in the 3´ UTR of ARE-containing transcripts, including ZFP36, upon treatment of murine macrophages with LPS (374).

In addition, recent evidence has shown that ZFP36 family members can influence mRNA translation not just by promoting mRNA degradation, but directly interfering with the translation machinery (375, 376). ZFP36 can directly interact with the 4EHP-GYF2 complex, a known translation repressor (377, 378), via its tetraproline-rich motifs. ZFP36L1 was also
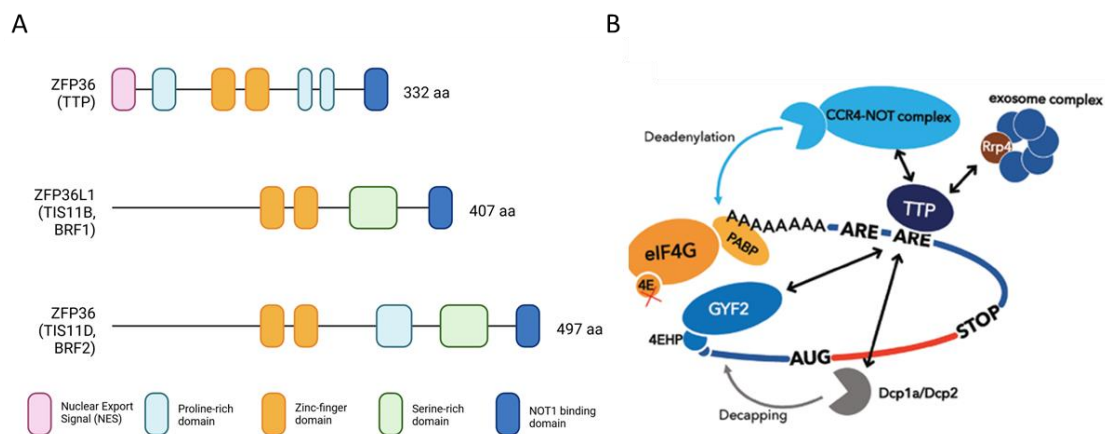
Figure 1.10: Structural overview of human ZFP36 family members and interactors of the prototypical ZFP36 protein. (A) Overview of the different domains identified in the three human ZFP36 family members. Alternative names for each protein are reported in brackets under the official protein name (left). The total length of the amino acid sequence is reported for each protein (left). Created with Biorender.com. (B) Schematic representation of the different interacting partners of ZFP36 and their functions. Adapted from H. Otsuka, A. Fukao, Y. Funakami, K. E. Duncan, T. Fujiwara, Emerging Evidence of Translational Control by AU-Rich Element-Binding Proteins. *Front. Genet.* **10** (2019).

recently found to block translation in parallel to previously described mechanisms of mRNA degradation (379). However, differently from what was observed for ZFP36, this inhibition was not due to the interaction with the 4EHP-GYF2 complex but rather via a CNOT1-dependent mechanism which did not require deadenylation of the target mRNA.

1.4.2 Functional studies

Total and tissue-specific knockouts of the *Zfp36* family members have been generated in mice to study their function, especially in the context of the immune system. The first to be described was a total knockout of *Zfp36,* which resulted in the development of a severe inflammatory syndrome characterized by destructive arthritis, cachexia, autoimmune response and myeloid hyperplasia (380). This phenotype was later associated with an increased expression of *Tnf* mRNA, which was identified to be a target of ZFP36 (381). The lack of *Zfp36* also resulted in the increased stabilization of the granulocyte colony-stimulating factor (CSF2) secreted by bone marrow-derived stromal cells, which contributed to the myeloid hyperplasia that was observed in *Zfp36* knockout mice (382). In their work, Carballo and colleagues were able to link ZFP36 with the deadenylation process: in bone marrow stromal cells from *Zfp36* knockout mice *Csf2* mRNA existed mainly in one larger form containing the polyA tail, while in the wild type animals the ratio between the larger and the smaller form of the mRNA, not containing the polyA, was around 50:50.

Zfp36l1 knockout mice showed a more severe phenotype, with embryonic lethality by day 11 (383). A *Zfp36l2* knockout mouse model resulted also in the death of the mice approximately 2 weeks after birth following the developing of anaemia, thrombocytopenia, and diffuse haemorrhages (384). The KO mice showed a generalized alteration of the hematopoietic processes, with a significant reduction in the levels of all the cellular components of the blood, as well as in the level of haemoglobin and platelets. These defects were due to a decrease in the hematopoietic progenitor cells in both the yolk sac and the foetal liver.

The generation of murine models in which one or more members of the ZFP36 family have been knocked out in a specific cell lineage or cell type allows to better understand the role played by these proteins in different physiological processes. For example, when ZFP36 was specifically knocked out in myeloid cells (357, 385), the phenotype did not mimic the severe inflammatory syndrome that was originally observed in the *Zfp36*-knock out mice (380).

However, when the mice were challenged with low doses of LPS they developed severe endotoxemia, in contrast with the wild type mice which did not show any significant response to the treatment (385). Endotoxemia was accompanied by increased serum levels of TNF, which were 110-fold higher in the KO mice than in the control. Since the absence of ZFP36 in the myeloid lineage does not entirely reproduce the phenotype observed in the *Zfp36*-knock out model, it is agreed that other cell types must be involved in the process (i.e. fibroblasts (386)). The murine model developed by Kratochvill and colleagues allowed the authors to confirm *in vivo* the mechanistic model they proposed to explain how ZFP36 regulates the transcription levels of TNF in a steady-state condition and after the treatment with LPS, which induces an inflammatory response (357). In their model, in the absence of inflammatory stimuli, ZFP36 regulates *Tnf* transcript levels together with ZP36L1 and ZFP36L2. When inflammation is induced, and the p38 pathway is activated, ZFP36 activity is reduced and ZFP36L1 and ZFP36L2 expression is repressed, resulting in the increased stability of target mRNAs. Interestingly, the authors reported that even at the peak of p38 activation 3 hours post LPS-treatment, *Tnf* mRNA stability in the control was significantly lower than in the knockout. Once the level of p38 activity starts fading and ZFP36 activity starts increasing, mRNAs that are targeted become more and more unstable and this allows a rapid clearance of pro-inflammatory chemokines and the resolution of inflammation.

The role played by ZFP36L1 and ZFP36L2 in macrophages was further investigated *in vitro* by Wang and colleagues (355). A *Zfp36l1* and *Zfp36l2* knockdown showed that, in the absence of LPS stimulation, *Zfp36l1* and *Zfp6l2* were responsible for *Dusp1* degradation. Due to the increased expression of *Dusp1*, the lack of *Zfp36l1* and *Zfp6l2* resulted in a reduced level of activation of the MAPK p38 pathway both in the unstimulated cells and after LPS treatment. The ability of DUSP1 to control p38 activation and therefore to modulate ZFP36 function is also central in the IL-10-mediated control of macrophage activation (387–389) as well as in the more recently discovered prostaglandin E2-mediated negative feedback loop (390). In the first case, IL-10, which is itself a target of ZFP36, induces STAT3 activation promoting at the same time DUSP1 and ZFP36 expression. DUSP1 is then able to control the activation of p38, preventing the inactivation of ZFP36. Increasingly higher amounts of active ZFP36 are then responsible for blocking the expression of IL-10 and blocking the feedback loop. A second negative feedback loop is regulated by prostaglandin E2 (PGE$_2$), which, by engaging in a paracrine fashion with its own receptor EP4, is able to induce DUSP1 as a result of the

activation of the cAMP signaling cascade. PGE_2 is induced in murine macrophages as a result of LPS treatment, which activates the p38-MK2 pathway, therefore, blocking ZFP36 activity. This results in the expression of cyclooxygenase 2, another target of ZFP36, which is responsible for the increased production of prostaglandin E2 and, consequently, inducing the feedback loop.

ZFP36 family members have been extensively investigated also for their function in the lymphocyte cell compartment. For example, ZFP36L1 has been demonstrated to play several important roles in B cell development. It has been shown that ZFP36L1 is involved in the development program responsible for the differentiation into marginal zone (MZ) B cells (391). Newman and colleagues showed that this is achieved by targeting two important transcription factors, KLF2 and IRF8, that are otherwise responsible for the differentiation into follicular B cells. ZFP36L1 has also been involved in the homing process that drives antibody secreting cells (ASCs) from the secondary lymphoid organs, where they undergo affinity maturation of immunoglobulins in the germinal centers, to the bone marrow. This process is highly regulated by the expression of CXCR4 and sphingosine-1-phosphate receptor 1 (S1PR1) (392), as well as of the integrins α4β1 (393) and α4β7 (394, 395). In this context, ZFP36L1 modulates the expression levels of the kinase G protein–coupled receptor kinase 2 (GRK2), which is a negative regulator of S1PR1, and of the integrins α4β1. Lack of ZFP36L1 results in an increased accumulation of ASC in the spleen and in the liver rather than the bone marrow niche (396).

ZFP36L1, together with ZFP36L2, is also responsible for maintaining cell quiescence in pre-B cells to allow variable-diversity-joining (VDJ) recombination (397). ZFP36L1 and ZFP36L2 redundantly direct transcripts of genes involved in the cell cycle regulation for degradation (i.e., *Ccne2*), preventing pre-B cells undergoing rearrangement from entering the cell cycle, which would otherwise inhibit the VDJ recombination. Interestingly, Galloway and colleagues described how cells lacking ZFP36L1 and ZFP36L2 do express the transcriptional program that allows pre-B cells to enter quiescence, but the post-transcriptional regulation mediated by the two proteins is necessary for the effective activation of these processes. The ability of ZFP36L1 and ZFP36L2 to regulate cell cycle progression plays a role not only during the development of B cells but also during the maturation of T cells in the thymus. In this context, during the double negative 3a stage, ZFP36L1 and ZFP36L2 target for degradation transcripts

encoding for protein involved in the cell cycle, allowing for productive VDJ recombination. Additionally, these two RNA binding proteins act on DNA damage response gene expression and limit the activation of the pathway. This prevents an abnormally activated DNA damage response from promoting cell cycle progression in the absence of a successfully rearranged pre-TCR (398). This fits with the development of T lymphoblastic leukaemia in mice lacking both ZFP36L1 and ZFP36L2 (399).

1.4.3 Role during infection

Despite ZFP36 family members´ well characterized role during inflammation, little evidence is available on their role in the context of viral infections. As for the activation of the p38 pathway, ZFP36 family members can play a pro- or anti-viral effect depending on the context.

The first evidence of the role played by ZFP36 in the context of viral infections comes from Moore and colleagues (400), which identified ZFP36 as a limiting factor for T cell activation. By performing HITS-CLIP, the authors identified the ability of ZFP36 to suppress T cell-associated mRNA abundance and translation via interaction with AU-rich elements present in the coding sequence rather than the 3' UTR. The functional effect of this mRNA degradation was the attenuation of activation marker expression, reduced T cell expansion and cell death. Interestingly, when mice lacking *Zfp36* were challenged with lymphocytic choriomeningitis virus (LCMV), clearance of the infection was reached faster as a result of greater expansion of specific T cells and increased secretion of effector cytokines such as interferon gamma and TNFα. Similarly, Ebner and colleagues (401) identified how ZFP36 regulates and limits neutrophil engagement with pathogens. In particular, they identified ZFP36 as a regulator of *Mcl1*, a gene belonging to the Bcl2 family which promotes cell survival by blocking apoptosis. A mouse model lacking *Zfp36* in the myeloid line showed a better clearance of bacterial infection, with increased accumulation of neutrophils in the infected region. The effect exerted by the lack of *Zfp36* was specific to neutrophils engaging with pathogens and not resting neutrophils and was not caused by increased accumulation of monocytes nor increased availability of myeloid progenitors or circulating myeloid cells. The authors proposed that the engagement of pathogens by neutrophils results in the activation of ZFP36 which, in turn, degrades Mcl1 promoting cell death, therefore, limiting the pool of activated neutrophils and

the inflammatory response which follows. This however comes at the expense of a more efficient immune response and more rapid control of the infection.

The expression and activity of proteins belonging to the ZFP36 family can also be hijacked and controlled by pathogens themselves. For example, the infection of murine hepatocytes and macrophages by MCMV induces the activation of the MK2 kinase which regulates IL-10 and other cytokines (IL-6, TNFα) by blocking ZFP36 activity. IL-10 secretion is important to limit the formation of a proper T cell response against MCMV, therefore promoting infection (402). Similarly, ZFP36 expression is strongly downregulated in different subpopulations of PBMC in patients chronically infected with the Hepatitis B virus (HBV). This downregulation is caused by two pro-inflammatory chemokines, IL-8 and RANTES, which are highly induced by HBV. As a consequence of the reduced levels of ZFP36, several cytokines and chemokines are significantly upregulated in the serum of these patients (403). Another example of ZFP36 inactivation by a viral protein which results in increased cytokine release occurs in cells infected by retroviruses. The oncoprotein Tax was shown to interact, via its C-terminal domain, with the C-terminal domain of ZFP36, promoting ZFP36 relocalization to the nucleus and preventing it from targeting TNFα mRNA for degradation, which results in increased TNFα expression (404).

Influenza virus infection of dendritic cells is known to induce the expression of several miRNAs, among which is miR-451. miR-451 can promote the degradation of 14-3-3ζ, a known interactor of ZFP36, and prevent ZFP36 inhibition. This leads to a reduced secretion of inflammatory cytokines with an unclear effect on the infection (405). In a similar fashion, coronavirus infection activates the MKK3-p38-MK2 cascade which simultaneously activates the expression of ZFP36 family members, as well as several pro-inflammatory chemokines and cytokines. This generates a negative feedback loop in which ZFP36 and its homologues are responsible for dampening the inflammatory response that is induced by the infection itself (406).

Recently, a more direct role for ZFP36L1 as a restriction factor for the Influenza A virus (IAV) was described, in which ZFP36L1 blocked the translation of the IAV HA, M1 and NS1 proteins, but did not affect their mRNA expression or stability. However, the ability of

ZFP36L1 to block IAV mRNA translation was independent of the binding to the AU-rich elements of the target mRNA but still required the protein-RNA interaction to occur (407).

2. Aims and objectives

In healthy humans, EBV infects mainly primary B cells, in which eventually develops a chronic latent infection that can periodically undergo episodes of lytic replication with virus production, but also occasionally epithelial cells (4). For many intracellular pathogens, the very early stages of infection are essential to downregulate the innate immune response that would otherwise block the incoming viral particles, thereby preventing the establishment of the infection. Despite their centrality in the EBV life cycle, little is known about these early events, with most of the studies focusing on events occurring after the EBV latency program has been activated (408–410). Modulation of signaling pathways by viruses is a well characterized mechanism that allows the virus to prevent the activation of pattern recognition receptors (PRR) or to counteract their effects (411). The inflammatory response that follows PRR activation after infection represents a double-edged sword for the virus as some cytokines facilitate infection, yet others block it (412–414). EBV infection of B cells gives rise to the secretion of pro-inflammatory cytokines (160, 415), as does the strong and generalized activation of the immune response against the virus during infectious mononucleosis (140). In addition, previous work has also identified EBV viral particles to be able to induce centrosome amplification and chromosomal instability independently from their ability to establish a successful latent infection (416). This highlights how the interaction between the host and the proteins contained within the viral particles can induce alterations in the infected cell with long-lasting effects and tumorigenic potential.

Therefore, the aims of this thesis are:

1) To determine the proteome and phosphoproteome in the first hours of the infection process.
2) To identify the cellular pathways modified by the viral infection early after infection.
3) To identify the steps of the infection process that are responsible for the modifications of the proteome and the activation of cellular pathways.
4) To identify the viral components (DNA, proteins) involved in the molecular events that follow infection.

3. Results

3.1 Early molecular events after EBV primary B cell infection.

3.1.1 Proteomic analysis.

To identify early molecular events occurring after EBV infection of primary B cells, I performed a high-throughput analysis of their proteome.
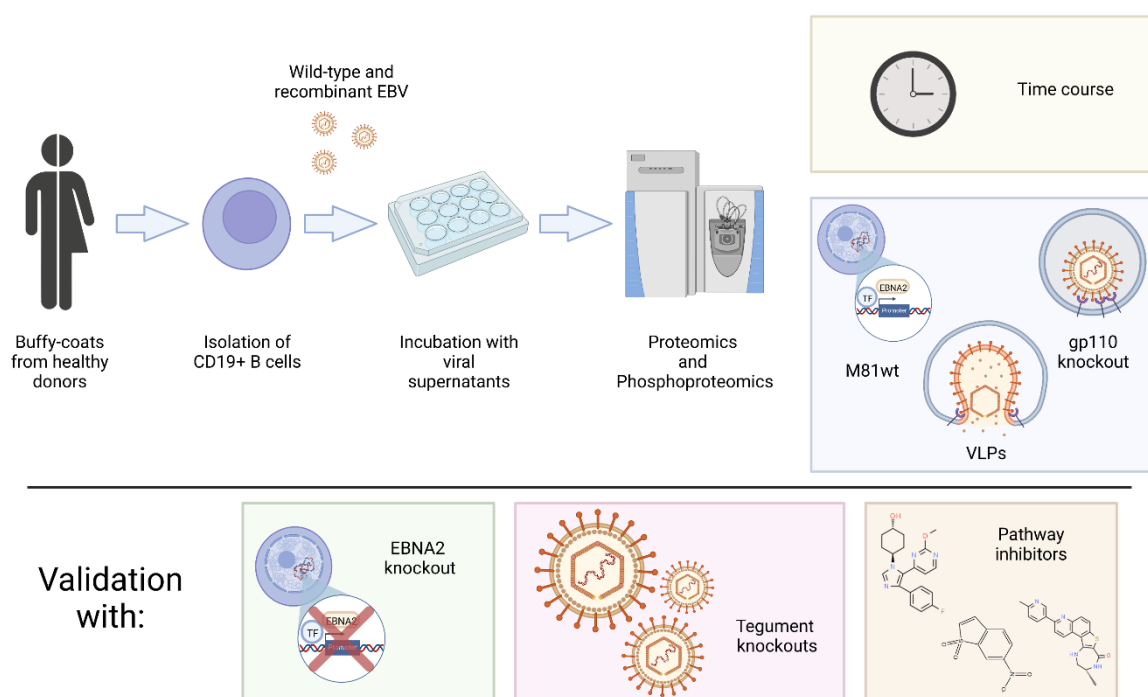
Figure 3.1: Schematic representation of the different methodologies employed to identify and characterize the events which occur shortly after EBV infection. Created with BioRender.com.

I first determined the proteome of two independent primary B cell samples infected with EBV M81 wild-type virus at 6 and 12 hours post infection. At 12 hours post infection, I found 12 proteins that were upregulated and 3 that were downregulated (Table 4, Fig. 3.2A). I performed pathway analysis which did not reveal any specific signature, in particular no interferon response. To validate this result, I quantified the interferon alpha release using ELISA at various time points after infection. This assay showed that secretion of this cytokine began after 16 hours and reached significant levels only 96 hours after infection (Fig. 3.2B). Among

the identified proteins, ZFP36L1 (also known as TIS11B or BRF1) was consistently upregulated already at 6 hours post infection (Fig. 3.2C).
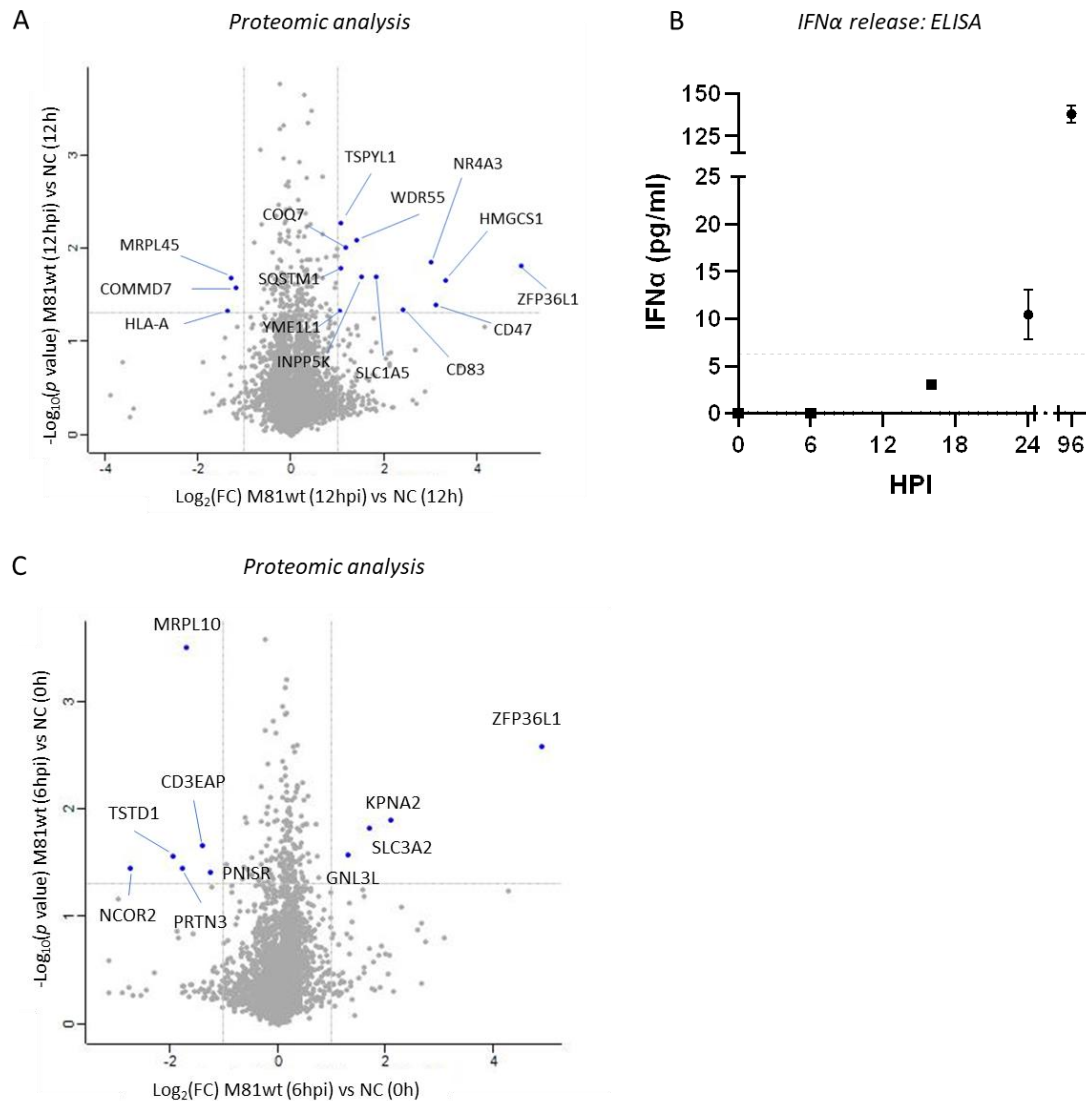
Figure 3.2: Proteomic analysis of primary infected B cells. (A) Volcano plot representation of significantly upregulated and downregulated proteins as identified by label-free mass spectrometry performed on two independent biological samples of primary human CD19+ B cells at 12 hours post infection with M81wt virus. A two-tailed paired t-test was performed. Targets were selected if their p value was < 0.05 and the absolute fold change versus the negative control was > 2. (B) Interferon α secretion was measured via ELISA at different time points after infection with M81wt virus of human primary B cells. The dotted line represents the lower detection limit of the kit used for the quantification as reported by the manufacturer. Two independent biological replicates were measured, and the data is shown as the mean ± SD. *(C)* Volcano plot representation of significantly upregulated and downregulated proteins as identified by label-free mass spectrometry performed on two independent biological samples of primary human CD19+ B cells at 6 hours post infection with M81wt virus. A two-tailed paired t-test was performed. Targets were selected if their p value was < 0.05 and the absolute fold change versus the negative control was > 2.

I then performed a second proteomic analysis at one single time point, 6 hours post infection, and I exposed B cells to M81wt, to an EBV/Δgp110 knockout that can bind to B cells, but cannot infect them, and to EBV virus-like particles (VLP) that enter B cells, but are devoid of DNA and cannot establish a chronic virus infection. Proteomic analysis of these samples showed that while ZFP36L1 was also clearly upregulated after exposure to EBV VLPs, though not to wild type levels, the effect on ZFP36L1 was only marginal after M81/Δgp110 binding (Fig. 3.3A). The generated data could also confirm recently identified cellular targets of the virus. At 6 hours post infection, I could confirm a significant reduction in the SMC6 protein both with the wild-type virus and the VLP control, but not the Δgp110 defective mutant (Fig. 3.3B) (417). Moreover, I also detected a statistically significant reduction in the levels of STAT2 protein after M81wt infection (Fig. 3.3C) (418).
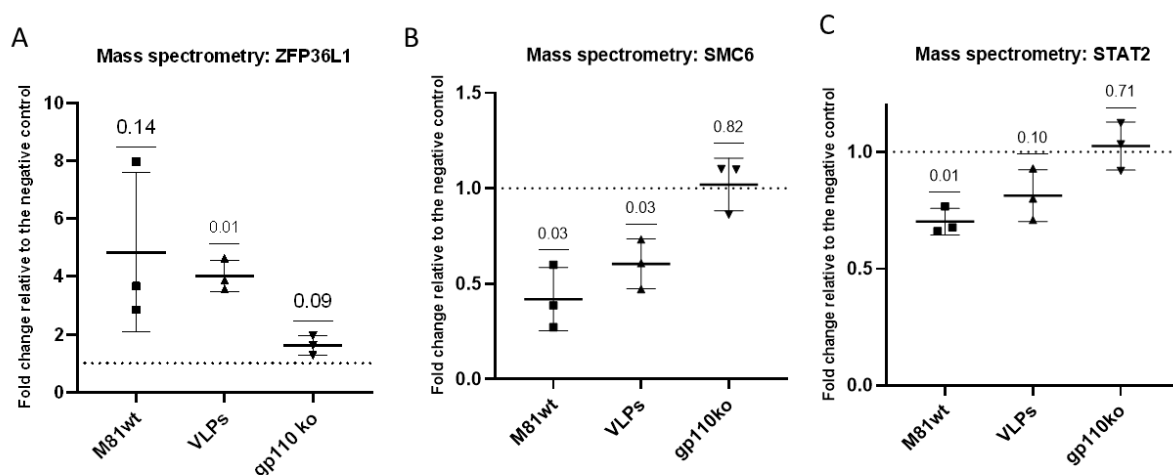
Figure 3.3: EBV induces dysregulation of ZFP36L1, SMC6 and STAT2 protein levels. (A-C) Variation in the protein levels of ZFP36L1 (A), SMC6 (B), and STAT2 (C) compared to the negative control in M81wt virus, VLPs, and gp110 knockout virus-infected B cells at 6 hours post infection as identified by mass spectrometry. The fold change for each independent biological replicate is reported, and the mean ± SD is indicated. A one sample t test ($\mu=1$) was performed. p values are reported above the comparison. $p<0.05$ was considered statistically significant.

3.1.2 Phosphoproteomic analysis.

Using a similar approach to the previously described experiment, I went on performing the phosphoproteomic analysis in order to identify phosphorylated peptides which are particularly enriched or depleted after infection. To do so, human primary B cells were infected with M81wt virus, VLPs or gp110 knockout virus for 6 hours. In order to obtain enough material to perform the analysis, the same amount of protein from several donors was pooled together to form a

biological replicate. A total of 3 biological replicates were analysed, each composed of 7 different donors. The phosphoproteome revealed multiple phosphoevents in the STAT3 protein, in members of the MAPK pathway, as well as in the RNA-binding proteins RMB7 and ZFP (ZFP36, ZFP36L1 and ZFP36L2) (Fig. 3.4A, Table 5). However, in the latter case, although the recorded values were all indicative of an increase in phosphoevents, the global analysis did not reach statistical significance because of a high level of standard deviation between values. Similar experiments performed with EBV VLPs led to the detection of more phosphoevents than after wild type infection, suggesting that some initial kinase targets of the virus revert at a later stage of infection (Fig. 3.4B). Binding of M81/Δgp110 also generated phosphoevents, some of which were common to those generated by EBV VLP and wild type infection (Fig. 3.4C and 3.4D, Table 5). In particular, phosphoevents in members of the ZFP36 family were common to all types of infection (Fig. 3.4E). Altogether, these high throughput screens identified an upregulation and phosphorylation of ZFP36L1, together with STAT3 phosphorylation, as important early events after EBV infection that were initiated by virus binding.

A — *Phosphoproteomic analysis*

B — *Phosphoproteomic analysis*

C — *Phosphoproteomic analysis*

D — p-value < 0.05 & Fold Change > 2 ; p-value < 0.05 & Fold Change < -2
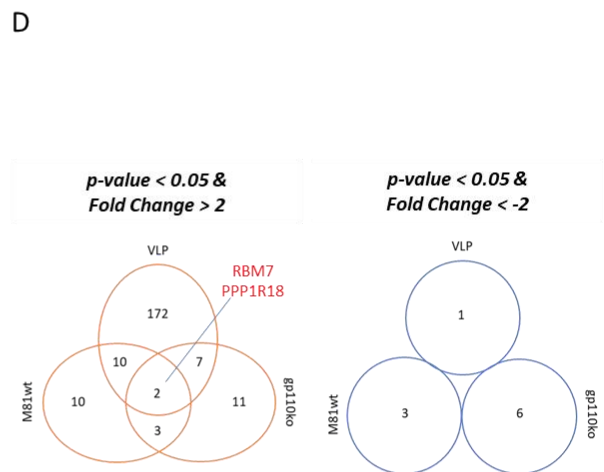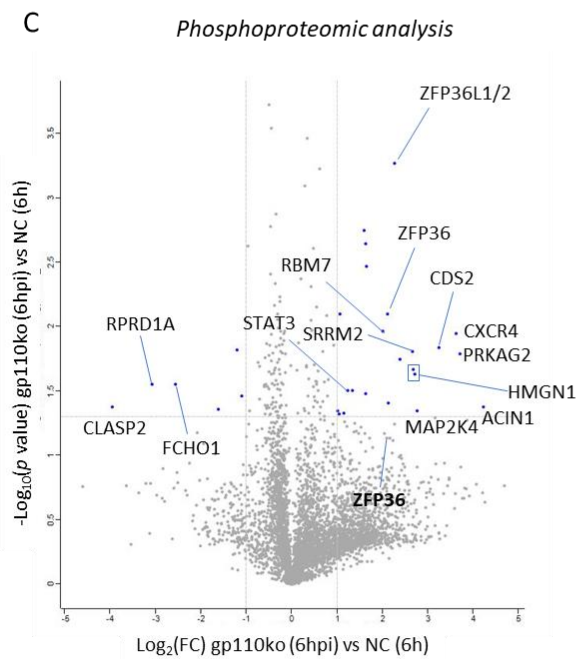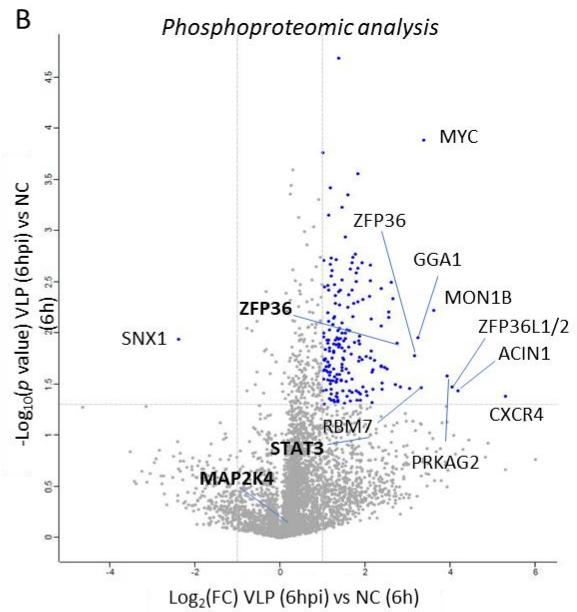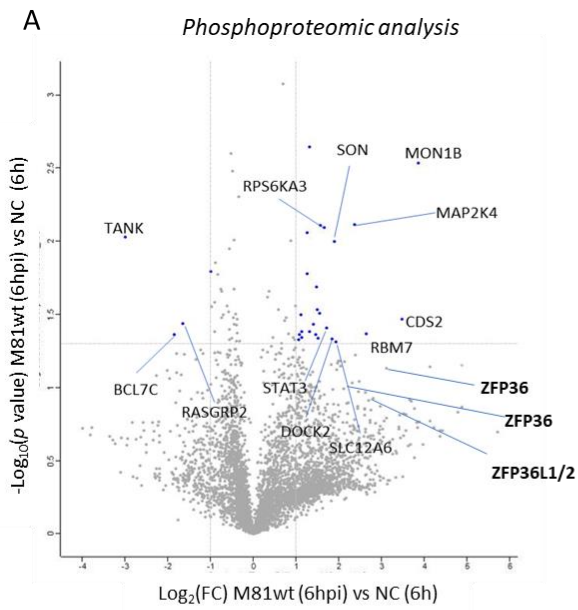
E — *Phosphorylation events detected for the ZFP36 family members*

Gene names	Positions within proteins	-log₁₀(p-value) M81wt_NC	log₂(fold change) M81wt_NC	-log₁₀(p-value) VLPs_NC	log₂(fold change) VLPs_NC	-log₁₀(p-value) gp110ko_NC	log₂(fold change) gp110ko_NC
ZFP36	192;203;186	1.13	3.11	1.78	3.16	2.10	2.10
ZFP36L2;ZFP36L1	490;334	0.93	2.80	1.48	4.05	3.27	2.26
ZFP36	329;340;323	0.99	2.12	1.91	2.76	1.13	2.09
ZFP36	99;110;93;100	0.71	4.37	0.92	4.88	0.82	3.47
ZFP36L1	54;32;60;123	0.73	3.83	0.37	2.71	0.83	3.06
ZFP36L1	92;70;98;161	1.02	1.33	0.01	-0.06	0.38	1.18
ZFP36L2	57	0.18	0.84	0.04	-0.33	0.08	0.41
ZFP36L2	59	0.15	0.65	0.12	-0.99	0.27	0.92

Figure 3.4: Phosphoproteomic analysis of M81wt, VLPs and gp110 knockout infected B cells. (A-C) Volcano plot representation of significantly upregulated and downregulated phosphopeptides as identified by phosphoproteomic in 3 independent biological pooled replicates of primary human CD19+ B cells treated with M81wt (A), VLPs (B) and gp110 knockout virus (C) at 6 hours post infection. A two-tailed paired t-test was performed in all cases. Targets were selected if their p value was < 0.05 (horizontal dotted line) and the absolute fold change versus the negative control was > 2 (vertical dotted lines). Selected upregulated candidates for which the p value is above significance are shown in bold. (D) Euler diagram representing the events identified by phosphoproteomic as up- (left) or downregulated (right) in the three conditions as compared to the negative control. Only the events with a p value <0.05 and an absolute fold change >2 were considered. The name of the two upregulated phosphoevents that are identified in all three conditions is indicated. (E) Table listing the phosphorylated residues for the ZFP36 family members that were identified by mass spectrometry in the three conditions. Fold change and p values are reported in the indicated logarithmic scale. Values in red indicate a p value <0.05, while values in green indicate a fold change >2.

3.2 EBV binding induces STAT3 activation via the BCR signaling.

3.2.1 EBV binding induces STAT3 activation.

From the list of phosphopeptides identified with the phosphoproteomic analysis, I decided to further investigate STAT3 activation. STAT3 activation was confirmed by performing western blot on samples infected either with wild type virus, its EBNA2 deletion mutant, with VLPs or with the M81/Δgp110 using a p-STAT3 (Tyr 705) specific antibody. All samples showed STAT3 activation, also after B cell exposure to the gp110 deletion mutant, thereby confirming that the activation takes place at a very early phase of infection (Fig. 3.5A). To rule out that this increase in phospho-STAT3 was the result of an increase in total STAT3, I performed immunoblotting on B cells infected with wild type EBV, which confirmed no modification in the levels of total STAT3, suggesting that posttranslational modifications were responsible for the observed STAT3 activation (Fig. 3.5B). These results were further confirmed by looking at the levels of total STAT3 as identified by the mass spectrometry experiment previously described (Fig. 3.5C). Phosphorylation of STAT3 is known to induce its translocation into the nucleus where it can act as a transcription factor (419). To confirm this, I performed cell fractionation which indeed showed that the increase in pSTAT3 upon EBV infection is mainly concentrated in the nucleus (Fig. 3.5D). Monitoring pSTAT3 expression overtime after wild type infection revealed that expression began 2 hours after infection and reached a plateau

between 6- and 24-hours post infection (Fig. 3.5E). STAT3 activation continued to increase after 24 hours post-infection and reached a maximum by 22 days post-infection (Fig. 3.5E). These results are in line with the observation that STAT3 is further upregulated in stably transformed LCLs under the influence of LMP1 (266).
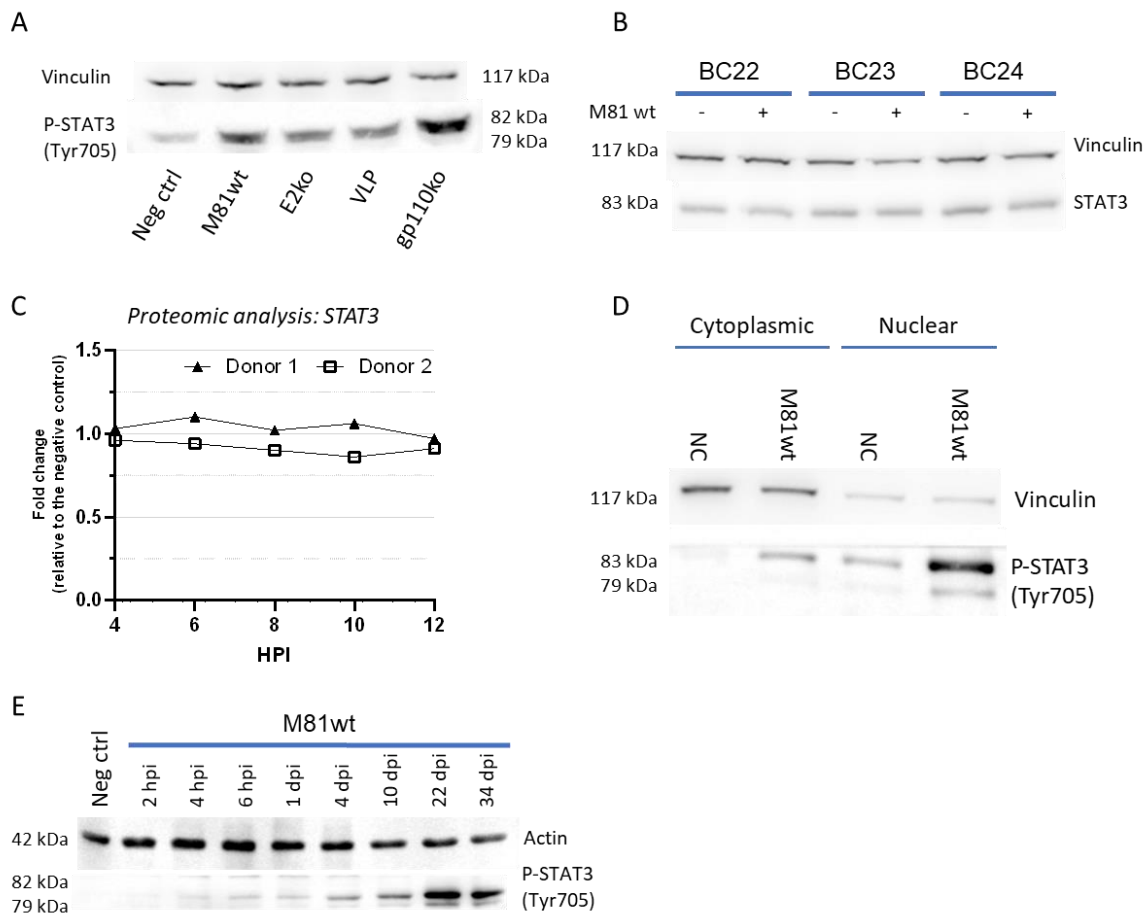
Figure 3.5: STAT3 activation occurs upon EBV binding. (A) Western blot analysis for activated STAT3 (Tyr705) was performed on human primary CD19+ B cells infected with M81wt, EBNA2 knockout, M81 VLPs, and gp110 knockout viruses at 6 hours post infection. (B) Western blot analysis of B cells infected or not with M81wt virus at 6 hours post infection from three independent donors. Total STAT3 was detected, and vinculin was used as loading control. (C) STAT3 protein levels as obtained by mass spectrometry performed on two independent biological replicates of M81wt infected B cells and expressed as fold change compared to the negative control at the different time points. The value of the fold change for each replicate is reported. (D) Cell fractionation performed on uninfected and M81wt infected human primary B cells at 6 hours post infection. Nuclear and cytoplasmic fractions were isolated and activated STAT3 was detected. Vinculin was used as a marker of cytoplasmic contamination. (E) Western blot performed on primary B cells infected with M81wt virus at different time points post infection. Phosphorylated STAT3 (Tyr705) was detected, and actin was used as loading control. (A, D, E) Each blot is representative of at least 3 biological replicates.

3.2.2 B cell receptor signaling is necessary for STAT3 activation.
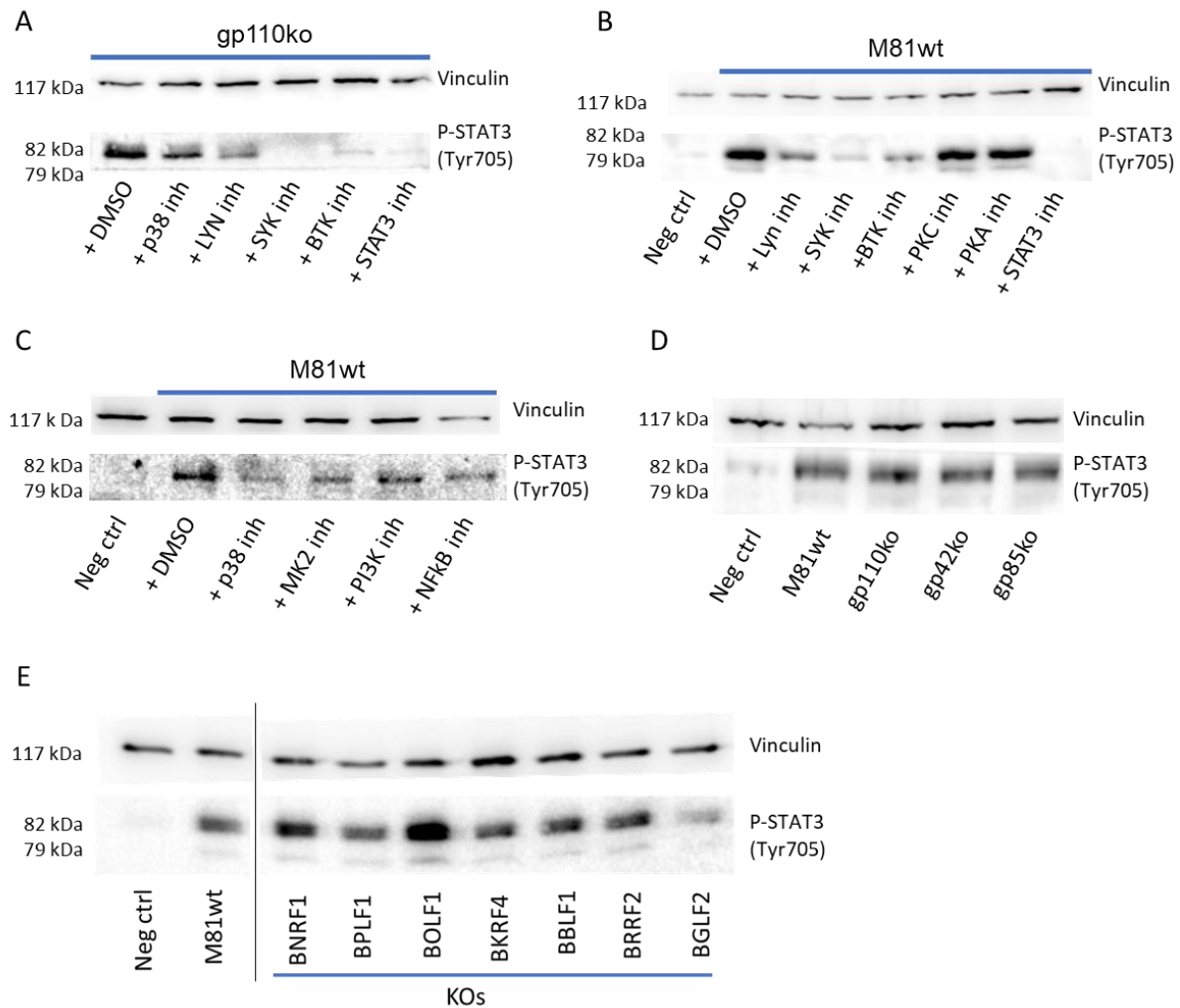
Figure 3.6: BCR signaling controls STAT3 activation. Western blot analysis for activated STAT3 (Tyr705) was performed on human primary CD19+ B cells: (A) exposed to the gp110 knockout virus or (B) infected with M81wt virus in the presence of inhibitors of B cell receptor signaling downstream mediators; (C) infected for 6 hours with M81wt virus in the presence of p38, MK2, PI3K and NF-κB pathway inhibitors; (D) exposed to M81wt gp85 and gp42 knockout viruses; (E) infected with different M81 tegument knockouts. (A-E) Phospho-STAT3 (Tyr705) was detected, and vinculin was used as loading control. Each blot is representative of at least 3 biological replicates.

I then attempted to identify the intracellular kinases involved in STAT3 Tyr705 phosphorylation. I began by exposing primary B cells to M81/Δgp110 virus in the presence of several pathway inhibitors selectively targeting downstream mediators of the B cell receptor signaling platform. Inhibition of SYK and BTK produced the strongest reduction in STAT3 Tyr705 phosphorylation levels, while LYN and p38 inhibition had a more limited effect (Fig. 3.6A). The same type of experiments using wild-type virus confirmed the importance of SYK

for STAT3 activation, although its inhibition did not completely block STAT3 phosphorylation (Fig. 3.6B). Furthermore, I could also identify a limited effect also from the inhibition of PI3K and NF-κB (Fig. 3.6B and C).

The results globally confirmed the validity of the phosphoproteome results and identified STAT3 phosphorylation as a major molecular event that follows virus binding. I then screened a panel of viruses devoid of surface proteins that retain full binding activity, but are unable to fuse with their target cells, for their ability to activate STAT3. This experiment showed that viral proteins involved in virus-cell fusion are not involved in STAT3 phosphorylation (Fig. 3.6D). The analysis was completed by infecting B cells with a panel of viruses lacking one of the EBV tegument proteins. BGLF2, and to a lesser extent BKRF4 and BPLF1, were found to be required for full STAT3 activation (Fig. 3.6E). Altogether, these results suggest that STAT3 is phosphorylated by SYK as the result of virus binding, but that P-STAT3 expression is further modulated by downstream events associated with virus entry.

3.3 EBV activates the p38-MK2-ZFP36L1 axis.

3.3.1 EBV virus-like particles are sufficient to activate ZFP36L1 expression.

Mass spectrometry results indicated that EBV infection was able to strongly induce ZFP36L1 expression shortly after infection. I performed western blot analyses which confirmed that while ZFP36L1 is hardly present in resting B cells, its expression was upregulated two hours after EBV infection and persisted for several days. (Fig. 3.7A). ZFP36L1 appeared as a ladder in western blot, suggesting the presence of differentially phosphorylated forms that have been previously reported in the literature (Fig. 3.7A) (420–424). I confirmed that this was indeed the case as the protein ladder reduced to a single band after treatment of the samples with a phosphatase (Fig. 3.7B) (355, 425). An RT-qPCR based analysis of transcription showed that the increase in ZFP36L1 protein production is paralleled by a short increase in transcription that reached a maximum at 6 hours post-infection but came back to baseline levels after two days (Fig. 3.7C). Treatment of infected B cells with actinomycin D and cycloheximide indicated that ZFP36L1 upregulation upon infection requires *de novo* transcription and translation (Fig. 3.7D).
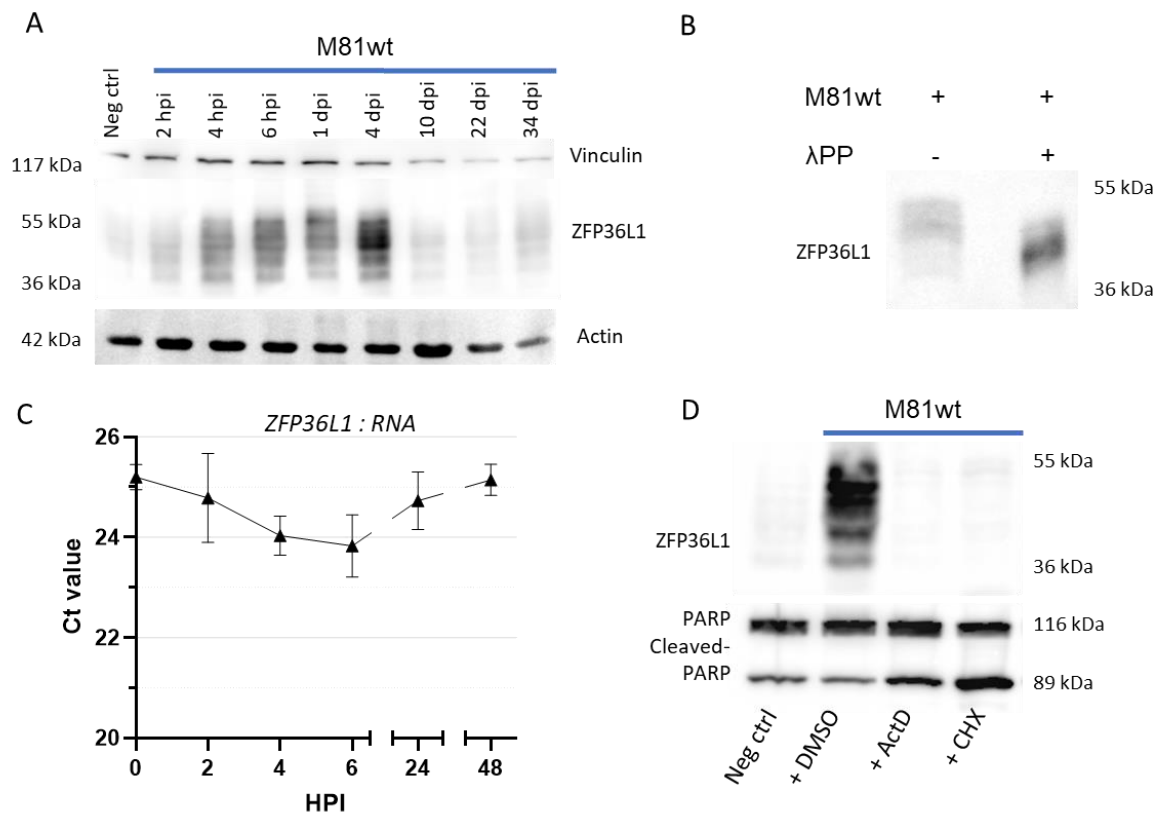
Figure 3.7: ZFP36L1 is highly upregulated upon EBV infection. (A) ZFP36L1 expression upon EBV infection as shown by western blot. A time course experiment was performed on primary human B cells infected with M81wt. ZFP36L1 was detected on samples obtained at the indicated time point post infection. (B) Cell lysates from M81wt infected B cells at 6 hours post infection were treated or not with λ protein phosphatase and immunoblotted for ZFP36L1. (C) ZFP36L1 mRNA quantification by RT-qPCR at different hours post M81wt virus infection. Ct values from 3 independent biological replicates are represented as mean ± SD. (D) Western blot analysis of primary human B cells infected with M81wt in presence of the vehicle only (DMSO) or actinomycin D (ActD), a transcriptional inhibitor, or cycloheximide (CHX), a translational repressor. The detection was performed using antibodies against ZFP36L1 and PARP/cleaved-PARP.

The infection experiments were extended to an M81/ΔEBNA2 virus deletion mutant, to virus-like particles and to M81/Δgp110. This assay showed ZFP36L1 induction after infection with VLPs or M81/ΔEBNA2 (6-fold versus 4-fold induction, on average), albeit at reduced levels relative to wild type infection (Fig. 3.8A and Fig. 3.2D). A very weak ZFP36L1 induction after M81/Δgp110 infection was also observed. Transcription analyses revealed a similar pattern, with exposure to VLPs or M81/ΔEBNA2 being less efficient at activating ZFP36L1 expression than wild type M81 (Fig. 3.8B). The binding of M81/Δgp110 to B cells proved unable to activate ZFP36L1 transcription.

Immunofluorescence stains for ZFP36L1 on freshly infected primary B cells showed increased ZFP36L1 expression upon EBV infection, with the accumulation of the protein in the cytoplasm where the protein can access its RNA targets (Fig. 3.8C) (336, 362, 364, 426). Here again, the wild-type virus proved to be more potent than the M81 VLPs or Δgp110 in stimulating ZFP36L1 protein production. Altogether, these experiments confirmed the data of the proteome and show that ZFP36L1 becomes increasingly activated as the infection progresses from virus binding to the inception of latent gene expression.
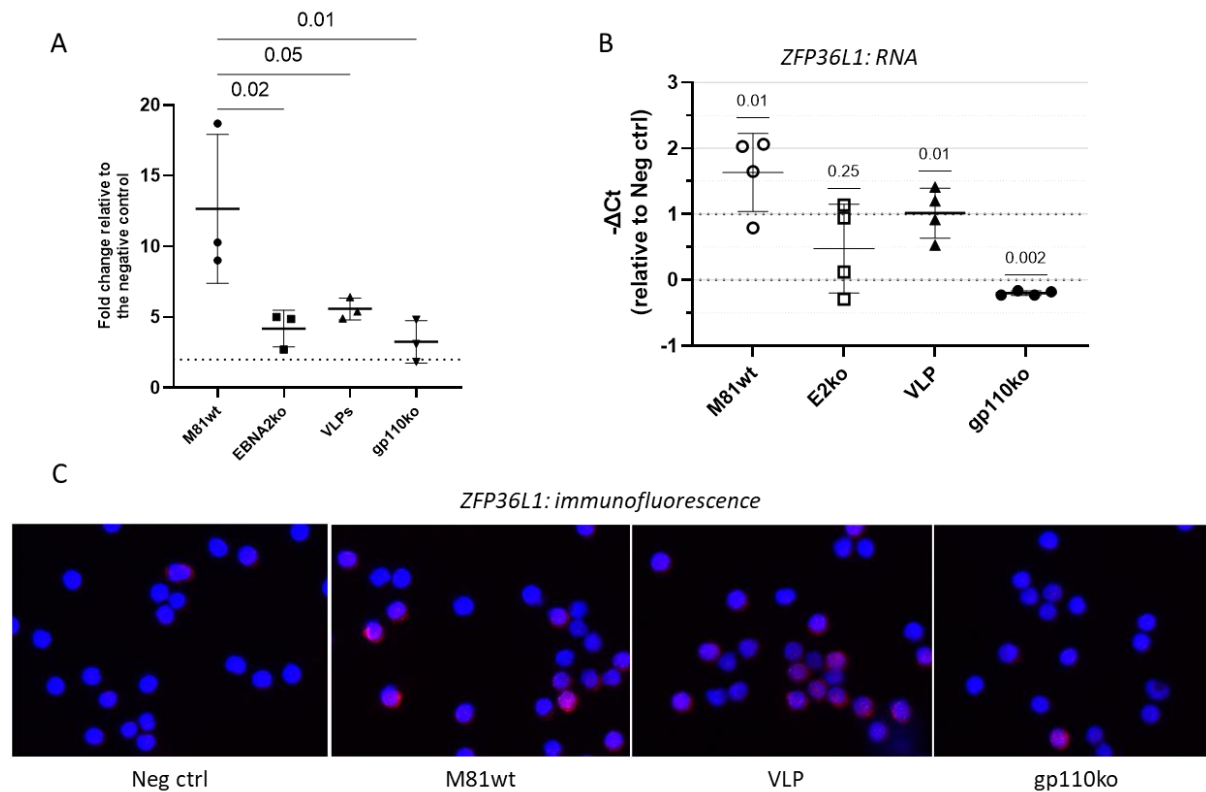
Figure 3.8: Latency initiation is required for full ZFP36L1 induction. (A) Protein expression levels of ZFP36L1 were detected by western blot after infection with M81wt, EBNA2 knockout, M81 VLPs, and gp110 knockout virus at 6 hours post infection. The signal for ZFP36L1 was quantified and normalized over the respective loading control. The fold change was calculated versus the negative control. The graph reports the values as the mean ± SD (n=3 independent biological replicates). (B) ZFP36L1 RNA expression levels were quantified via reverse transcription quantitative PCR (RT-qPCR) at 6 hours post infection with M81wt, EBNA2 knockout, VLPs or gp110 knockout virus and represented as difference versus the negative control. The difference for each independent replicate is plotted, and the mean ± SD is reported (n=4 independent biological replicates). (C) Immunofluorescence staining of primary human CD19+ B cells untreated or treated with M81wt, M81 VLPs or gp110 knockout virus at 6 hours post infection. Cells were stained for ZFP36L1 (red). Nuclei were counterstained with DAPI (blue). (A-B) A paired two-tailed t-test (A) or a one sample t-test (μ=0) (B) was performed. p values are reported above the comparison. p<0.05 was considered statistically significant.

3.3.2 Exposure of B cells to EBV induces MK2, the ZFP36L1 master regulator.

Because MK2 was previously reported to regulate the expression and phosphorylation of the ZFP36 protein family members to which ZFP36L1 belongs, I used phospho-specific antibodies to detect MAPK p38 activation, together with its downstream target MK2 (Fig. 3.9A) (421, 427–429). This assay confirmed the activation of MAPK p38 and MK2 upon infection (Fig. 3.9B). The accumulation of phosphorylated p38 was not paralleled by an increase in total p38
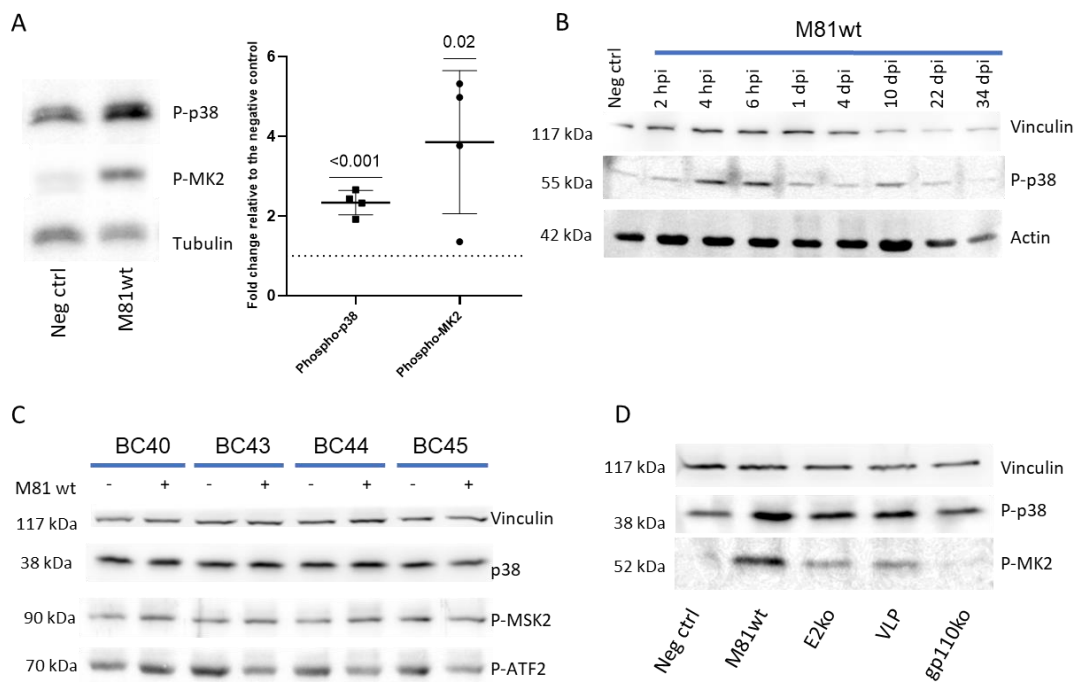
Figure 3.9: EBV infection induces p38-MK2 activation. (A) EBV M81wt infected B cells at 6 hours post infection were analysed for their levels of p38 and MK2 activation using immunoblotting for phosphorylated p38 (Thr180/Tyr182) and phosphorylated MK2 (Thr334), respectively. An example of a blot is shown (left panel). The intensity of the signal of the bands was quantified via ImageJ and normalized over the loading control. The fold change is calculated versus the uninfected control (n=4 independent biological replicates). Single values are plotted, and the mean ± SD is shown (right panel). A one sample t-test (μ=1) was performed. p values are reported above the comparison. p<0.05 was considered statistically significant. (B) p38 activation was detected in M81wt infected primary B cells at different time points after infection. (C) Total p38 levels, as well as MSK2 and ATF2 activation status (Ser196 for MSK2 and Thr71 for ATF2) were assessed in B cells at 6 hours post infection with M81wt virus in 4 independent biological replicates. (D) p38 and MK2 activation was detected via immunoblotting in human primary B cells at 6 hours post infection with M81wt virus, EBNA2 knockout, M81 VLPs or gp110 knockout. Phospho-p38 and phospho-MK2 were detected, and vinculin was used as loading control. Vinculin was used as loading control (B-D).

and did not result in the activation of other downstream branches of the p38 pathway such as MSK2 or ATF2 (Fig. 3.9C). While p38 activation and ZFP36L1 expression showed a simultaneous increase two hours after infection, phospho-p38 already went back to baseline levels after one day (Fig. 3.9B). Exposure of primary B cells to EBV VLPs or M81/ΔEBNA2 also led to the induction of p38 and MK2, although it could not reach levels seen after wild type infection, particularly for the latter kinase (Fig. 3.9D). Infection with the gp110 null mutant did not activate the p38/MK2 pathway at all (Fig. 3.9D).

I also assessed two other major MAPK pathways, PI3K-AKT and ERK1/2, and did not observe any significant changes in their phosphorylation status (Fig. 3.10A). Since NF-κB was previously reported to be activated after early EBV infection events, I investigated the activation status of its canonical branch (430, 431). Phospho-p65 and IκBa expression was already observed in resting B cells and did not consistently increase upon infection (Fig. 3.10B).
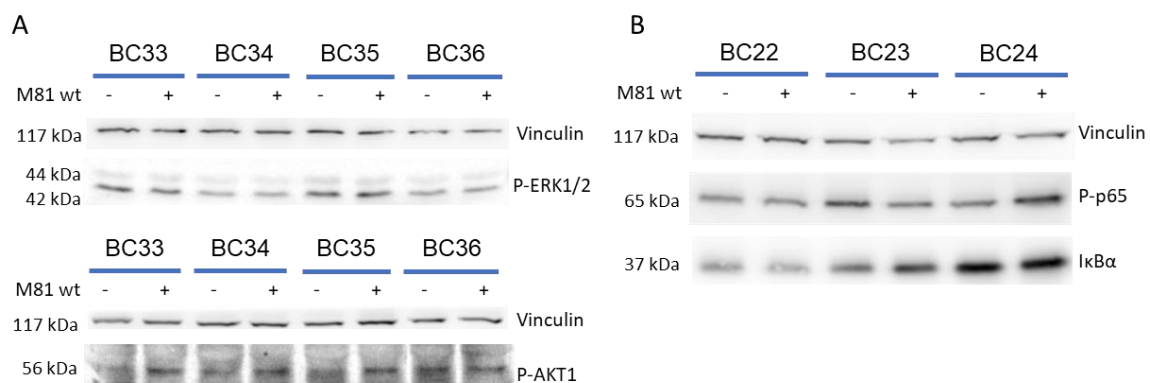
Figure 3.10: EBV does not induce ERK1/2 or NF-κB. (A) ERK1/2 and AKT activation status was measured by western blot at 6 hours post infection with M81wt virus in 4 independent replicates by detection of phospho-ERK Thr202/Tyr204 and of phospho-AKT1 Ser473. (B) Phospho-p65 and total IκBα levels were investigated in 3 independent donors at 6 hours post infection with M81wt virus. Vinculin was used as loading control.

3.3.3 Several pathways regulate ZFP36L1 induction.

I then tested whether other kinases could be involved in the activation of the p38-MK2 axis and, consequently, of ZFP36L1 induction. For this purpose, a panel of selective inhibitors against SYK, LYN, BTK, PI3K, PKA, NF-κB, PKC, and STAT3 was tested. Inhibitors targeting SYK, LYN, BTK, PI3K, PKA, NF-κB and PKC did not have any effect on p38 or pMK2 expression (Fig. 3.11A & Fig. 3.11B). Interestingly, exposure to a STAT3 inhibitor

increased pMK2 and pp38 levels, a phenomenon previously observed by Guha and colleagues which indicates a possible interplay between these two pathways (432). The impact of this panel of inhibitors on ZFP36L1 was broader, with the LYN, SYK, BTK and STAT3 inhibitors
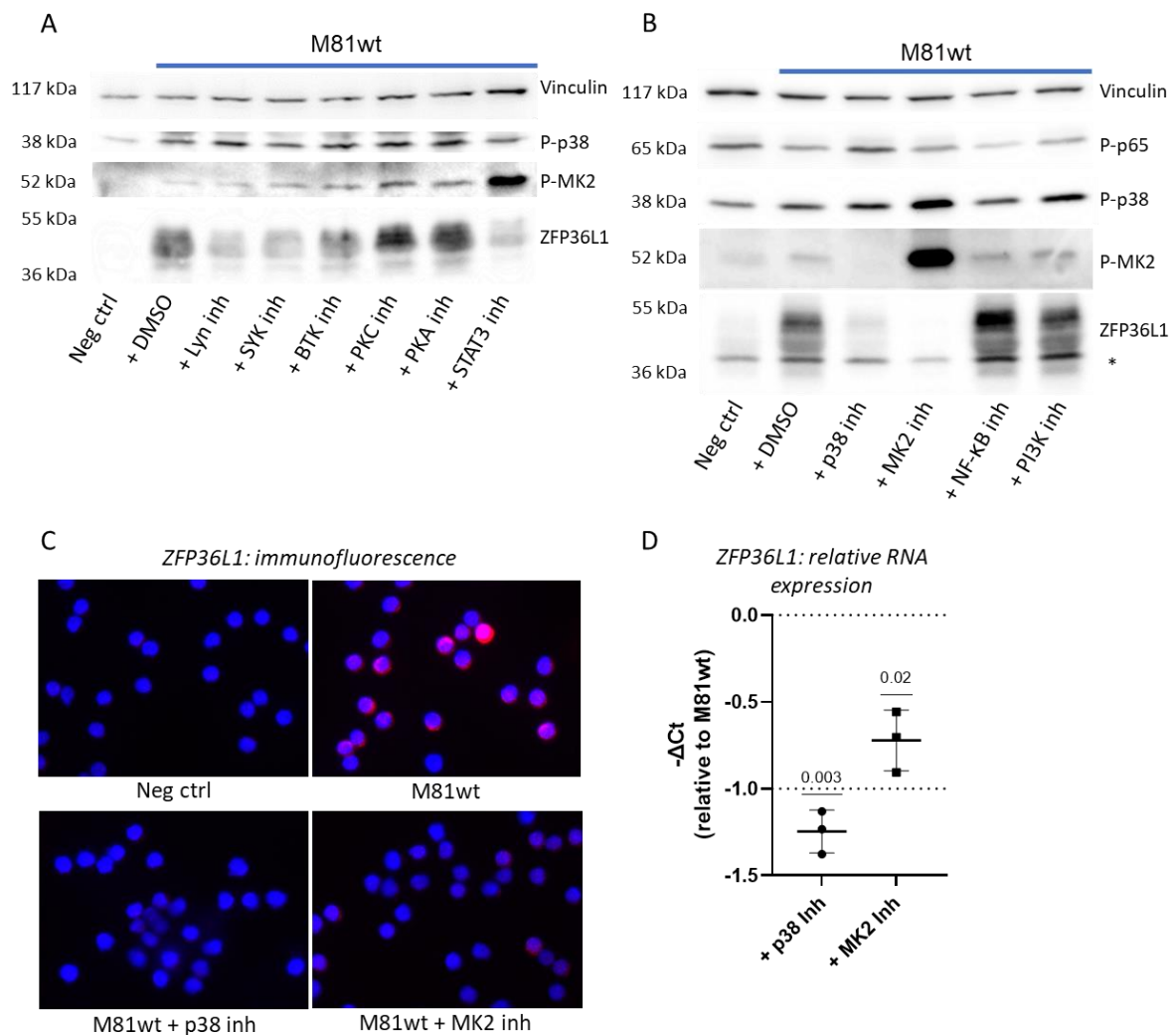
Figure 3.11: ZFP36L1 induction is dependent on the activation of p38/MK2. (A) Anti-phospho p38 and anti-phospho MK2, together with an anti-ZFP36L1 antibody, were used to stain primary B cells infected with M81wt virus in the presence of inhibitors of the downstream mediators of the BCR signaling cascade. (B) Western blot analysis of p38/MK2 and NF-κB activation levels, and ZFP36L1 expression in human primary B cells infected with M81wt virus and treated with p38, MK2, NF-κB and PI3K pathway inhibitors. (C) Immunofluorescence staining for the detection of ZFP36L1 in human primary B cells infected with M81wt virus in the presence of p38 or MK2 inhibitors at 6 hours post infection. ZFP36L1 signal is shown in red, while nuclei are counterstained with DAPI (blue). (D) ZFP36L1 mRNA expression was evaluated by RT-qPCR in B cells infected for 6 hours with M81wt in presence or not of the p38 or MK2 inhibitors. The difference between the Ct value of the target in the treated sample and in the untreated control for each independent replicate is shown, and the mean ± SD is reported. (A-B) Each blot is representative of at least 3 biological replicates (n=3). * indicates phospho-p38.

leading to a significant decrease in ZFP36L1 abundance. As expected, the MK2 and p38 inhibitors markedly reduced ZFP36L1 transcription, protein expression, as well as phosphorylation (Fig. 3.11B-D). This confirms the importance of the p38 pathway in controlling ZFP36L1 expression levels, but also shows that other kinases modulate its abundance and phosphorylation pattern.

3.4 IL-6 and TNFα are induced by a multistep mechanism which is controlled by several pathways.

3.4.1 EBV infection leads to a two-step activation of IL-6 and TNFα.

The results on the early stages of infection gathered so far showed an induction of MK2, ZFP36L1 and STAT3 within two hours, three pathways involved in the control of the inflammatory response. The ZFP family members bind to RNAs carrying an AU rich stretch in their 3'UTR and inactivate them through a combination of decapping and deadenylation (352). In particular, TNFα and IL-6 mRNAs have been shown to be regulated by these proteins (380, 433, 434). This is particularly interesting as both cytokines have been reported to be released upon virus binding to its target B cells (435, 436). Therefore, I closely monitored the ability of infected B cells to secrete both cytokines shortly after infection. Infected cells were seeded at the same concentration and cultured for 6 hours at each time point before ELISA quantification was performed on the conditioned medium. The secretion ability for IL-6 peaked within the first day after infection, with a 5-fold increase, and then decreased back to baseline. TNFα secretion ability was instead highest at the last time point considered (96 hpi), although was already significantly increased in the first 6 hours post infection, at which point a 2-fold increase compared to the baseline was observed (Fig. 3.12A). Interestingly, the cytokine release observed after EBV infection of primary CD19+ B cells could be further increased upon induction with TPA, LPS or anti-BCR antibodies (Fig. 3.12B). Investigation of a panel of 14 independent primary B cell samples infected with EBV showed that although the infection always led to an increase in IL-6 and TNFα release, the recorded levels varied more 20-fold (from 20 to 450 pg/mL) for the former and 8-fold for the latter (10 to 80 pg/mL, suggesting the role of genetic polymorphisms governing the intensity of the response to the virus (Fig. 3.12C). I then looked at the transcriptional activation of IL-6 and TNFα and found that both transcripts tripled in numbers within 2 hours after the infection, but went back to baseline levels within 6

hours (Fig. 3.12D). While IL-6 transcripts further diminished in abundance after 24 hours, TNFα transcripts increased again in abundance at that time point. ZFP36L1 transcripts evolved exactly in the opposite direction, increasing when TNFα transcripts decreased and vice versa.
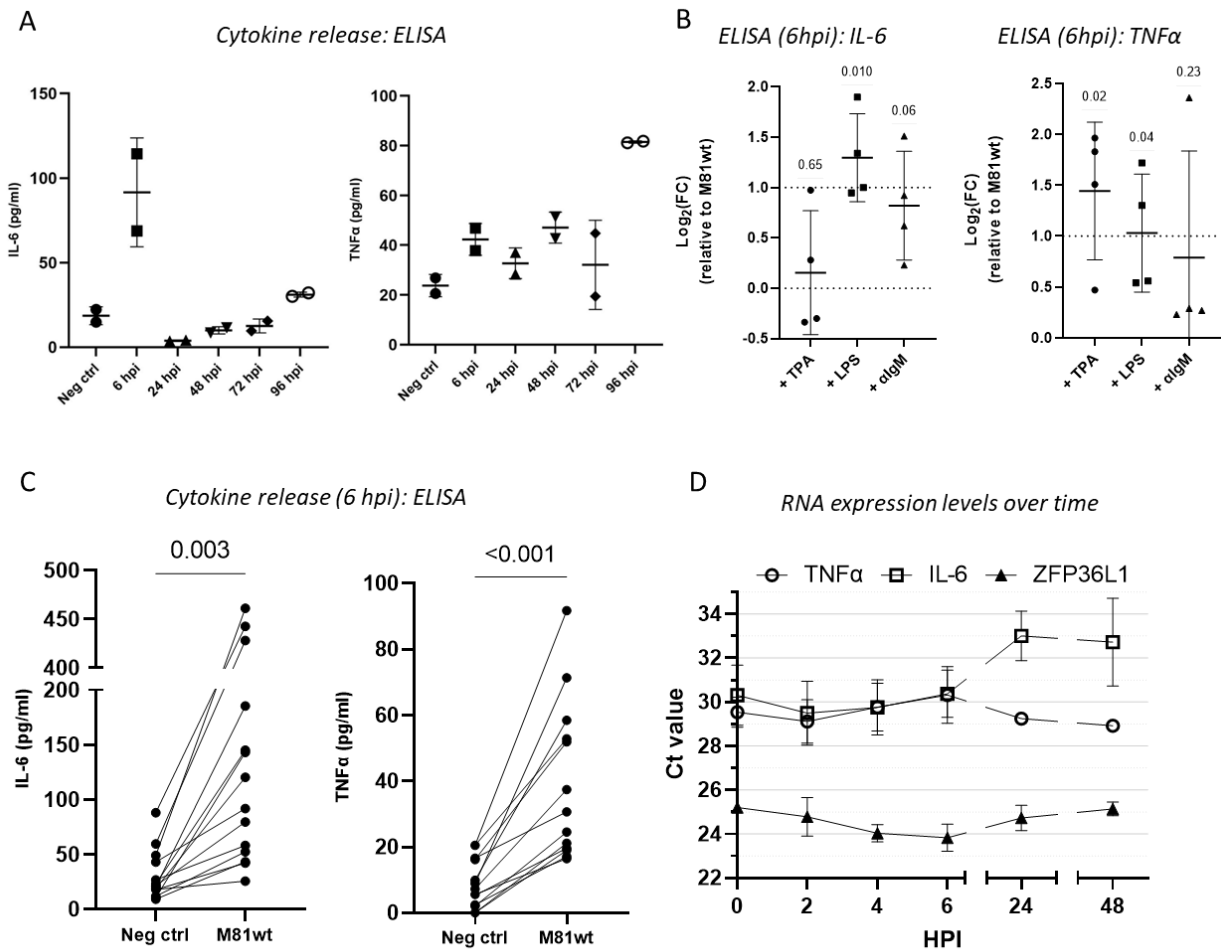
Figure 3.12: EBV infection induces IL-6 and TNFα secretion. (A) IL-6 and TNFα secretion by primary human CD19+ B cells infected with M81wt virus. At each time point cells were seeded at the same cell concentration and incubated for 6 hours. The release of the two cytokines was measured by ELISA. Single values were plotted and the mean ± SD is shown (n=2 independent biological replicates). (B) Quantification of IL-6 and TNFα secretion by ELISA in M81wt infected B cells at 6 hours post infection untreated or treated with TPA, LPS or crosslinked with IgM (n=4 independent biological replicates). The Log2(Fold change) is calculated relative to the untreated M81wt infected B cells. A one sample t test (μ=0) was performed. p values are reported above the comparison. p<0.05 was considered statistically significant. (C) ELISA quantification of IL-6 and TNFα secretion at 6 hours upon infection with M81wt virus in 14 independent donors. Single values are reported. A great variability is observed among different healthy donors. A paired two-tailed t-test was performed. p values are reported above the comparison. p<0.05 was considered statistically significant. (D) IL-6, TNFα, and ZFP36L1 mRNA expression as quantified by reverse transcription quantitative PCR at different time points upon infection with M81wt virus. Ct values are reported as the mean ± SD (n=3 independent biological replicates).

I then repeated the cytokine induction experiment with B cells infected by M81/ΔEBNA2, EBV VLPs or with the M81/Δgp110 virus. Quantification of cytokine release showed that exposure to EBV VLPs or with the M81/Δgp110 virus doubled on average cytokine release relative to uninfected cells, but remained three times lower than after wild type infection. Exposure of B cells to M81/ΔEBNA2 resulted in intermediate cytokine release levels, reaching 50% of wild type levels (Fig. 3.13A). Analysis of cytokine transcript levels showed a similar pattern, with EBV VLPs or M81/Δgp110 infection giving rise to a lower expression than wild type infection and infection with M81/ΔEBNA2 delivering intermediate results (Fig. 3.13B and 3.8B for comparison with ZFP36L1 expression). From these results it can be concluded that virus binding gives rise to a limited IL-6 and TNFα transitory release, and that both the presence of the viral DNA within infectious particles and in particular latent gene expression are required to reach maximal cytokine transcription and release. This suggests that events linked to latency inception further modulate cytokine production.
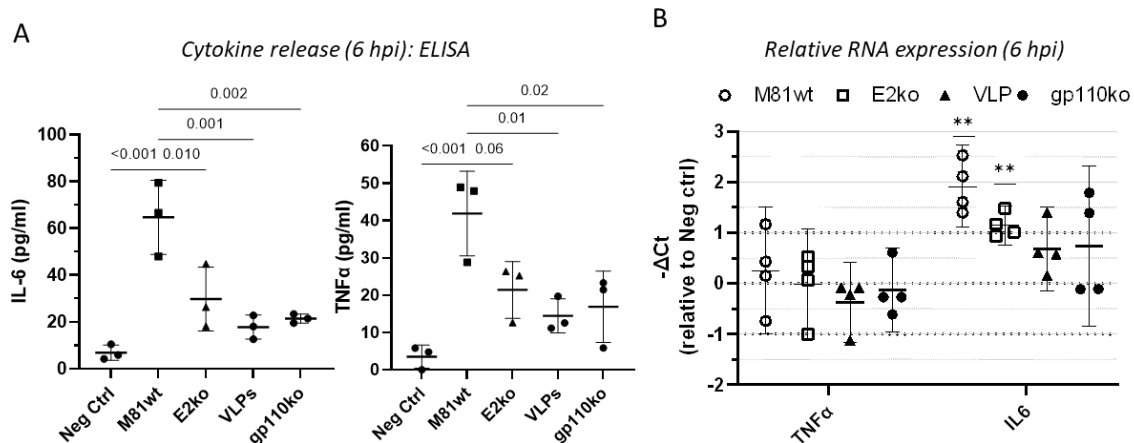
Figure 3.13: Maximal IL-6 and TNFα production requires a successful infection. (A-B) IL-6, TNFα protein secretion and mRNA expression as quantified respectively by ELISA (A) and RT-qPCR (B) at 6 hours post infection with M81wt virus, EBNA2 knockout, M81 VLPs, and gp110 knockout virus. Values obtained from 3 (A) or 4 (B) independent primary samples are reported, together with the mean ± SD. For the mRNA quantification, values are shown as the difference versus the negative control. A paired two-tailed t-test (A) or a one sample t-test ($\mu=0$) (B) was performed. p values are reported above the comparison or indicated with a star notation (**, $p \leq 0.01$). $p<0.05$ was considered statistically significant.

3.4.2 Several pathways control IL-6 and TNFα secretion after infection.

The secretion of pro-inflammatory cytokines like IL-6 and TNFα is controlled by several pathways. In order to assess their contribution, I used a panel of pathway inhibitors and determined their effect in terms of cytokines reduction. When B cells were infected with the

wild-type virus in the presence of inhibitors of BCR-associated kinases, both IL-6 and TNFα were variably affected, with the SYK inhibitor producing the strongest effect (Fig. 3.14A).
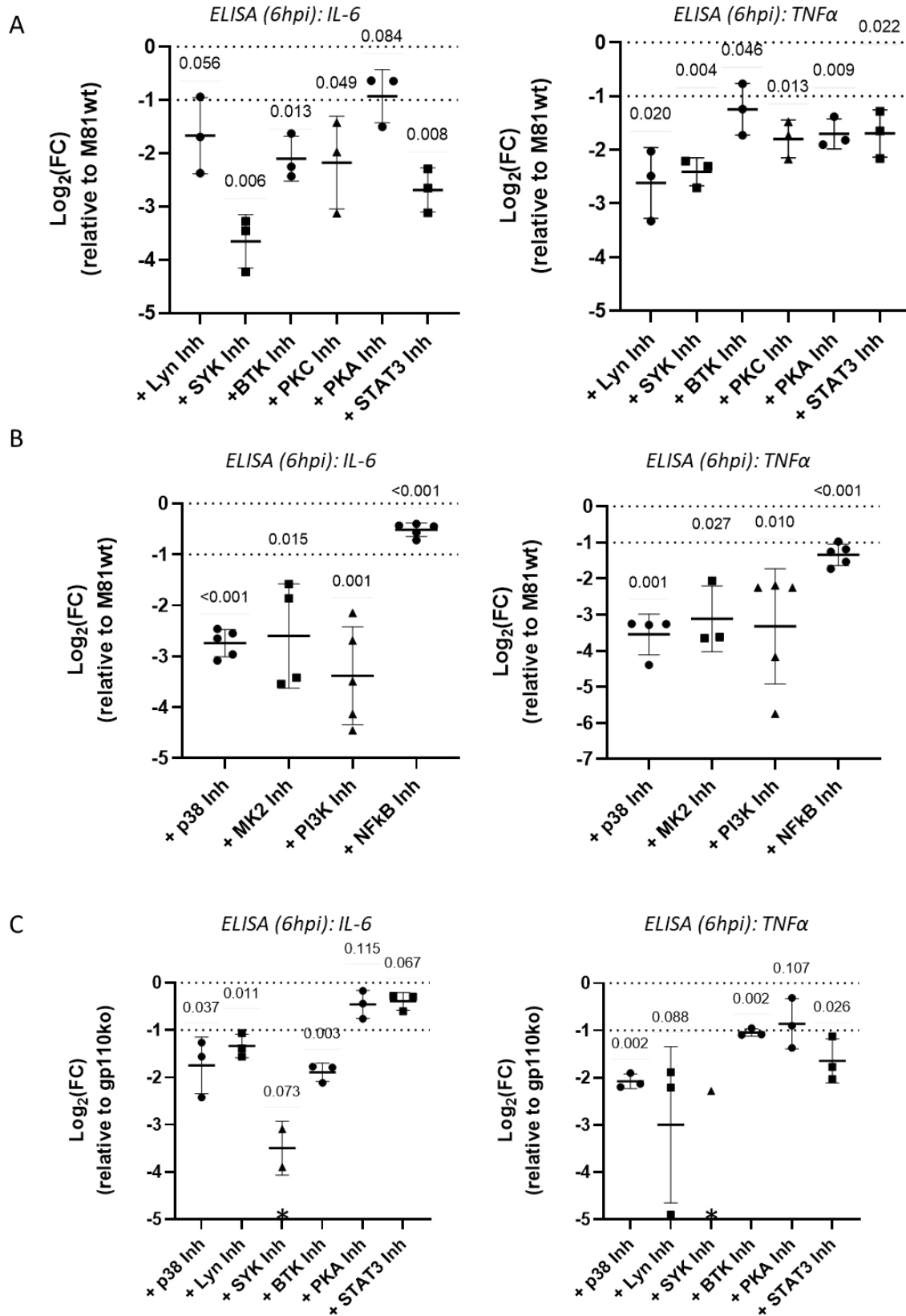
Figure 3.14: Several pathways are involved in the regulation of EBV-induced IL-6 and TNFα secretion. In order to investigate the role that the different pathways have on the secretion of IL-6 and TNFα upon EBV stimulation, IL-6 and TNFα were quantified using ELISA from conditioned medium at 6 hours post infection in primary B cells that were infected with M81wt virus in the presence of (A) BCR signaling inhibitors or (B) p38, MK2, PI3K, or NF-κB inhibitors. (C) The same experiment as in (A) was performed using the gp110 knockout virus to treat the cells. Values are expressed as Log2(Fold change) relative to (A-B) M81wt or (C) gp110 knockout infected cells. 3 (A, C) or 5 (B) independent biological replicates were analysed. A one sample t-test was performed (μ=0). p values are reported above the comparison. p<0.05 was considered statistically significant. An asterisk is used to indicate when samples were below the detection limit and could not be quantified.

Interestingly, the inhibitory effect was different for the two cytokines, pointing towards different regulatory mechanisms. I observed a significant reduction in both IL-6 and TNFα secretion when cells were treated with p38, MK2 and PI3K inhibitors, but only a limited effect was detected by inhibiting NF-κB (Fig. 3.14B). Similar effects on IL-6 and TNFα release were observed when B cells were exposed to M81/Δgp110 in the presence of BCR signaling inhibitors (Fig. 3.14C). In this context, the already low level of cytokine expression occurring upon M81/Δgp110 binding was nearly completely abolished by the SYK inhibition. Altogether, these results show that cytokine release after EBV infection is limited both in time and intensity, with interindividual variations, resulting both from virus binding and latency activation and is controlled by signaling pathways activated by virus infection.

3.5 EBV tegument proteins induce MK2 and ZFP36L1.

Because EBV VLPs can induce p38-MK2 activation and ZFP36L1 transcription and translation in the absence of viral DNA, the most likely explanation was that components of the VLPs are responsible for this effect. I focused my attention on the tegument proteins and to understand their role in this process, I infected B cells with a panel of tegument knockout viruses available in the lab. In the absence of BBLF1 or BGLF2, p38, and to a lesser extent ZFP36L1, failed to be activated upon infection (Fig. 3.15A). B cell infection with the BKRF4 null mutant also reduced p-MK2 levels. Quantification of cytokine release after infection with these defective mutants showed a similar pattern. In the absence of BBLF1, BGLF2 or BKRF4, TNFα and IL-6 release were markedly reduced (Fig. 3.15B). Unexpectedly, infection with the ΔBNRF1 deletion mutant gave rise to cytokine release levels comparable to or even higher than after infection with wild type EBV (Fig. 3.15B).
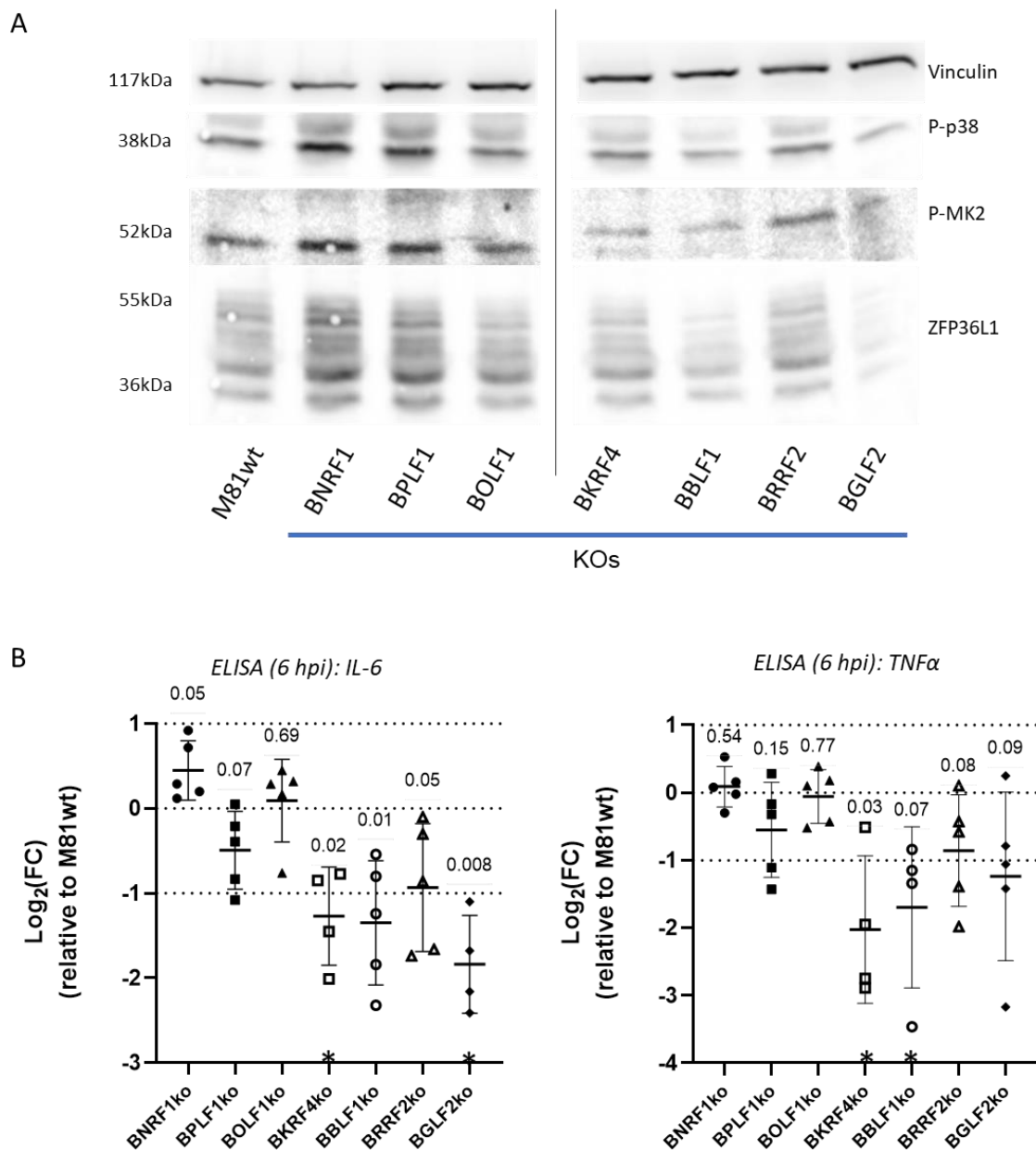
Figure 3.15: EBV tegument proteins induce p38/MK2 activation and ZFP36L1 expression. (A) Primary CD19+ B cells were infected for 6 hours with different tegument protein knockouts and immunoblotted to detect p38 and MK2 activation and ZFP36L1 expression. Vinculin was used as a loading control. n=5 independent biological replicates. (B) The conditioned medium from (A) was used to quantify via ELISA the secretion of IL-6 and TNFα. Values are expressed as Log2(Fold change) relative to M81wt infected cell. The value for each single replicate is shown and the mean ± SD is reported (n=5 independent biological replicates). An asterisk is used to indicate when samples were below the detection limit and could not be quantified. Statistical analysis was performed using a one sample t-test ($\mu=0$). p values are reported above the comparison. $p<0.05$ was considered statistically significant.

3.6 STAT3 and p38/MK2 signaling allow early latent gene expression.

In the last part of my work, I set out to elucidate the role played by the different signaling pathways activated during the early stages of the EBV infection. To this end, I treated B cells exposed to wild type virus with an extended panel of inhibitors and assessed EBV infection by detection of the viral protein EBNA2 at 3 days post infection (Fig. 3.16A) or, in the case of the STAT3 inhibitor Stattic, at 20 hours post infection (Fig. 3.16B). Indeed, Stattic is highly toxic for eukaryotic cells and its effect can only be evaluated for a short period of time. The strongest reduction in the number of EBNA2 positive cells was observed when the infection was performed in presence of the p38-MK2 axis or the STAT3 inhibitors. Inhibition of the BCR signaling complex also resulted in a moderate reduction of latently infected B cells.
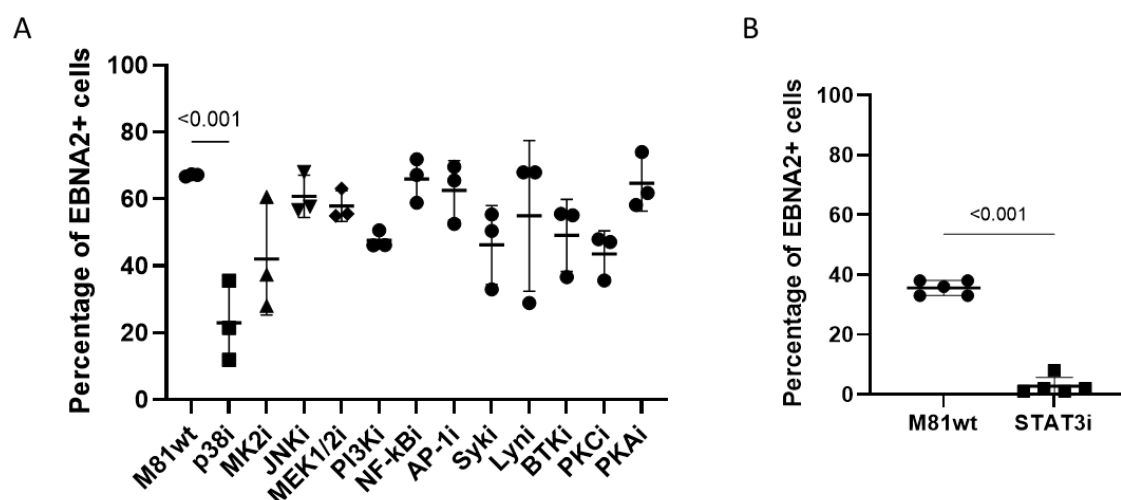
Figure 3.16: p38-MK2 and STAT3 activation are required for latency establishment. (A-B) The role played by several signaling pathways in the establishment of EBV infection was evaluated using selective pathway inhibitors. EBNA2 immunofluorescence staining was performed at 3 days post infection (A) or at 20 hours post infection (B). The percentage of EBNA2 positive cells is reported, with each single replicate being shown, as well as the mean ± SD. 3 (A) or 5 (B) independent biological replicates were analysed. Statistical analysis was performed using a paired two-tailed t-test. p values are reported above the comparison. p<0.05 was considered statistically significant.

Since a reduction in EBNA2 positive cells could be the result of either a reduced transfer of EBV viral genomes to the host nucleus or a reduction in the expression levels of viral genes, I performed fluorescent *in situ* hybridization (FISH) with a probe specific to the viral genome (Fig. 3.17A). This assay showed that inhibition of the p38 pathway, but not of STAT3, led to a 30% reduction in the efficiency of episome transfer to the nucleus. When I performed a

similar analysis using B cells exposed to ΔBGLF2 knockout, I obtained an even stronger effect with a 90% reduction in cells carrying the viral genome, suggesting that the functions of this tegument protein extend further than just p38 activation (Fig. 3.17B). Indeed, recent work has for example shown that BGLF2 has a profound effect on miRNA expression (437).
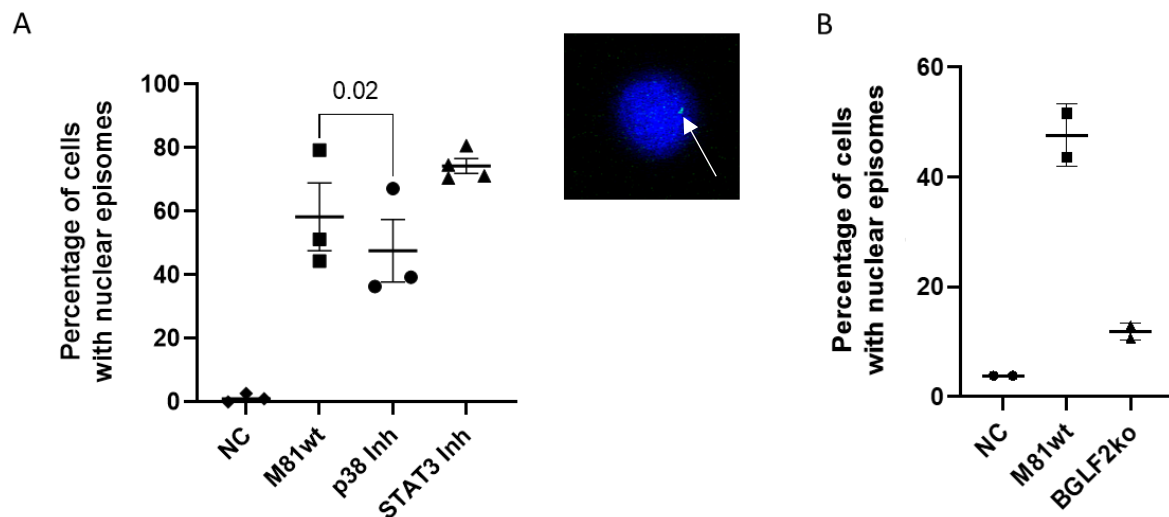
Figure 3.17: p38-MK2 activation allows viral DNA transport. (A-B) Fluorescent *in situ* hybridization (FISH) was used to detect EBV episomal DNA in freshly M81wt-infected CD19+ B cells in the presence or absence of the p38 inhibitor or of the STAT3 inhibitor (A) or in BGLF2 knockout infected cells (B) (3 hours post infection). The percentage of cells showing nuclear episomes is reported, with each single replicate being shown, as well as the mean ± SD. (A) 3 (p38 inhibitor-treated), 5 (STAT3 inhibitor-treated) or (B) 2 (BGLF2 knockout) independent biological replicates were analysed. An exemplificative image of an EBV nuclear episome is shown (center). The EBV episomal DNA is shown in green (arrow), while the nucleus was counterstained with DAPI (blue). (A) Statistical analysis was performed using a paired two-tailed t-test. p values are reported above the comparison. $p < 0.05$ was considered statistically significant.

Since the inhibition of the p38-MK2 axis only mildly affected the nuclear transfer of EBV genomes, while STAT3 inhibition did not affect it at all, I looked at the expression levels of early latency genes, EBNA2 and genes expressed from the Wp promoter, which are expressed shortly after infection and whose expression is the first step in the establishment of latency (Fig. 3.18A and B). I found that blocking p38 or MK2 activation resulted in a strong reduction in the expression of both EBNA2 and Wp promoter-driven transcripts. This effect was stronger for p38 inhibition than for MK2 inhibition, suggesting a possible broader activation of the p38

signaling cascade than the sole engagement of the MK2 branch. The reduction in transcription from the Cp/Wp promoter and EBNA2 transcription was even stronger for STAT3 inhibition.
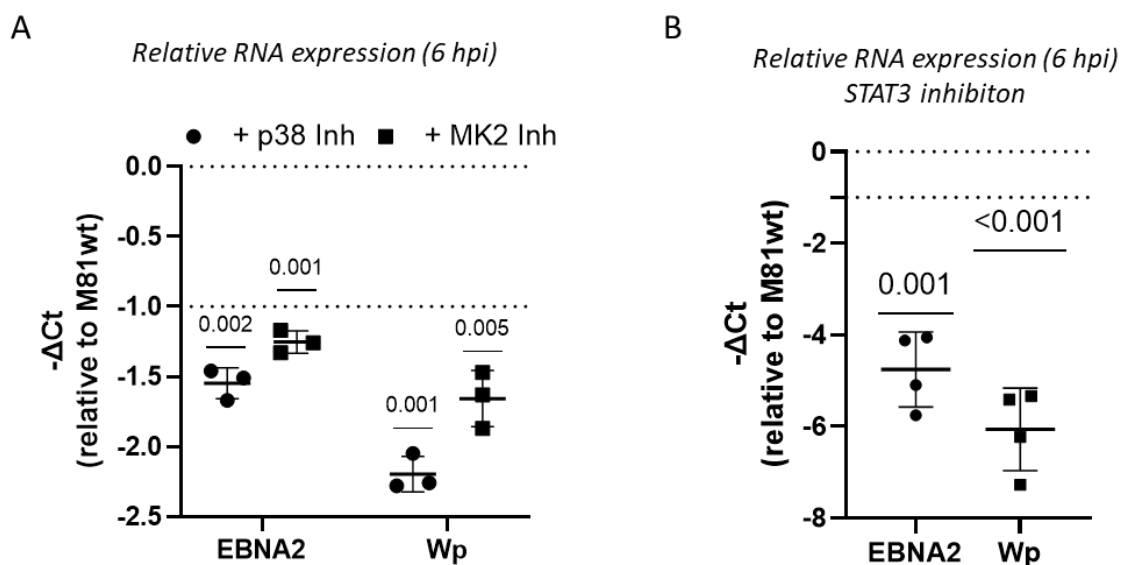
Figure 3.18: p38-MK2 and STAT3 activation are involved in early latent gene expression. mRNA expression levels for EBNA2 and Wp promoter-originated transcripts were quantified via RT-qPCR in CD19+ B cells exposed to M81wt virus in the presence of either the p38 inhibitor, the MK2 inhibitor (A), and STAT3 inhibitor (B) at 6 hours post infection. The difference between the Ct value of the treated sample and the untreated is reported for each replicate, and the mean ± SD is also shown (n=3 independent biological replicates). (A, B) Statistical analysis was performed using a one sample t-test ($\mu=0$). p values are reported above the comparison. $p<0.05$ was considered statistically significant.

4. Discussion

4.1 The role of STAT3 and p38-MK2 activation

Epstein-Barr virus infects B cells and establishes a life-long latent infection which has been extensively studied due to its oncogenic potential. However, the very early stages of infection during which the virus overcomes and controls the host's innate immune response, as well as rewiring the cell's internal circuits, are still largely uncharacterized. By combining mass spectrometry analysis with a panel of knockouts in which the infection process is stopped at different stages, I was able to identify two pivotal events which are essential for viral infection, the activation of STAT3 and of the p38-MK2-ZFP36L1 axis. By activating these two pathways, EBV virus particles were able to facilitate the establishment of latency and limit, both in time and intensity, cytokine release.

The involvement of STAT3 and of p38-MK2 in regulating early latent gene transcription is of particular interest. Alpha- and Betaherpesviruses have long been known to package transactivators such as VP16 and pp71 in their tegument to directly activate transcription of viral Immediate Early (IE) genes upon release, but this direct mechanism has apparently not been conserved for EBV (438, 439). Although BNRF1 shares the ability of VP16 to disrupt the ATRX-Daxx interaction and BPLF1 is a sequence homolog of pp71, I did not find any evidence that these two EBV proteins directly activate viral transcription (18, 440). Additionally, when the EBV M81 wild-type genome was investigated for STAT3 binding sites, two were identified directly upstream of the main exon of EBNA2 (nucleotide 35265 to 35275 (TTTTTGGGAAT) and 36200-36210 (CTACCAGGAAC)), suggesting a possible role of STAT3 in directly regulating EBNA2 transcription.
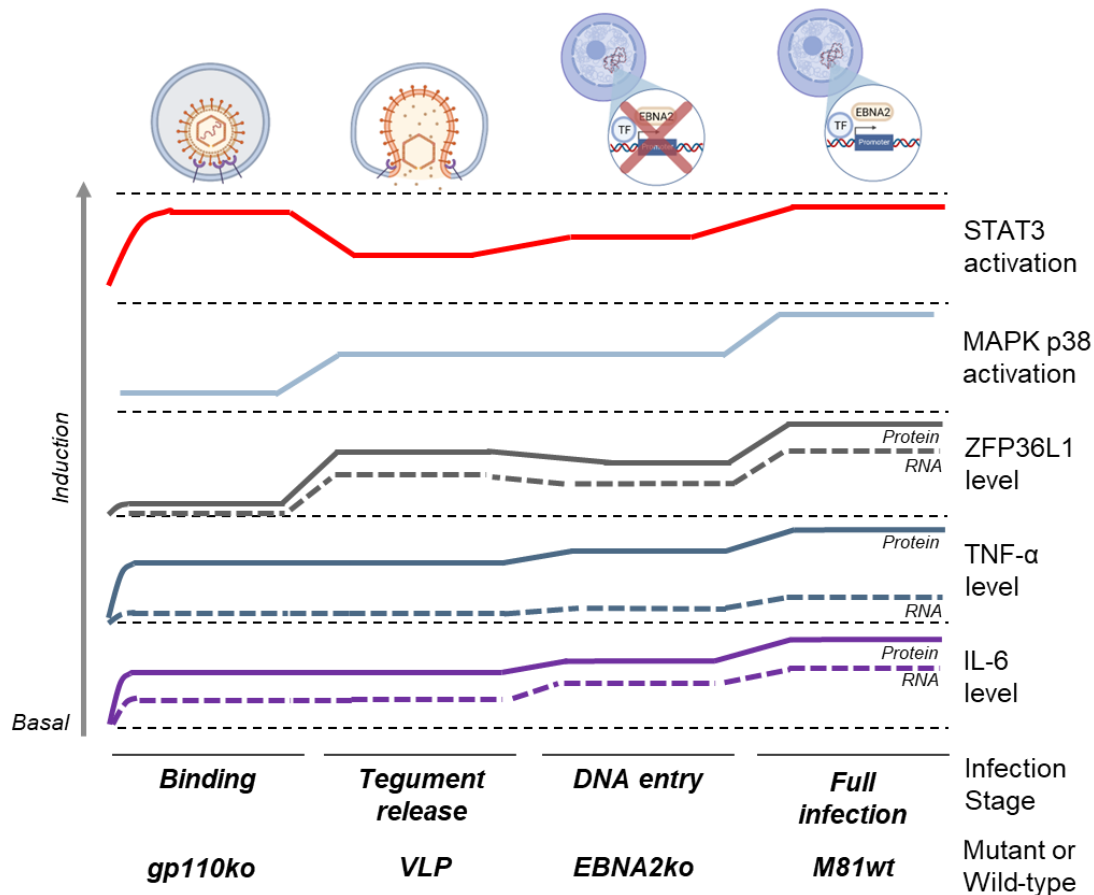
Figure 4.1: Graphical summary of the results. The induction levels for each of the target investigated is shown relatively to the recombinant virus used and, therefore, to the infection stage at which the infection is blocked. Created with Biorender.com.

4.2 EBV controls IL6 and TNFα secretion

The STAT3 and p38-MK2 pathways typically induce an inflammatory response, especially in immune cells, with potentially negative consequences for the virus (275, 296, 441). Indeed, in EBV-infected B cells, STAT3 and p38 inactivation by selective inhibitors dampened cytokine release. However, STAT3 and p38 induced the simultaneous expression and phosphorylation of ZFP36L1, an RNA binding protein that negatively regulates cytokine transcription and is likely responsible for the time-limited cytokine release that takes place in the first hours of infection. More generally, quantification of TNFα and IL-6 release showed that this process is inefficient and could be additionally boosted by further stimulating the B cells with other stimuli such as TPA or LPS.

With my results, I could show that the observed cytokine release is regulated via a two-step mechanism. Virus binding itself led to a limited cytokine release as has been reported before, although no effect on cytokine transcription was identified (431). Tegument release or nuclear transfer of viral DNA had limited to no additional effect in terms of both cytokine transcription and release. Only latent gene expression induction was able to significantly boost both IL-6 and TNFα, although this event was limited at the very early hours post infection. Indeed, this early induction was followed by a significant reduction in terms of transcript levels within the first 24 hours post infection, suggesting that cytokine release is actively repressed in infected cells. Given the previously described function of ZFP36L1, whose expression both at the mRNA level and at the protein level significantly increases shortly after infection, a pattern exactly opposite to those of the cytokines, it can be suggested that ZFP36L1 plays a significant role in this process. The evidence obtained with my work, therefore, suggests the hypothesis that EBV particles can promote the activation of latent gene expression with a limited cost in terms of the immune response. However, it is important to note that in a few individuals, the infection was followed by much higher levels of cytokine release. This suggests that genetic factors condition the cytokine response against EBV infection. These polymorphisms might have potential clinical consequences, for example in the case of infectious mononucleosis during which intense cytokine release is observed (164).

4.3 BCR signaling regulates STAT3 activation

In order to better define the precise molecular mechanism responsible for STAT3 activation, I combined the usage of several tegument knockouts with treating the cells with selective pathway inhibitors. Using this approach, I was able to identify that STAT3 phosphorylation was an event which occurred after virus binding independently of virus fusion. I could not detect any difference in the level of activation of STAT3 compared to the wild-type when different knockout variants lacking each a glycoprotein involved in secondary binding to B cell and activation of the fusion machinery was used, suggesting that the event was directly mediated by gp350 itself interacting with CD21 or CD35. For this reason, selective pathway inhibitors targeting the B cell receptor signaling immediate downstream mediators were used, and I was able to show that STAT3 phosphorylation was modulated by intracytoplasmic kinases, in particular SYK. SYK was previously shown to phosphorylate STAT3 at Y705 in response to oxidative stress in acute lymphoblastic leukemia cells or following activation of

the signaling cascade induced by Mac-1 or FcγRI in acute myeloid leukemia (191–193). I then investigated whether tegument proteins contained in the virion could play a role in STAT3 Y705 phosphorylation. Unexpectedly, tegument proteins such as BKRF4 and BGLF2 were also necessary to maintain full STAT3 induction after infection with wild type EBV. It is possible that this effect results from the stimulating effects of these tegument proteins on p38/MK2 which itself potentiates STAT3 activation (442, 443). It is well documented in the literature that established LCLs express high STAT3 levels under the influence of LMP1. STAT3 activation has also been proposed to allow infected B cells to progress through the cell cycle at the early stages of transformation by altering the ATR-mediated DNA damage response (260, 262, 263). Koganti and colleagues (260) previously showed that pSTAT3 705 is expressed shortly after EBV infection and protected cells from undergoing apoptosis. My work recognizes new functions for STAT3 early after infection and identifies virus binding as its activating cue.

4.4 Activation of the p38-MK2 signaling cascade

The use of DNA-free EBV VLPs allowed me to identify the p38-MK2 pathway as another target of the infectious particle, although latent gene expression was required to obtain full activation of this pathway. Thanks to the panel of tegument knockouts I was able to identify that the tegument proteins BKRF4, BBLF1, BPLF1 and BGLF2 were necessary for p38-MK2 activation, as well as STAT3 activation as described before. The details of the molecular interactions between these cellular and viral proteins remain to be determined, but it is noteworthy that a link between p38 and BGLF2 has already been identified during viral lytic replication (271, 418, 444). My observations suggest that this interaction is also important in the initial phase of virus-cell interactions. Because BBLF1 acts as a chaperone for BGLF2 (16), and BPLF1 acts as a platform for many tegument proteins, it is likely that the deficits in p38 induction observed in their absence are due to their action on BGLF2. Although BOLF1, another tegument protein, was speculated to interact indirectly with BGLF2 via BKRF4, I found here that a BOLF1 null virus fully activated p38 and ZFP36L1 (445).

4.5 EBV infection induces ZFP36L1

Another important consequence of virus entry was the expression and phosphorylation of ZFP36L1. Using MK2 and p38 inhibitors, I found that the p38-MK2 axis is essential for ZFP36L1 induction. This observation is in line with previous work showing that MK2 both activates ZFP36 family proteins transcription and phosphorylates the resulting ZFP36L1 proteins (427–429). Although there were signs of both p38 and ZFP36L1 activation such as the presence of phospho-events and a minimal induction already after virus binding, the intensity of activation was minimal in comparison to downstream events such as virus entry and latent protein production. ZFP36L1 can be phosphorylated at multiple sites that can be either activating (424) or inactivating (420, 421, 446). ZFP36L1 phosphorylation allows direct interaction with the chaperone 14-3-3 and thereby its stabilization. However, these events also inactivate the ability of the protein to promote the degradation of its RNA targets. The observation that expression of ZFP36L1 is followed by a reduction in the abundance of IL-6 and TNFα transcripts, two well characterized targets of the ZFP36 family of proteins, suggests that ZFP36L1 is, at least initially, active and responsible for the sharp decrease in cytokine expression one day after infection. Although MK2 is considered the main regulator of ZFP36L1 phosphorylation, other kinases such as PKA (424), PKB (420, 446) have been shown to target this RNA binding protein. In addition to these described regulators, I also found here that LYN, BTK and STAT3 can directly or indirectly influence the ZFP36L1 phosphorylation status.

Modulation of the p38-MK2-ZFP36L1 pathway has been previously reported after infection with other members of the *Herpesviridae* family. However, these events occurred in already infected cells and were thus independently of the virion (326, 327). For example, infection with the gammaherpesvirus Kaposi Sarcoma Herpesvirus (KSHV) induces the p38-MK2 pathway via expression of the Kaposin B protein (333). Phosphorylated MK2 is responsible for the activation of the MK2-HSP27-p115RhoGEF-RhoA signaling axis which, in turn, results in the disruption of the P-body network, a set of cytoplasmic hubs involved in the processing of mRNA targeted for degradation (334, 447). In contrast to EBV, KSHV-infected cells produce large amounts of cytokines that are beneficial to cell growth. Because of this positive effect on the infected cells, KSHV does not need to block the cytokine release following MK2 activation (448). Another member of the *Herpesviridae* family to control the p38-MK2-ZFP36L1

pathway is MCMV. In contrast to EBV infection, MCMV infection leads to an activation of MK2 to which follows the repression of ZFP36 function. In this case, MCMV blocks ZFP36 activity in order to maintain high levels of IL-10 transcription and secretion, despite MK2 being associated with an increased secretion also of antiviral cytokines. However, the presence of high levels of IL-10, which is secreted by the infected macrophages and hepatocytes, allows the virus to dampen a T cell response against infected cells (402).

4.6 NF-κB is not activated immediately after infection

Early studies performed using either recombinant soluble gp350 or wild-type EBV showed IL-6 secretion upon binding which was explained by the activation of the NF-κB p65/p50 transcriptional factors and of NF-IL-6 (431). However, in my experimental model, I could not identify an increase in the level of phosphorylated p65. The results obtained using the selective inhibitor PS-1145 clearly showed a very limited effect on IL-6 and TNFα secretion. Furthermore, more recent lines of evidence have identified the tegument proteins BPLF1 and BGLF2 as active repressors of NF-κB, interfering with its activation both during virus production but also during the early phases of infection (449, 450). This supports the idea that NF-κB activation is tightly regulated by the incoming virus shortly after infection to prevent the mounting of a significant immune response, and it is later modulated via LMP1.

4.7 Limitations of the study

This study used high-throughput approaches, proteomics and phosphoproteomics, to identify targets significantly modulated by EBV upon infection. These techniques present intrinsic limitations in the type of proteins detected (e.g. protein size, protein localization), as well as variability in between sample runs, due to sample preparation techniques and instrument detection ability (451). In addition, protein sample preparation for the phosphoproteomic analysis required the pooling of many donors in order to have the required amount of material for phosphopeptide enrichment, introducing variability between the biological replicates. These limitations affected the number of statistically significant events identified and, therefore, the ability of the analysis to provide a clear picture of the modifications induced by EBV infection. In addition, most of the events identified in the phosphoproteomic analysis do

not have a well-defined effect in terms of biological function, limiting the significance of bioinformatic approaches for data mining (i.e. pathway enrichment analysis).

Another limiting aspect of my work was the lack of a suitable technical approach to genetically engineer primary B cells to perform functional studies on the identified proteins of interest. In recent years a few publications described techniques to induce the expression of exogenous sequences or to generate knockouts in human primary B cells by electroporation of CRISPR-Cas9 ribonucleoprotein complexes (452, 453). However, these systems rely on concomitant B cell activation by a mixture of cytokines or infection with EBV, making them ill-suited for investigating the role played by the target protein during the early stages of infection.

4.8 Future directions

Several open questions remain to be investigated to fully understand the biological processes occurring shortly after EBV infection. The role played by both p38-MK2 and STAT3 in regulating the transcription of latency genes I uncovered will require a more extensive evaluation of the role played by different cellular transcriptional factors in the expression of early latency genes (83, 454–456). In particular, although not confirmed, the bioinformatic identification of STAT3 binding sites in proximity to the only exon coding for EBNA2 represents another hint for possible direct involvement of STAT3 in the process. On the other hand, p38 role in the transcriptional regulation of Wp-originated transcripts most likely relies on the effect it has on downstream mediators, including transcription factors. Interestingly, p38 effect on transcription initiation might not be restricted to the activation of transcription factors, but, considering the results from the FISH analysis, could extend to the regulation of the cytoskeleton or of the molecular machinery responsible for delivering the viral capsid to the nucleus. For this reason, further investigating the role played by p38 could shed new light on how the viral genome is delivered to the nucleus.

Another aspect which requires additional study is the role played by IL-6 and TNFα. As previously discussed, the expression of these two cytokines is suppressed a few hours post infection but follows different kinetics at later stages. Why is TNFα expression increasing after 24 hours post infection? One possible explanation is that TNFα has an autocrine and/or paracrine effect, promoting an overall effect which is beneficial for the survival and growth of the infected cell. For this reason, investigating the effect of these cytokines either by

supplementing or depleting them during the early phases of infection, both in the context of a pure B cell population or in the presence of other subtypes of immune cells, could provide a better insight into why EBV differently regulates them.

As previously mentioned, IL-6 and TNFα showed great variability between donors, with possible clinical relevance. Indeed, not only EBV is responsible for the development of infectious mononucleosis in a fraction of infected individuals, but several autoimmune conditions have been proposed to be linked to EBV infection (4). One recent publication by Bjornevik and colleagues was able to confirm the epidemiological link between EBV infection and the development of multiple sclerosis, a rare autoimmune condition which affects the central nervous system (9). Investigating possible genetic variations in the genes associated with the STAT3 or p38-MK2 signaling pathways, as well as in ZFP36L1, could allow the identification of genetic markers or risk factors associated with these diseases. Interestingly, several SNPs within or in the proximity of the ZFP36L1 coding sequence have been linked via genome-wide association studies with various autoimmune conditions, including multiple sclerosis (rs12434551) (457).

One future development of this work is also to test whether STAT3, p38-MK2, or ZFP36L1 activation can be used as a readout of EBV entry in cell types which are not known to be EBV targets and in which EBV is not able to establish latent infection. Given the activatory signals induced by EBV binding and tegument release independently of latency establishment, the question arises on whether EBV interaction with other types of cells can have a similar effect. By analysing the levels of activation of these pathways upon exposure to EBV particles it could be possible to extend the current knowledge of cells permissive to EBV entry.

5. *Materials and Methods*

5.1 Materials

5.1.1 Eukaryotic cell lines and primary cells

Virus producer cell lines are HEK293 cells stably transfected to carry either the M81 wild-type EBV BAC or one of the recombinant EBV virus BACs (section 5.1.5) were previously generated in the laboratory via transfection and were maintained by constant selection with 100 μg/mL hygromycin.

Primary human CD19+ B cells were isolated from anonymous buffy coats purchased from the *DRK-Blutspendedienst Baden-Württemberg - Hessen gemeinnützige GmbH* using a Ficoll cushion and a MACS positive selection method.

5.1.2 Cell culture media

Producer cells were kept in culture using RPMI-1640 (Gibco by Life Technologies) supplemented with 10% fetal bovine serum (SIGMA).

Primary CD19+ cells were cultured using RPMI-1640 (Gibco by Life Technologies) supplemented with 20% fetal bovine serum (SIGMA), and 1 mM sodium pyruvate (Gibco by Life Technologies).

5.1.3 Plasmids

The following plasmids were used for the induction of producer cell lines (virus production):

- p509, a pRK5 backbone plasmid encoding for BZLF1 from the B95-8 EBV strain under control of a CMV promoter;
- p2130, a pRK5 backbone plasmid encoding for BRLF1 from the B95-8 EBV strain under control of a CMV promoter:
- pRA, a pRK5 backbone plasmid encoding for BALF4 (=gB=gp110) derived from the B95-8 EBV strain. This plasmid was used to increase B cell infectivity:

5.1.4 Oligonucleotides

Internal #	Name	Sequence
335	hGAPDH cDNA	GATCTCGCTCCTGGAA
333	W2W1 cDNA	CCTAGGCCCTGAAGG
334	EBNA2 cDNA	GCAAGATAGAATGTAGGCAT
363	W0 fwd	CGCCAGGAGTCCACACAAAT
364	W0	GAGGGGACCCTCTGGCC
342	W probe	FAM-ACCGAAGTGAAGGCCCTGGACCAAC-TAMRA
349	EBNA2 fwd type1	GCTTAGCCAGTAACCCAGCACT
344	EBNA2 rev	TGCTTAGAAGGTTGTTGGCATG
343	EBNA2 probe	FAM-CCCAACCACAGGTTCAGGCAAAACTTT-TAMRA
3845	hTFRC fwd	AATCCTGGGGGTTATGTGGC
3846	hTFRC rev	GGTGATTTTCCCTGCTCTGAC
4358	hTFRC probe	JOE-AGGCTGCAACAGTTACTGGT-BHQ
3473	hIL-6 fwd	CTTCGGTCCAGTTGCCTTCTC

3474	hIL-6 rev	TTACATGTCTCCTTTCTCAGGGC
3587	hIL-6 probe	FAM-AATTCGGTACATCCTCGACG-TAMRA
3475	hTNF-a fwd	GCTGCACTTTGGAGTGATCG
3476	hTNF-a rev	GCTTGAGGGTTTGCTACAACA
3583	hTNF-a probe	FAM-GAGTGACAAGCCTGTAGCCC-TAMRA
3417	hZFP36L1 fwd	AGTTTAAAGCTCCTCCTCCCCC
3418	hZFP36L1 rev	TTTCTGTCCAGCAGGCAACC

5.1.5 Recombinant EBV (rEBV)

Internal #	*Name*	*Description*
B110	*M81wt*	*Recombinant M81 wild-type virus*
B279	*M81 BZLF2-kan-KO*	*Recombinant M81 in which the BZLF2 (=gp42) CDS has been replaced by the kanamycin resistance cassette from pCP15*
B975	*M81 EBNA2-kan-KO*	*Recombinant M81 in which the EBNA2 CDS has been replaced by the kanamycin resistance cassette from pCP15*

B1001	*M81 BALF4(Δnts42-1730)-kan-KO*	*Recombinant M81 in which the nts42-1730 of the BALF4 (=gp110) CDS have been replaced with the kanamycin resistance cassette from pCP15*
B1050	*M81 BFLF1/BFRF1A-KO BBRF1-KO BALF4-kan-KO*	*Recombinant M81 B1001 containing the following deletions: BFLF1Δnts-43/+1394; BFRF1A Δnts1-45; BBRF1 Δnts299-1237*
B1099	*M81 BNRF1(aa1-428.expressed)-kan-KO*	*Recombinant M81 in which the BNRF1 CDS has been disrupted by inserting the kanamycin cassette from pCP15 (aa 1-428 are expressed)*
B1580	*M81 BPLF1(aa60-3147end)*	*Recombinant M81 in which the BPLF1 CDS has been disrupted by inserting an ampicillin resistance cassette to replace aa 60-3147 (end)*
B1636	*M81 BOLF1(stop.codon.after.aa2)-KO*	*Recombinant M81 in which the BOLF1 CDS has been disrupted by inserting a stop codon after aa2*
B1637	*M81 BSRF1(2stop.codons.after.aa7)-KO*	*Recombinant M81 in which the BSRF1 CDS has been disrupted by inserting two stop codons after aa7*
B1641	*M81 BKRF4-kan-KO*	*Recombinant M81 in which the BKRF4 CDS has been replaced by the kanamycin resistance cassette from pCP15*
B1651	*M81 BBLF1(2stop.codons.after.aa8)-KO*	*Recombinant M81 in which the BBLF1 CDS has been disrupted by inserting two stop codons after aa8*
B1669	*M81 BRRF2(1stop.codon+shift.after.aa13)-KO*	*Recombinant M81 in which the BRRF2 CDS has been disrupted by inserting a stop codon after aa13 together with a frameshift*

B1672	*M81 BGLF2(ATG-->ACG+2stop.codons.after.aa8-KO*	*Recombinant M81 in which the BGLF2 CDS has been disrupted by replacing the ATG with ACG, and inserting two stop codons after aa8*
B1789	*M81 BXLF2(aa19-686)-tet-KO*	*Recombinant M81 in which the BXLF2 (=gH) CDS has been disrupted by inserting a tetracycline resistance cassette to replace aa 19-686*

5.1.6 Antibodies

Target	*Usage*	*Species and clonality*	*Dilution*	*Supplier*
EBNA2	IFA	Mouse, monoclonal (PE2)	1:35	Hybridoma cell line
ZFP36L1/2	IFA/WB	Rabbit, monoclonal	1:200 (IFA); 1:1000 (WB)	Cell Signaling Technology, #2119
IκBα	WB	Mouse, monoclonal	1:1000	BioLegend, #609101
phospho-p65 (Ser536)	WB	Rabbit, monoclonal	1:1000	Cell Signaling Technology, #3033
phospho-ERK (Thr202/Tyr204)	WB	Rabbit, monoclonal	1:1000	Cell Signaling Technology, #4370
phospho-AKT1 (Ser473)	WB	Rabbit, monoclonal	1:10000	Abcam, #ab81283

STAT3	WB	Rabbit, monoclonal	1:1000	Cell Signaling Technology, #4904
phospho-STAT3 (Tyr705)	WB	Rabbit, monoclonal	1:1000	Cell Signaling Technology, #9131
p38	WB	Rabbit, monoclonal	1:1000	Cell Signaling Technology, #9212
phospho-p38 (Thr180/Tyr182)	WB	Rabbit, monoclonal	1:1000	Cell Signaling Technology, #9211
phospho-MK2 (Thr334)	WB	Rabbit, monoclonal	1:1000	Cell Signaling Technology, #3007
phospho-ATF2 (Thr71)	WB	Mouse, monoclonal	1:200	Santa Cruz Biotechnology, sc-8398
phospho MSK2 (Ser196)	WB	Rabbit, polyclonal	1:500	R&D, #AF189
Actin	WB	Mouse, monoclonal	1:1000	Santa Cruz Biotechnology, sc-8432
Vinculin	WB	Mouse, monoclonal	1:1000	Santa Cruz Biotechnology, sc-73614
Cy-3 conj. Anti-mouse	IFA/FC-viral quantification	Goat	1:300	Dianova, #115-165-174

Cy-3 conj. Anti-rabbit	IFA	Goat	1:300	Dianova, #111-165-003
HRP conj. Anti-mouse	WB	Goat	1:40000	Promega, #W4011
HRP conj. Anti-rabbit	WB	Goat	1:10000	Promega, #W4021

5.1.7 Pathway Inhibitors

Name	*Target*	*Concentration*
SB239063	p38	10 μM
PF-3644022	MK2	10 μM
SP600125	JNK	10 μM
Trametinib	MEK1/2	0.1 μM
ZSTK474	PI3K	1 μM
PS-1145	NF-kB	3 μM
T-5224	AP-1	20 μM
PRT-062607	Syk	2 μM

Bafetinib	Lyn	5 μM
Ibrutinib	BTK	10 nM
Bisindolylmaleimide I	PKC	5 μM
H-89	PKA	5 μM
Stattic	STAT3	2,5 μM
Actinomycin D	Transcription	2 μg/mL
Cycloheximide	Translation	15 μg/mL

5.1.8 Chemicals, reagents, kits

Name	*Used for*	*Supplier*
Sodium orthovanadate	Phosphoproteomics	New England Biolabs
phosphoSTOP phosphatases inhibitors	Phosphoproteomics	Roche
complete mini EDTA free protease inhibitors	Phosphoproteomics	Roche

Halt™ Protease and Phosphatase Inhibitor	WB	Thermo Fisher Scientific
ROTI® Nanoquant	WB	Carl Roth GmbH + Co. KG
Acrylamide: 30% stock, with 0-8% bisacrylamide	WB	Carl Roth GmbH + Co. KG
Page Ruler Prestained Protein Ladder	WB	Thermo Fisher Scientific
SDS solution (20%)	WB	Santa Cruz Biotechnology
β-mercaptoethanol	WB	Sigma Aldrich
Ponceau S	WB	Sigma Aldrich
Bovine serum albumin	WB/ELISA	Sigma Aldrich
Pierce™ ECL Western Blotting Substrate	WB	Thermo Fisher Scientific
Tween 20	WB/ELISA	GE Healthcare
Triton X-100	IFA	AppliChem

Paraformaldehyde	IFA	AppliChem
Glycerol	IFA/FISH	Sigma Aldrich
DABCO	IFA/FISH	Sigma Aldrich
DAPI	IFA/FISH	Sigma Aldrich
Human IL-6 ELISABASIC kit (HRP)	ELISA	Mabtech
Human TNFα ELISABASIC kit (HRP)	ELISA	Mabtech
Human IFN-α pan ELISABASIC kit (HRP)	ELISA	Mabtech
TMB substrate	ELISA	BD Biosciences
RNeasy Mini kit	RNA extraction	Qiagen
RNase-Free DNase Set	RNA extraction	Qiagen
Random hexamers	cDNA synthesis	Thermo Fisher Scientific
dNTP mix 10mM	cDNA synthesis	Thermo Fisher Scientific

RNase inhibitor	cDNA synthesis	Promega
Methanol	FISH	Carl Roth GmbH + Co. KG
Acetic acid	FISH/WB	Carl Roth GmbH + Co. KG
Formamide	FISH	Sigma Aldrich
Biotin-16-dUTP	FISH	Roche
Streptavidin, Alexa488 conj.	FISH	Invitrogen
Heparin sodium salt	CD19+ B cell isolation	Sigma Aldrich
Ficoll Plus	CD19+ B cell isolation	Cytiva
Dynabeads™ CD19 Pan B	CD19+ B cell isolation	Thermo Fisher Scientific
DETACHaBEAD™ CD19	CD19+ B cell isolation	Thermo Fisher Scientific
PBS tablets	Cell culture	Thermo Fisher Scientific
DMSO	Cell culture	Sigma Aldrich

Trypan Blue solution	Cell culture	Sigma Aldrich
Trypsin EDTA 0.05%	Cell culture	Thermo Fisher Scientific
Hygromycin B	Cell culture	Thermo Fisher Scientific
Metafectene	Cell transfection	Biontex

5.1.9 Enzymes

Name	*Used for*	*Supplier*
DNase I	Viral titre quantification	Thermo Fisher Scientific
Proteinase K	Viral titre quantification	Roche
TaqMan Universal PCR Master Mix	Viral titre quantification	Thermo Fisher Scientific
Benzonase, purity >90%	Phosphoproteomics	Merck Millipore
Lambda protein phosphatase	Dephosphorylation of proteins	New England Biolabs
***E. coli* DNA polymerase I**	FISH	Roche

AMV Reverse Transcriptase	cDNA synthesis	New England Biolabs

5.1.10 Buffer solutions

Name	*Used for*	*Composition*
Phosphate Buffered Saline (PBS)	IFA/FC/ELISA	137 mM NaCl, 2,7 mM KCl, 10 mM Na_2HPO_4, 1,8 mM KH_2PO_4; pH=7,4
Lysis buffer for phosphoproteomics	MS	100 mM Tris-HCl pH 8.5, 7 M Urea, 1 % Triton, 10 U/mL DNase I, 1 mM magnesium chloride, 1% benzonase, 1 mM sodium orthovanadate, phosphoSTOP phosphatases inhibitors, complete mini EDTA free protease inhibitors
5X RIPA buffer	WB	100 mM Tris-HCl (pH 7,5), 750 mM NaCl, 25 mM EDTA, 2,5 % NP-40 and 5% Sodium deoxycholate
4x Protein loading buffer	WB	200 mM Tris-HCl (pH 6,8), 8 % SDS, 1% bromophenol blue, 40% glycerol and 10% 2-mercaptoethanol
Ponceau S staining solution	WB	0,1% (w/v) Ponceau S, 5% acetic acid (glacial)
10X TBS	WB	200 mM Tris-HCl (pH 7.6), 1,5 M NaCl
TBS-T	WB	1X TBS + 0.1% Tween 20
Blocking buffer	WB	TBS-T + 5% skim milk powder

TBS-T + BSA	WB	TBS-T + 3% BSA
Polyacrylamide stacking gel (4,5 %)	WB	125 mM Tris (pH 6.8), 15% (v/v) acrylamide stock, 4 mM EDTA
Polyacrylamide separating gel (12,5 %)	WB	335 mM Tris (pH 8,9), 42% (v/v) acrylamide stock, 3,3 mM EDTA
10X SDS-running buffer	WB	250 mM Tris, 1,92 M glycine, 1% SDS; pH=8,5
Blotting buffer	WB	25 mM Tris, 150 mM glycine, 20% methanol
Buffer A	Subcellular fractionation	10 mM HEPES pH 7.9, 10 mM KCl, 0.1 mM EDTA, 1mM DTT, 1x protease and phosphatase inhibitor cocktail
Buffer B	Subcellular fractionation	20 mM HEPES pH 7.9, 400 mM NaCl, 1 mM EDTA, 1mM DTT, 1x protease and phosphatase inhibitor cocktail
Permeabilization buffer	IFA	1X PBS + 0,5% Triton X-100
Antibody incubation buffer	IFA	1X PBS + 10% heat-inactivated goat serum
Embedding buffer	IFA/FISH	25 mg/mL DABCO, 0,2 M Tris-HCl (pH 8,0), glycerol 90%
10X hypotonic solution	FISH	402 mM KCl, 5,2 mM EGTA, 75,5 mM HEPES; pH=7,0
Fixation buffer	FISH	66% methanol, 33% acetic acid (glacial)
20X SSC buffer	FISH	3M NaCl, 0,3 M Sodium Citrate; pH 7,0

10X nick translation buffer	FISH	0,5 M Tris-HCl (pH 8,0), 50 mM $MgCl_2$, 0,5 mg/mL BSA
Denaturation buffer	FISH	2X SSC + 70% deionised formamide (pH=7,0)
Hybridization buffer	FISH	4X SSC + 20% dextran sulphate (MW 500000)
Wash buffer A	FISH	4X SSC + 50% formamide
Wash buffer B	FISH	4X SSC + 0,1% Tween 20
Blocking buffer	FISH	4X SSC + 3% BSA + 0,1% Tween 20
Detection buffer	FISH	4X SSC + 1% BSA + 0,1% Tween 20
Incubation buffer	ELISA	1X PBS + 0,05% Tween 20 + 0,1% BSA

5.2 Methods

5.2.1 Eukaryotic cell culture

5.2.1.1 Cell maintenance

Eukaryotic cells were cultured using the appropriate medium (section 5.1.2) in the incubator at 37°C with 5% CO_2. HEK293-derived cell lines were passaged using 0.05% Trypsin-EDTA twice a week or when 70-80% optical confluency was reached.

5.2.1.2 CD19+ B cell isolation

Human CD19+ B cells used in this study were freshly isolated from buffy coats (section 5.1.1) using the Dynabeads™ CD19 Pan B positive selection kit combined with the DETACHaBEAD™ CD19 beads removal kit.

The buffy coats were initially diluted using an equal volume of 1X PBS containing heparin and layered on top of a volume of Ficoll equal to 1/3 of the blood:PBS mix. Samples were centrifuged at room temperature for 30 minutes at 400 x g. The layer containing mononuclear cells was then recovered and washed 3 times with 1X PBS. Cells were then resuspended in RPMI-1640 + 1% FBS and pre-washed Dynabeads™ CD19 Pan B magnetic beads were added according to manufacturer's instructions. The cell suspension was then incubated at 4°C rolling for 30 minutes. CD19+ B cells were then isolated by using a magnet and washed 3 times with RPMI-1640 + 1% FBS before adding the DETACHaBEAD™ CD19 beads removal reagent according to manufacturer's instructions. Beads-free B cells were obtained after incubating with the reagent for 1 hour at room temperature rolling followed by 3 washing steps. Isolated CD19+ B cells were kept in RPMI-1640 + 20% FBS on ice until further use.

5.2.1.3 Virus induction

In order to induce lytic replication and produce viral supernatants, cells were counted and seeded at a concentration of $1,5 \times 10^5$ viable cells/mL in 2 mL of complete medium in a 6-well plate and incubated overnight at 37°C. The following day, cells were transfected with a total of 1,25 µg of pDNA per well: 0,5 µg of p509, encoding BZLF1, and 0,25 µg of p2130, encoding BRLF1, to induce lytic replication; 0,5 µg of pRA encoding BALF4 to increase B cell infectivity (458). For the BALF4 knockout producer cell line, the induction was performed without the BALF4 encoding-plasmid, which was replaced with the same amount of empty pRK5 plasmid. Transfections were performed using the liposome-based reagent Metafectene according to the manufacturer's instructions. In summary, for each well of a 6-well plate, two solutions were mixed:

- solution A, 100 µL of RPMI-1640 medium without additions to which the pDNA was added;
- solution B, 100 µL of RPMI-1640 medium without additions to which 3,75 µL of metafectene was added.

The resulting solution was incubated for 20 minutes at room temperature. 1 mL of complete medium was removed from each well and 200 µL of transfection solution was added to each well in a drop-wise fashion. Cells were incubated for 8 to 12 hours before the medium was

replaced with fresh complete medium. Three days after transfection, viral supernatants were collected, centrifuged at 400 x g for 10 minutes and filtered through a 0.45 μm filter.

5.2.1.4 Quantification of viral titres using qPCR

To evaluate EBV genome equivalents per millilitre of supernatant, viral supernatants were quantified via qPCR (459). Prior to performing the qPCR, viral supernatants were treated with DNase I, in order to remove viral DNA copies freely present in suspension, followed by subsequent treatment with proteinase K to release the viral genome contained inside the capsid. A set of internal controls were used to guarantee the successful completion of each step: a negative control containing only water to control for contamination; a positive control with known viral titre; a water-based suspension containing EBV BAC DNA to control for DNase I treatment efficiency. For each condition, 1 μL of DNase I 1 U/μL plus 5 μL of 10X DNase I reaction buffer was added to 44 μL of solution or supernatant. Samples were then incubated in a thermocycler for 1 hour at 37°C and at 70°C for 10 minutes to inactivate the reaction. For proteinase K treatment, 5 μL of each of the DNase I-treated samples was mixed with 5 μL of a prediluted proteinase K solution (1:100 in water, stock 10 mg/mL) and incubated in a thermocycler at 50°C for 1 hour and at 75°C for 20 minutes to inactivate the reaction. Each sample was then diluted 1:10 (final volume 100 μL) with PCR-grade water.

Following the dilution of the sample, the qPCR reaction was prepared. qPCR was performed with primers and probe specific for the non-repetitive EBV BALF5 gene sequence to measure the EBV copy numbers in the supernatants. The following reaction mixture was set up for each sample:

Volume	Reagent
12,5 μL	TaqMan Universal PCR Master mix (2x)
2,5 μL	Forward primer
2,5 μL	Reverse primer

1,0 µL	Probe
1,5 µL	H_2O
5 µL	DNase I and Proteinase K treated sample
25 µL	*Total volume*

The PCR reaction was performed using the ABI STEP ONE PLUS Real-Time PCR System (Applied Biosystems) with the following thermocycling conditions:

Temperature (°C)	Time (mm:ss)	Number of cycles
50	02:00	1x
95	10:00	1x
95	00:15	40x
60	01:00	

Using a standard curve in which the linear relationship between threshold cycle (C_T) values and genome copies/mL has been previously established, I was able to calculate the genome-containing particles per millilitre.

5.2.1.5 Quantification of gp350+ particles

For those experiments in which a panel of recombinant EBV viruses including VLPs was used, quantification of gp350+ particles was performed by flow cytometry. For this purpose, M81

wild-type virus, previously quantified with qPCR, was titrated (1, 0.75, 0.5, and 0.25 x 10^7 genome containing particles) and bound to $3x10^5$ human primary B cells at 4°C. In parallel, different dilutions of viral supernatants to be quantified were incubated with the same number of human primary B in the same conditions. After 2 hours, cells were washed with ice-cold PBS, resuspended in 100 μL of PBS and fixed for 15 minutes on ice using an equal volume of PBS + 4% FA. After washing the cells twice with PBS, they were stained with α-gp350 (clone 72A1, dilution 1:3) in PBS + 2% FBS for 30 minutes at room temperature followed by the staining with the secondary antibody α-mouse IgG-Cy3 antibody for 30 minutes. Cells were then analysed via flow cytometry using a BD FACSCalibur™. Median fluorescence intensity (MFI) values were determined, and a standard curve was generated for EBV genomes vs MFI. MFI values obtained for VLPs/KOs were extrapolated off the standard curve to quantify VLPs/KOs (460).

5.2.1.6 B cell infections

Purified CD19+ human B cells were exposed to viral supernatant with a multiplicity of infection of 30, as determined by qPCR or gp350 quantification, by rolling for two hours at 4°C. Cells were then cultured at a density of $2x10^6$ cell/mL for the indicated amount of time with RPMI-1640 supplemented with 20% FBS + 1% HEPES at 37°C. For the experiments in which pathway inhibitors were used, these were added to primary B cells at the concentration indicated for 1 hour prior to the incubation with virus supernatant. The inhibitors were then added in each of the following steps maintaining the same final concentration.

5.2.2 Protein analysis

5.2.2.1 Proteomic analysis

Both proteomic and phosphoproteomic analyses were performed at the DKFZ Genomics and Proteomics Core Facility. Samples were prepared and submitted to the Core Facility for further processing. The following methods were provided by Dr Dominic Helm.

Sample Preparation

$4x10^6$ primary B cells from human healthy donors were left uninfected or infected with M81wt for a different amount of time. At each time point, cells were washed with ice-cold PBS, lysed

with 1X RIPA buffer containing protease and phosphatase inhibitors and quantified using the Bradford quantification assay.

Proteins (10 ug) were separated for 0.5 cm via SDS-PAGE. After Commassie staining the total sample was cut out and used for subsequent Trypsin digestion according to a slightly modified protocol described by Shevchenko et al. (461) on a DigestPro MSi robotic system (INTAVIS Bioanalytical Instruments AG).

Mass spectrometry run

LC-MS/MS analysis was performed using an Ultimate 3000 UPLC system connected to a Q-Exactive HF-X mass spectrometer. The UPLC was operated using a trap-elute set-up. Peptides were first loaded on a trap column (Acclaim PepMap300 C18, 5µm, 300Å wide pore; Thermo Fisher Scientific) for 5 min and 30 µL/min of 0.05% TFA in water. During the analytical gradient (Solvent A: water with 0.1% formic acid; Solvent B; 80% acetonitrile, 20% and 0.1% formic acid) the concentration of solvent B was ramped from 2% to 25% (150 min) and 25%-40% (30 min) on a nanoEase MZ Peptide analytical column (300Å, 1.7 µm, 75 µm x 200 mm; Waters). Eluting peptides were analysed by a Q-Exactive-HF-X mass spectrometer (Thermo Fisher Scientific) running in data depend acquisition mode. A full scan at 120 k resolution was followed by up to 35 MS/MS scans at 15 k resolution. Precursors were isolated for MS/MS scans via a quadrupole isolation window of 1.6 m/z and fragmented via a collision energy of 27 NCE. Unassigned and singly charged peptides were excluded from fragmentation and dynamic exclusion was set to 60 s.

Data analysis

Data analysis was performed by MaxQuant (462) (version 1.6.0.16) using an organism specific database extracted from Uniprot.org under default settings. Identification FDR cut-offs were 0.01 on peptide level and 0.01 on protein level. Match between runs option was enabled to transfer peptide identifications across Raw files based on accurate retention time and m/z.

Quantification was done using a label free quantification approach based on the MaxLFQ algorithm (463). A minimum of 2 quantified peptides per protein was required for protein quantification.

Data have been further processed by in-house compiled R-scripts to plot and filter data.

Statistics

The Perseus software package (version 1.6.7.0) using default settings for further statistical analysis (464) of LFQ data (http://www.coxdocs.org/doku.php?id=perseus:user:use_cases:interactions) was used. Adapted from the Perseus recommendations (464) protein groups with non-zero intensity values in 70% of the samples of at least one of the conditions were used and imputation with random values drawn from a downshifted (1.8 standard deviation) and narrowed (0.3 standard deviation) intensity distribution of the individual sample.

5.2.2.2 Phosphoproteomic analysis

Sample Preparation

$4x10^6$ primary B cells from human healthy donors were left uninfected or infected with M81wt, VLPs, or gp110 knockout virus for 6 hours. A total of 21 donors were used, and the same amount of protein was pooled from 7 donors for each condition to generate 3 independent pooled biological replicates.

Samples have been prepared according to a slightly modified protocol described by Potel et al. (465). Briefly, cell pellets were resuspended with lysis buffer (see section 5.1.10) and lysed by sonication. Cell debris was removed by centrifugation (21k x g for 15 minutes at 4 °C). Protein concentration was determined via Bradford assay and followed by Chloroform/Methanol precipitation as described by Wessel et al. (466).

Pellets were resuspended in digestion buffer (8 M Urea, 100 mM NaCl, 50 mM TEAB, pH 8.5), followed by reduction in 10 mM DTT for 1 h at 27°C, alkylation by 30 mM Iodoacetamide for 30 min at room temperature in the dark and quenching the reaction by adding additional 10 mM DTT. Samples have subsequently been digested by Lys-C at an enzyme:protein ratio of 1:00 for 3 -4 h at 30°C, diluted with 50 mM TEAB to a resulting Urea concentration of 1.6 M and further digestion with Trypsin overnight at 37°C in an enzyme:protein ration of 1:50. Digestion was stopped by acidification, adding 0.02%(vol/vol) TFA. Digested peptides have been desalted using C18 SepPack Cardridges and resuspended in 0.07 % (v/v) TFA in 30 %

(v/v) ACN and fractionated by on-column FE3+- IMAC enrichment on an Ultimate 300 LC system using the method described by Ruprecht et al. (467). The two fractions per sample, containing mainly either unphosphorylated or phosphorylated peptides, have been desalted by StageTips (468) and resolved in 50mM citric acid and 0.1 % TFA.

Mass spectrometry run

LC-MS/MS analysis was performed using an Ultimate 3000 UPLC system connected to a Q-Exactive HF-X mass spectrometer. The UPLC was operated using a trap-elute set-up. Peptides were first loaded on a trap column (Acclaim PepMap300 C18, 5µm, 300Å wide pore; Thermo Fisher Scientific) for 5 min and 30 ul/min of 0.05% TFA in water. During the analytical gradient (Solvent A: water with 0.1% formic acid; Solvent B; 80% acetonitrile, 20% and 0.1% formic acid) for the phospho-fraction the concentration of solvent B was ramped from 2% to 8% (15 min), 8%-25% (135 min) and 25%-40% (20 min) and for the full proteome samples the concentration of solvent B was ramped from 2% to 25% (150 min) and 25%-40% (30 min). For separation a nanoEase MZ Peptide analytical column (300Å, 1.7 µm, 75 µm x 200 mm; Waters) was used. Eluting peptides were analysed by a Q-Exactive-HF-X mass spectrometer (Thermo Fisher Scientific) running in data depend acquisition mode. A full scan at 120 k resolution was followed by up to 35 MS/MS scans at 15 k resolution. Precursors were isolated for MS/MS scans via a quadrupole isolation window of 1.6 m/z and fragmented via a collision energy of 27 NCE. Unassigned and singly charged peptides were excluded from fragmentation and dynamic exclusion was set to 60 s.

Data analysis

Data analysis was carried out by MaxQuant (462) using an organism specific database extracted from Uniprot.org under default settings. Identification FDR cut-offs were 0.01 on peptide level and 0.01 on protein level. Match between runs option was enabled to transfer peptide identifications across Raw files based on accurate retention time and m/z. Quantification was done using a label free quantification approach based on the MaxLFQ algorithm (463). A minimum of 2 quantified peptides per protein was required for protein quantification. Data have been further processed by in-house compiled R-scripts to plot and filter data.

Statistics

The Perseus software package (version 1.6.7.0) using default settings for further statistical analysis (464) of LFQ data (http://www.coxdocs.org/doku.php?id=perseus:user:use_cases:interactions) and phospho data (http://www.coxdocs.org/doku.php?id=perseus:user:use_cases:modifications) was used. Adapted from the Perseus recommendations (464) protein groups with non-zero intensity values in 70% of the samples of at least one of the conditions were used and imputation with random values drawn from a downshifted (1.8 standard deviation) and narrowed (0.3 standard deviation) intensity distribution of the individual sample.

5.2.2.3 Subcellular fractionation

The subcellular fractionation protocol was modified from a previously published method (469). In summary, $6x10^6$ uninfected or M81wt-infected primary CD19+ B cells were washed once with PBS 1X and gently resuspended in 40 µL of buffer A (see section 5.1.10). Cells were then incubated on ice for 15 minutes and then 2.5 µL of 10% NP-40 was added before being vortexed at minimum speed for 10 seconds and incubated on ice for 2 minutes. The supernatant was collected after centrifuging the samples for 6 minutes at 600 x g at 4°C and identified as the cytoplasmic fraction. The pellet was then gently washed once with 100 µL of buffer A, centrifuged for 5 minutes at 600 x g at 4°C and resuspended in 15 µL of buffer B (see section 5.1.10). Resuspended pellets were then vortexed at maximum speed for 15 seconds, incubated on ice for 15 minutes, and vortexed once more prior to proceeding to sonication. Samples were then centrifuged at maximum speed for 5 minutes at 4°C and the supernatant was identified as the nuclear fraction. Both the cytoplasmic and the nuclear fraction were quantified via Bradford assay and further processed for western blot.

5.2.2.4 Lambda phosphatase treatment

Total protein lysate prepared with EDTA-free RIPA buffer and protease inhibitors was treated for 30 minutes at 30°C with lambda protein phosphatase according to manufacturer´s instructions. An untreated control was processed similarly in the absence of the enzyme. Samples were then analysed by western blot.

5.2.2.5 Western blot analysis

Proteins were extracted from cell pellets with 1X RIPA buffer supplemented with protease and phosphatase inhibitor cocktail for 15 min on ice followed by sonication to shear the genomic DNA. Up to 30 μg of proteins was denatured in 4X protein loading buffer (see section 5.1.10) for 10 minutes at 95°C and loaded on a 12.5% SDS–polyacrylamide gel. The run was performed in 1X SDS-running buffer for 90 minutes at 90V constant and for 3 hours at 120V constant or until the front of the samples reached the bottom of the gel. Protein transfer was performed in blotting buffer (see section 5.1.10) onto a 0.22 μm nitrocellulose membrane (Hybond C, Amersham) for 90 minutes at 25V constant. The nitrocellulose membrane was then washed briefly in double-distilled water and stained with Ponceau S staining solution (see section 5.1.10). A blocking step was performed for 1 hour at room temperature by incubating the blots in blocking buffer (see section 5.2.10), after which the antibody against the target protein was added and the blot was incubated overnight at 4°C. Antibodies recognizing phosphorylated proteins were incubated in TBS with 0.1% Tween 20 and 5% BSA. After extensive washing in TBS with 0.1% Tween 20, the blot was incubated for 1 hour at room temperature with suitable secondary antibodies coupled to horseradish peroxidase (goat anti-mouse or goat anti-rabbit lgG). Bound antibodies were detected using the ECL detection reagent using the GE Amersham Imager 680 detection system.

5.2.2.6 Immunostaining

Cells were dropped on a glass slide and allowed to air dry. Fixation was performed with 4% paraformaldehyde in PBS for 20 minutes at room temperature and permeabilization was performed with permeabilization buffer (see section 5.1.10) for 10 minutes at room temperature. The staining was performed by incubating the primary antibody diluted in antibody incubation buffer (see section 5.1.10) for 1 hour at 37°C. Slides were then washed in PBS three times and incubated with an anti-mouse or anti-rabbit secondary antibody conjugated to Cy-3 for 30 minutes at 37°C. Nuclear staining was performed by incubation with PBS + 40 ng/mL DAPI for 5 minutes. Slides were embedded with a DABCO/glycerol embedding solution (see section 5.1.10) and stored at 4°C until acquisition was performed with the Leica DM5000B fluorescence microscope.

5.2.2.7 ELISA

Human primary B cells were infected and cultured for the indicated amount of time. Cell culture supernatants were collected after centrifuging the cell suspension and analysed for IL-6, TNFα, and IFN-α production using the Human IL-6 ELISABASIC kit (HRP), the Human TNFα ELISABASIC kit (HRP), and the Human IFN-α pan ELISABASIC kit (HRP) following the manufacturer's protocol (see section 5.1.8). In summary, a high-bond 96-well ELISA plate was coated with 100 μL of coating antibody diluted in 1X PBS overnight at 4°C. The plate was then washed 3 times with 300 μL of 1X PBS + 0,05% Tween 20 and then blocked with 200 μL of ELISA incubation buffer (see section 5.1.10) for 1 hour at room temperature. After washing the plate 3 times, 100 μL of the sample was added and incubated for 2 hours at room temperature. A standard curve was included by serially diluting the reconstituted standard according to the dynamic range of the assay. After incubation, the plate was washed and 100 μL of biotinylated capture antibody diluted in incubation buffer was added and incubated for 1 hour at room temperature, followed by an additional washing step and 1 hour incubation with HRP-conjugated streptavidin diluted in incubation buffer. After one final washing step, 100 μL of premixed TMB substrate was added to each well and incubated for maximum 15 minutes. The reaction was stopped by adding 50 μL of 2M H_2SO_4 solution. The measurement of the absorbance was performed at 450 nm and 540 nm using the Tecan Infinite M Nano Plus plate reader. The absorbance readings for the reference wavelength 540 nm were subtracted from the measure obtained at 450 nm and the concentration of the samples was determined by interpolation of the obtained absorbance value from the standard curve.

5.2.3 RNA expression analysis

5.2.3.1 RNA isolation

At the indicated time point, $2x10^6$ infected cells were pelleted and washed twice with ice-cold PBS 1X. Cell pellets were then lysed using the RLT buffer from the RNeasy Mini kit. RNA isolation was performed on-column according to the manufacturer´s protocol. DNase treatment was performed on-column using the RNase-Free DNase Set for 15 minutes at room temperature. RNA concentration and purity were assessed by Nanodrop quantification. Samples were stored at -80°C if not immediately used.

5.2.3.2 cDNA synthesis

For cDNA synthesis, 250 ng of RNA was used to generate cDNA. The reaction was performed using random hexamers (for ZFP36L1, IL-6, and TNFα) or specific primers (for EBNA2 and Wp) and the AMV Reverse Transcriptase. RNA samples were denatured by heating them up at 65°C for 5 minutes and then incubated on ice until the reverse transcription reaction was prepared. The reaction was set up as follows:

Volume	Reagent
1,0 μL	10 mM dNTPs
2,0 μL	Primer mix or Random hexamers
2,0 μL	10X Reaction buffer
0,2 μL	RNase inhibitor (40 U/μL)
0,8 μL	Reverse Transcriptase (10 U/μL)
14 μL	RNA
20 μL	*Total volume*

The reaction was performed in a thermocycler using the following cycling conditions:

Temperature (°C)	Time (mm:ss)	Number of cycles
25	05:00	1x (only if random hexamers are used)
42	60:00	1x
80	05:00	1x

cDNA samples were then diluted 1:5 with PCR-grade water (total volume 100 µL) and stored at -20°C until further use.

5.2.3.3 Reverse transcription quantitative PCR (RT-qPCR)

All RT–qPCRs included samples not treated with reverse transcriptase that served as negative controls. All samples were run in duplicate, together with primers specific for the human TFRC gene to normalize for variations in cDNA recovery.

The primers and probes used to detect ZFP36L1, IL-6, TNFα, EBNA2, Wp, and TFRC are listed in section 5.1.4. For each target, as well as for TFRC, primers and probe were premixed to have a working concentration of 2,5 µM for each primer and 1,67 µM for the probe. For the reaction, the TaqMan™ Universal PCR Master Mix was used and the reaction was set up as follows:

Volume	Reagent
12,5 µL	TaqMan Universal PCR Master mix (2x)
3,0 µL	Primers and probe mix

3,0 µL	Primers and probe mix (TFRC)
1,5 µL	H_2O
5 µL	cDNA
25 µL	*Total volume*

The PCR reaction was performed using the ABI STEP ONE PLUS Real-Time PCR System (Applied Biosystems) with the following thermocycling conditions:

Temperature (°C)	Time (mm:ss)	Number of cycles
50	02:00	1x
95	10:00	1x
95	00:15	40x
60	01:00	

5.2.4 Fluorescent In Situ Hybridization (FISH)

5.2.4.1 Probe preparation

The EBV-specific probe was generated by nick translation of the complete B95-8 BAC as described before (470). In summary, the following reaction was set up:

Volume	Reagent
10,0 μL	10X nick translation buffer (see section 5.1.10)
10,0 μL	0,1 M 2-mercaptoethanol
5,0 μL	1 mM dNTPs
5,0 μL	1 mM Biotin-16-dUTP
7,5 μL	DNase I (dilute 1:6000)
4,0 μL	*E. coli* DNA polymerase I
48,5 μL	H_2O
10 μL	B95-8 BAC DNA (μg)
100 μL	*Total volume*

The reaction was incubated for 1 hour at 15°C and then stored on ice. A sample of the reaction was then denatured for 3 minutes at 95°C, mixed with DNA loading buffer and loaded onto a 2% agarose gel to check for the probe size. If the probe had an average size of 300 nt ca, 3 μL of 0,5 M EDTA and 1 μL of 10% SDS were added to the reaction which was then heated up to 68°C to inactivate the DNase I. The probe was then precipitated using sodium acetate and ethanol and resuspended in deionised formamide. The probe was stored at -20°C.

5.2.4.2 Cell preparation

Cells were washed twice with prewarmed PBS and resuspended in 1 mL of prewarmed (37°C) hypotonic solution (see section 5.1.10) added in a dropwise fashion. Cells were then incubated for 10 minutes at 37°C before adding 100 μL of ice-cold fixation buffer (see section 5.1.10). Cells were then pelleted, resuspended by flicking in 1 mL of fixation buffer and incubated on ice for 25 minutes. After fixation, cells were washed twice with fixative. Cells were stored in fixative at -20°C until further processed.

5.2.4.3 Staining

Cells were concentrated in a final volume of 50-100 μL (based on pellet size) and dropped on a glass slide. A chemical aging step was performed by adding 100% ethanol to cover the slide and heating it at 94°C for 10 seconds. Chemical aging was followed by a denaturation step in which the slide was covered with denaturation buffer (see section 5.1.10) and incubated at 75°C for 100 seconds. Slides were then let to cool down and washed in 4X SSC buffer before being dehydrated with an increasingly concentrated alcohol solution (70%-100%). After air drying the slide, the biotin-labelled probe was mixed with the hybridisation buffer (see section 5.1.10) and denatured at 75°C for 5 minutes and immediately plunged on ice for approximately 5 minutes. After denaturation, the probe was added to the slide and incubated overnight at 37°C in a humid chamber. To prevent evaporation, the slide was covered with a coverslip and sealed with rubber gum. The slide was then washed three times with wash buffer A (see section 5.1.10) at 42°C and then once with 4X SSC. An incubation step with blocking buffer (section 5.1.10) was performed at 37°C for 30 minutes, followed by the incubation for 30 minutes at 37°C with Alexa488-conjugated streptavidin diluted in detection buffer (see section 5.1.10). The slide was then washed in wash Buffer B (see section 5.1.10) at 42°C, counterstained with DAPI and mounted using DABCO/glycerol mounting solution (see section 5.1.10). The acquisition was performed with the Leica DM5000B fluorescence microscope.

5.2.5 Statistical analysis

All experiments were analysed with a paired *t*-test (one sample or two-tailed) and p-values equal to 0.05 or less were considered significant unless otherwise indicated. The statistical

analyses were performed with the GraphPad Prism 9 software. Mass spectrometry data were statistically analysed using the software Perseus as described above.

Tables

Table 1

Tegument proteins and their described functions.

Name	Function
BNRF1	Upon entry, disrupts the ATRX-DAXX complex, promoting viral early gene expression (18). Induces the degradation of the SMC5/6 cohesin complex both during *de novo* infection and lytic replication (417). Induces centrosomal amplification (416).
BPLF1	Deubiquitinase, deneddylase. Promotes the degradation of cullin-RING ubiquitin ligases in the nucleus (471), interferes with DDR (472–474), prevents the activation of NF-κB during lytic replication (475), contributes to innate immune evasion by blocking TLR (476) and interferon signaling (477). Blocks selective autophagy (478).
BOLF1	Possibly involved in infectivity (445).
BBLF1	Interacts with BGLF2, it is required for virus production (16, 479).
BGLF4	Serine/threonine protein kinase. Phosphorylates several viral and cellular proteins. Involved in virus production. Reviewed in (480)
BSRF1	Required for virus production (481, 482).
BKRF4	Interacts with BGLF2, it is required for virus production (483). Acts as histone chaperone and it is involved in the DDR (484–486).
BGLF2	Required for virus production (16, 483). Involved in infectivity (487), and in promoting lytic reactivation (271, 418, 444). Interferes with NF-κB activation (450) and RISC activity (437).
BRRF2	Required for virus production (488, 489).
BLRF2	Required for virus production (490, 491).

Table 2

EBV expression pattern during the different latency programs. Stage of infection associated with each latency program, as well as association with EBV-related malignancies, is also reported.

Latency type	EBNA1	EBNA2	EBNA-LP	EBNA3 (A, B, C)	LMP1	LMP2	EBERs	BHRF1	BARTs	Inf. stage	Disease
0	No	No	No	No	No	No	Yes	No	?	Resting memory B cells	--
I	Yes (Qp)	No	No	No	No	No	Yes	No	Yes	Dividing memory B cells	BL, GC
IIa	Yes (Qp)	No	No	No	Yes	Yes	Yes	No	Yes	Germinal center B cells	HL, NPC, TCL, DLBCL
IIb	Yes	Yes	Yes	Yes	No	No	Yes	Yes	Yes	Naïve B cells	IM, CLL
III	Yes	Yes	Yes	Yes	Yes	Yes	Yes	Yes	Yes	Naïve B cells	IM, PTLD, DLBCL

Qp: Q promoter;
BL: Burkitt lymphoma;
GC: gastric carcinoma;
HL: Hodgkin lymphoma;
NPC: nasopharyngeal carcinoma;
TCL: T-cell lymphoma;
DLBCL: diffuse large B cell lymphoma;
IM: infectious mononucleosis;
CLL: chronic lymphoid leukaemia;
PTLD: posttransplant lymphoproliferative disease.

EBV gene expression profile for some of the listed malignancies may vary from what indicated in a proportion of cases

Table 3

List of proteins and non-coding RNAs expressed during the latency phase. Described functions as well as oncogene or tumor suppressor activity are reported based on previously published reviews (4, 25, 105, 492–496)*.*

Latent protein	Function	Role in oncogenesis
EBNA1	Responsible for the maintenance of the viral genome during cell replication in latently infected cells. Modulates signaling pathways to promote cell survival and proliferation.	Required for *in* vitro transformation of B cells. Promotes the expression of growth transforming factors. Increases metastatic potential in NPC.
EBNA2	Transcriptional coactivator. Initiates latency transcription program. Controls the expression of several viral and cellular genes.	Required for *in vitro* transformation of B cells. Induces MYC expression. Promotes the induction of rapid cell division within 3 days post-infection.
EBNA-LP	Transcriptional coactivator. Interacts with EBNA2 during the early stages of latency. Regulates the expression of viral and cellular genes.	Required for *in vitro* transformation of B cells.
EBNA3A, B, C	Can positively/negatively regulate gene expression. Compete with EBNA2 for the binding to RBP-Jκ. EBNA3A and EBNA3C block the plasmablast differentiation program.	EBNA3A and EBNA3C are required for *in vitro* transformation of B cells. They can promote cell cycle and block apoptosis. EBNA3C blocks the ATR/Chk2-mediated DDR. EBNA3B acts as a tumor suppressor.
LMP1	Mimics CD40 signaling. Controls the activation of several signaling pathways, including NF-κB, JNK, p-38, ERK, PI3K, and JAK-STAT. Modulates many downstream targets. Induces UPR to boost its own expression. Induces changes in the expression profile similarly to the antigen-induced B cell activation. Can be released via extracellular vesicles, affecting the surrounding microenvironment.	Required for *in vitro* transformation of B cells. Acts as oncogene in *in vitro* and *in vivo* experiments. Promotes cell growth and proliferation while blocking apoptosis. Remodels cellular metabolism, potentiating glycolysis. Increases telomerase activity. Promotes tumor migration. Induces EGFR expression and epithelial-mesenchymal transition in NPC.

LMP2A, B	LMP2a mimics the B cell receptor signaling. It recruits Lyn and Syk to initiate signal transduction. Provides pro-survival signals which are required to sustain cell growth. In epithelial cells, it can negatively regulate LMP1 expression. LMP2B might augment LMP1 signaling and negatively regulate LMP2A activity	Both LMP2A and LMP2B are not essential for *in vitro* transformation of B cells, although they can provide a growth advantage. Promotes survival and blocks apoptosis. *In vivo*, LMP2A expression allows BCR-negative B cells to leave the bone marrow and reach the secondary lymphoid organs by constitutive activation of BCR transduction mediators. LMP2A supports tumorigenesis in a *in vivo* model of MYC-driven lymphomagenesis. Can affect normal B cell development. Can induce hyperproliferation and alter differentiation in epithelial cells.
Noncoding RNA	***Function***	***Role in oncogenesis***
EBERs	Can bind to AREs in the 3'UTR of transcripts. Can regulate LMP1 and LMP2 expression by binding to PAX5. Can modulate lytic replication by promoting IL-8 secretion. Induces IL-6 and IL-10 production by activation of the interferon response.	Not required for *in vitro* transformation of B cells. Accelerate cell growth in a strain-dependent manner. EBER-induced cytokine production has a positive autocrine effect in several EBV-associated malignancies.
BARTs	Negatively regulate the expression of several host genes, promoting immunoevasion. Negatively regulate antigen presentation. Can block lytic replication. Can target LMP1, LMP2A, BZLF1, and BALF5 transcripts. Can induce BCR desensitization by targeting downstream mediators of the BCR signaling.	Not required for *in vitro* transformation of B cells. Highly expressed in latently infected epithelial cells (including NPC, GC) and in EBV-infected primary effusion lymphoma. Promotes tumor growth in a *in vivo* model of GC. Can target tumor suppressor gene mRNAs for degradation. Block apoptosis and promote cell cycle progression. Supports migration and metastasis formation in *in vitro* and *in vivo* models of NPC and GC.
BHRF1	Can target latent gene mRNAs (EBNA2, LMP1, LMP2). Promote viral particle secretion by modulating SUMOylation. Can induce BCR desensitization by targeting downstream mediators of the BCR signaling. Can act as immunoevasin.	Lack of BHRF1 reduces *in vitro* transformation and *in vivo* infection. Block apoptosis and promote cell cycle progression. Downregulate PTEN and p27.

Table 4

List of targets which are Up- or downregulated (Absolute Fold change>2) and statistically significant (p-value<0.05) at 12h post infection

Gene names	p-value M81wt_NC (12hpi)	Fold change M81wt_NC (12hpi)
ZFP36L1	0.02	30.97
HMGCS1	0.02	9.95
CD47	0.04	8.68
NR4A3	0.01	8.06
CD83	0.04	5.32
SLC1A5	0.02	3.57
INPP5K	0.02	2.84
WDR55	0.01	2.64
COQ7	0.01	2.25
SQSTM1	0.02	2.10
TSPYL1	0.01	2.08
YME1L1	0.05	2.06
COMMD7	0.03	-2.28
MRPL45	0.02	-2.45
HLA-A	0.05	-2.60

Table 5

List of detected phospho-events which are upregulated (fold change>2), statistically significant (p value<0.05) and shared by different conditions.

	Protein	Position
Events in common to all three conditions	PPP1R18	368;368;43
	RBM7	205;84;204
Events in common to M81wt and VLP	AIM1	892;484
	MON1B	59
	DOCK2	1685;1177
	PRRC2C	2107;2105;2058;1862
	JUND	90
	SON	94
	DYNC1I2	81
	FAM134C	26
	DDX42	754;635
	CDC23	562;444
Events in common to M81wt and gp110ko	CDS2	23
	STAT3	704,705
	MAP2K4	80;91
Events in common to VLP and gp110ko	ZFP36	192;203;186
	ZFP36L2;ZFP36L1	490;334
	CXCR4	321;325
	TAF9	149
	PRKAG2	78;122
	ACIN1	400;342;360
	TRAPPC8	971

Bibliography

1. M. A. Epstein, B. G. Achong, Y. M. Barr, VIRUS PARTICLES IN CULTURED LYMPHOBLASTS FROM BURKITT'S LYMPHOMA. *Lancet (London, England)* **1**, 702–703 (1964).

2. B. Ehlers, *et al.*, Lymphocryptovirus phylogeny and the origins of Epstein-Barr virus. *J. Gen. Virol.* **91**, 630–642 (2010).

3. A. Moghaddam, J. Koch, B. Annis, F. Wang, Infection of Human B Lymphocytes with Lymphocryptoviruses Related to Epstein-Barr Virus. *J. Virol.* **72**, 3205 (1998).

4. C. Münz, Ed., *Epstein Barr Virus Volume 1* (Springer International Publishing, 2015).

5. T. Bakheet, E. Hitti, K. S. A. Khabar, ARED-Plus: An updated and expanded database of AU-rich element-containing mRNAs and pre-mRNAs. *Nucleic Acids Res.* **46**, D218–D220 (2018).

6. E. L. Thacker, F. Mirzaei, A. Ascherio, Infectious mononucleosis and risk for multiple sclerosis: a meta-analysis. *Ann. Neurol.* **59**, 499–503 (2006).

7. M. Biström, *et al.*, Epstein-Barr virus infection after adolescence and human herpesvirus 6A as risk factors for multiple sclerosis. *Eur. J. Neurol.* **28**, 579–586 (2021).

8. Y. Xu, *et al.*, Association of Infectious Mononucleosis in Childhood and Adolescence with Risk for a Subsequent Multiple Sclerosis Diagnosis among Siblings. *JAMA Netw. Open* **4** (2021).

9. K. Bjornevik, *et al.*, Longitudinal analysis reveals high prevalence of Epstein-Barr virus associated with multiple sclerosis. *Science (80-.).* **375**, 296–301 (2022).

10. G. Houen, N. H. Trier, Epstein-Barr Virus and Systemic Autoimmune Diseases. *Front. Immunol.* **11**, 587380 (2020).

11. W. Liu, *et al.*, Structures of capsid and capsid-associated tegument complex inside the Epstein-Barr virus. *Nat. Microbiol.* **5**, 1285–1298 (2020).

12. Z. Li, *et al.*, CryoEM structure of the tegumented capsid of Epstein-Barr virus. *Cell Res.* **30**, 873–884 (2020).

13. R. Germi, *et al.*, Three-dimensional structure of the Epstein-Barr virus capsid. *J. Gen. Virol.* **93**, 1769–1773 (2012).

14. T. Murata, "Encyclopedia of EBV-encoded lytic genes: An update" in *Advances in Experimental Medicine and Biology*, (Adv Exp Med Biol, 2018), pp. 395–412.

15. E. Johannsen, *et al.*, Proteins of purified Epstein-Barr virus. *Proc. Natl. Acad. Sci.* **101**, 16286–16291 (2004).

16. C. H. Hung, *et al.*, Interaction Between BGLF2 and BBLF1 Is Required for the Efficient Production of Infectious Epstein–Barr Virus Particles. *Front. Microbiol.* **10** (2020).

17. R. Feederle, *et al.*, Epstein-Barr virus BNRF1 protein allows efficient transfer from the endosomal compartment to the nucleus of primary B lymphocytes. *J. Virol.* **80**, 9435–43 (2006).

18. K. Tsai, N. Thikmyanova, J. A. Wojcechowskyj, H.-J. J. Delecluse, P. M. Lieberman, EBV tegument protein BNRF1 disrupts DAXX-ATRX to activate viral early gene transcription. *PLoS Pathog.* **7**, e1002376 (2011).

19.   B. S. Möhl, J. Chen, K. Sathiyamoorthy, T. S. Jardetzky, R. Longnecker, Structural and Mechanistic Insights into the Tropism of Epstein-Barr Virus. *Mol. Cells* **39**, 286–291 (2016).

20.   A. M. Gram, *et al.*, The Epstein-Barr Virus Glycoprotein gp150 Forms an Immune-Evasive Glycan Shield at the Surface of Infected Cells. *PLoS Pathog.* **12**, 1–28 (2016).

21.   L. L. Quinn, *et al.*, The Missing Link in Epstein-Barr Virus Immune Evasion: the BDLF3 Gene Induces Ubiquitination and Downregulation of Major Histocompatibility Complex Class I (MHC-I) and MHC-II. *J. Virol.* **90**, 356–367 (2016).

22.   H. Changotra, *et al.*, Epstein-Barr virus glycoprotein gM can interact with the cellular protein p32 and knockdown of p32 impairs virus. *Virology* **489**, 223–32 (2016).

23.   M. Gore, L. M. Hutt-Fletcher, The BDLF2 protein of Epstein-Barr virus is a type II glycosylated envelope protein whose processing is dependent on coexpression with the BMRF2 protein. *Virology* **383**, 162 (2009).

24.   L. M. Hutt-Fletcher, EBV glycoproteins: Where are we now? *Future Virol.* **10**, 1155–1162 (2015).

25.   P. M. Howley, D. M. Knipe, J. L. Cohen, B. A. Damania, *Fields Virology: DNA Viruses*, 7th Ed. (Wolters Kluwer Health, 2021) (August 19, 2022).

26.   A. Adams, T. Lindahl, Epstein-Barr virus genomes with properties of circular DNA molecules in carrier cells. *Proc. Natl. Acad. Sci. U. S. A.* **72**, 1477–1481 (1975).

27.   W. Hammerschmidt, B. Sugden, Identification and characterization of oriLyt, a lytic origin of DNA replication of Epstein-Barr virus. *Cell* **55**, 427–433 (1988).

28.   J. Yates, N. Warren, D. Reisman, B. Sugden, A cis-acting element from the Epstein-Barr viral genome that permits stable replication of recombinant plasmids in latently infected cells. *Proc. Natl. Acad. Sci. U. S. A.* **81**, 3806–3810 (1984).

29.   C. R. Kintner, B. Sugden, The structure of the termini of the DNA of Epstein-Barr virus. *Cell* **17**, 661–671 (1979).

30.   E. A. Hurley, D. A. Thorley-Lawson, B cell activation and the establishment of Epstein-Barr virus latency. *J. Exp. Med.* **168**, 2059 (1988).

31.   J. Zimmermann, W. Hammerschmidt, Structure and role of the terminal repeats of Epstein-Barr virus in processing and packaging of virion DNA. *J. Virol.* **69**, 3147–3155 (1995).

32.   K. Sathiyamoorthy, J. Chen, R. Longnecker, T. S. Jardetzky, The COMPLEXity in herpesvirus entry. *Curr. Opin. Virol.* **24**, 97–104 (2017).

33.   E. E. Heldwein, GH/gL supercomplexes at early stages of herpesvirus entry. *Curr. Opin. Virol.* **18**, 1–8 (2016).

34.   G. R. Nemerow, N. R. Cooper, Early events in the infection of human B lymphocytes by Epstein-Barr virus: the internalization process. *Virology* **132**, 186–198 (1984).

35.   J. Tanner, J. Weis, D. Fearon, Y. Whang, E. Kieff, Epstein-barr virus gp350/220 binding to the B lymphocyte C3d receptor mediates adsorption, capping, and endocytosis. *Cell* **50**, 203–213 (1987).

36.   H. Molina, *et al.*, Analysis of Epstein-Barr virus-binding sites on complement receptor 2 (CR2/CD21) using human-mouse chimeras and peptides: At least two distinct sites are necessary for ligand-receptor interaction. *J. Biol. Chem.* **266**, 12173–12179 (1991).

37.   H. Molina, *et al.*, Characterization of a complement receptor 2 (CR2, CD21) ligand binding site for C3: An initial model of ligand interaction with two linked short consensus repeat modules. *J. Immunol.* **154**, 5426–5435 (1995).

38.   J.-C. Carel, B. L. Myones, B. Frazier, V. M. Holers, Structural requirements for C3d,g/Epstein-Barr virus receptor (CR2/CD21) ligand binding, internalization, and viral infection. *J. Biol. Chem.* **265**, 12293–12299 (1990).

39.   G. Szakonyi, *et al.*, Structure of complement receptor 2 in complex with its C3d ligand. *Science (80-.).* **292**, 1725–1728 (2001).

40.   A. E. Prota, D. R. Sage, T. Stehle, J. D. Fingeroth, The crystal structure of human CD21: Implications for Epstein-Barr virus and C3d binding. *Proc. Natl. Acad. Sci. U. S. A.* **99**, 10641–10646 (2002).

41.   J. M. Ahearn, D. T. Fearon, Structure and Function of the Complement Receptors, CR1 (CD35) and CR2 (CD21). *Adv. Immunol.* **46**, 183–219 (1989).

42.   D. T. Fearon, R. H. Carter, The CD19/CR2/TAPA-1 complex of B lymphocytes: Linking natural to acquired immunity. *Annu. Rev. Immunol.* **13**, 127–149 (1995).

43.   M. Balbo, *et al.*, Pep34, a synthetic peptide whose sequence corresponds to the intracytoplasmic domain of the Epstein-Barr virus receptor (CR2, CD21), regulates human B lymphocyte proliferation triggered through CR2. *Mol. Immunol.* **32**, 1295–1298 (1995).

44.   S. Bouillie, M. Barel, R. Frade, Signaling through the Epstein-Barr virus/C3d receptor (gp140, CR2, CD21) in human B lymphocytes: Activation of phosphatidylinositol 3-kinase via a CD19 independent pathway. *Mol. Immunol.* **35**, 350 (1998).

45.   M. Barel, M. Le Romancer, R. Frade, Activation of the EBV/C3d Receptor (CR2, CD21) on Human B Lymphocyte Surface Triggers Tyrosine Phosphorylation of the 95-kDa Nucleolin and Its Interaction with Phosphatidylinositol 3 Kinase. *J. Immunol.* **166**, 3167–3173 (2001).

46.   M. Barel, M. Balbo, M. Le Romancer, R. Frade, Activation of Epstein-Barr virus/C3d receptor (gp140, CR2, CD21) on human cell surface triggers pp60src and Akt-GSK3 activities upstream and downstream to Pl 3-kinase, respectively. *Eur. J. Immunol.* **33**, 2557–2566 (2003).

47.   S. Lottin-Divoux, D. Jean, M. Le Romancer, R. Frade, Activation of Epstein-Barr virus/C3d receptor (gp140, CR2, CD21) on human B lymphoma cell surface triggers Cbl tyrosine phosphorylation, its association with p85 subunit, Crk-L and Syk and its dissociation with Vav. *Cell. Signal.* **18**, 1219–1225 (2006).

48.   M. S. Arredouani, *et al.*, Analysis of Host Gene Expression Changes Reveals Distinct Roles for the Cytoplasmic Domain of the Epstein-Barr Virus Receptor/CD21 in B-Cell Maturation, Activation, and Initiation of Virus Infection. *J. Virol.* **88**, 5559–5577 (2014).

49.   J. G. Ogembo, *et al.*, Human Complement Receptor Type 1/CD35 Is an Epstein-Barr Virus Receptor. *Cell Rep.* **3**, 371–385 (2013).

50.   Q. Li, *et al.*, Epstein-Barr virus uses HLA class II as a cofactor for infection of B lymphocytes. *J. Virol.* **71**, 4657–4662 (1997).

51.   K. M. Haan, W. W. Kwok, R. Longnecker, P. Speck, Epstein-Barr Virus Entry Utilizing HLA-DP or HLA-DQ as a Coreceptor. *J. Virol.* **74**, 2451–2454 (2000).

52.   R. Jiang, X. Gu, C. A. Nathan, L. Hutt-Fletcher, Laser-capture microdissection of oropharyngeal epithelium indicates restriction of Epstein-Barr virus receptor/CD21 mRNA to tonsil epithelial cells. *J. Oral Pathol. Med.* **37**, 626–633 (2008).

53. L. S. Chesnokova, S. L. Nishimura, L. M. Hutt-Fletcher, Fusion of epithelial cells by Epstein-Barr virus proteins is triggered by binding of viral glycoproteins gHgL to integrins alphavbeta6 or alphavbeta8. *Proc. Natl. Acad. Sci. U. S. A.* **106**, 20464–9 (2009).

54. L. S. Chesnokova, L. M. Hutt-Fletcher, Fusion of Epstein-Barr virus with epithelial cells can be triggered by αvβ5 in addition to αvβ6 and αvβ8, and integrin binding triggers a conformational change in glycoproteins gHgL. *J. Virol.* **85**, 13214–13223 (2011).

55. H. Matsuura, A. N. Kirschner, R. Longnecker, T. S. Jardetzky, Crystal structure of the Epstein-Barr virus (EBV) glycoprotein H/glycoprotein L (gH/gL) complex. *Proc. Natl. Acad. Sci. U. S. A.* **107**, 22641–22646 (2010).

56. J. Chen, *et al.*, Ephrin receptor A2 is a functional entry receptor for Epstein-Barr virus. *Nat. Microbiol.* **3**, 172–180 (2018).

57. H. Zhang, *et al.*, Ephrin receptor A2 is an epithelial cell receptor for Epstein-Barr virus entry. *Nat. Microbiol.* **3**, 164–171 (2018).

58. D. Xiong, *et al.*, Nonmuscle myosin heavy chain IIA mediates Epstein-Barr virus infection of nasopharyngeal epithelial cells. *Proc. Natl. Acad. Sci. U. S. A.* **112**, 11036–11041 (2015).

59. S. M. Tugizov, J. W. Berline, J. M. Palefsky, Epstein-Barr virus infection of polarized tongue and nasopharyngeal epithelial cells. *Nat. Med.* **9**, 307–314 (2003).

60. J. Xiao, J. M. Palefsky, R. Herrera, S. M. Tugizov, Characterization of the Epstein-Barr virus glycoprotein BMRF-2. *Virology* **359**, 382–396 (2007).

61. J. Xiao, J. M. Palefsky, R. Herrera, J. Berline, S. M. Tugizov, The Epstein-Barr virus BMRF-2 protein facilitates virus attachment to oral epithelial cells. *Virology* **370**, 430–42 (2008).

62. H.-B. B. Wang, *et al.*, Neuropilin 1 is an entry factor that promotes EBV infection of nasopharyngeal epithelial cells. *Nat. Commun.* **6**, 6240 (2015).

63. I. C. Zachary, How neuropilin-1 regulates receptor tyrosine kinase signalling: the knowns and known unknowns. *Biochem. Soc. Trans.* **39**, 1583–1591 (2011).

64. C. D. Shannon-Lowe, B. Neuhierl, G. Baldwin, A. B. Rickinson, H. J. Delecluse, Resting B cells as a transfer vehicle for Epstein-Barr virus infection of epithelial cells. *Proc. Natl. Acad. Sci. U. S. A.* **103**, 7065–7070 (2006).

65. C. Shannon-Lowe, M. Rowe, Epstein-Barr Virus Infection of Polarized Epithelial Cells Via the Basolateral Surface By Memory B Cell-Mediated Transfer Infection. *PLoS Pathog.* **7** (2011).

66. S. Imai, J. Nishikawa, K. Takada, Cell-to-cell contact as an efficient mode of Epstein-Barr virus infection of diverse human epithelial cells. *J. Virol.* **72**, 4371–4378 (1998).

67. C. Ni, *et al.*, In-cell infection: A novel pathway for Epstein-Barr virus infection mediated by cell-in-cell structures. *Cell Res.* **25**, 785–800 (2015).

68. A. M. Joseph, G. J. Babcock, D. A. Thorley-Lawson, Cells expressing the Epstein-Barr virus growth program are present in and restricted to the naive B-cell subset of healthy tonsils. *J. Virol.* **74**, 9964–9971 (2000).

69. G. J. Babcock, D. Hochberg, D. A. Thorley-Lawson, The expression pattern of Epstein-Barr virus latent genes in vivo is dependent upon the differentiation stage of the infected B cell. *Immunity* **13**, 497–506 (2000).

70. G. J. Babcock, L. L. Decker, M. Volk, D. A. Thorley-Lawson, EBV persistence in memory B cells in vivo. *Immunity* **9**, 395–404 (1998).

71. D. Hochberg, *et al.*, Acute Infection with Epstein-Barr Virus Targets and Overwhelms the Peripheral Memory B-Cell Compartment with Resting, Latently Infected Cells. *J. Virol.* **78**, 5194–5204 (2004).

72. E. M. Miyashita, B. Yang, G. J. Babcock, D. A. Thorley-Lawson, Identification of the site of Epstein-Barr virus persistence in vivo as a resting B cell. *J. Virol.* **71**, 4882–4891 (1997).

73. W. Henle, V. Diehl, G. Kohn, H. Zur Hausen, G. Henle, Herpes-type virus and chromosome marker in normal leukocytes after growth with irradiated Burkitt cells. *Science* **157**, 1064–1065 (1967).

74. J. H. Pope, M. K. Horne, W. Scott, Transformation of foetal human keukocytes in vitro by filtrates of a human leukaemic cell line containing herpes-like virus. *Int. J. cancer* **3**, 857–866 (1968).

75. D. A. Thorley-Lawson, K. P. Mann, Early events in Epstein-Barr virus infection provide a model for B cell activation. *J. Exp. Med.* **162**, 45–59 (1985).

76. S. Schlager, S. H. Speck, M. Woisetschläger, Transcription of the Epstein-Barr virus nuclear antigen 1 (EBNA1) gene occurs before induction of the BCR2 (Cp) EBNA gene promoter during the initial stages of infection in B cells. *J. Virol.* **70**, 3561–3570 (1996).

77. M. Woisetschlaeger, C. N. Yandava, L. A. Furmanski, J. L. Strominger, S. H. Speck, Promoter switching in Epstein-Barr virus during the initial stages of infection of B lymphocytes. *Proc. Natl. Acad. Sci. U. S. A.* **87**, 1725–1729 (1990).

78. C. Alfieri, M. Birkenbach, E. Kieff, Early events in Epstein-Barr virus infection of human B lymphocytes. *Virology* **181**, 595–608 (1991).

79. C. Shannon-Lowe, *et al.*, Epstein-Barr virus-induced B-cell transformation: Quantitating events from virus binding to cell outgrowth. *J. Gen. Virol.* **86**, 3009–3019 (2005).

80. M. Bodescot, M. Perricaudet, P. J. Farrell, A promoter for the highly spliced EBNA family of RNAs of Epstein-Barr virus. *J. Virol.* **61**, 3424–3430 (1987).

81. M. Woisetschlaeger, *et al.*, Role for the Epstein-Barr virus nuclear antigen 2 in viral promoter switching during initial stages of infection. *Proc. Natl. Acad. Sci. U. S. A.* **88**, 3942–3946 (1991).

82. R. Tierney, H. Kirby, J. Nagra, A. Rickinson, A. Bell, The Epstein-Barr virus promoter initiating B-cell transformation is activated by RFX proteins and the B-cell-specific activator protein BSAP/Pax5. *J. Virol.* **74**, 10458–10467 (2000).

83. R. Tierney, *et al.*, Epstein-Barr Virus Exploits BSAP/Pax5 To Achieve the B-Cell Specificity of Its Growth-Transforming Program. *J. Virol.* **81**, 10092–10100 (2007).

84. D. J. Hughes, C. A. Dickerson, M. S. Shaner, C. E. Sample, J. T. Sample, trans-Repression of protein expression dependent on the Epstein-Barr virus promoter Wp during latency. *J. Virol.* **85**, 11435–11447 (2011).

85. M. T. Puglielli, N. Desai, S. H. Speck, Regulation of EBNA gene transcription in lymphoblastoid cell lines: characterization of sequences downstream of BCR2 (Cp). *J. Virol.* **71**, 120–128 (1997).

86. T. Murata, *et al.*, Induction of Epstein-Barr Virus Oncoprotein LMP1 by Transcription Factors AP-2 and Early B Cell Factor. *J. Virol.* **90**, 3873–3889 (2016).

87. C. Demetriades, G. Mosialos, The LMP1 promoter can be transactivated directly by NF-kappaB. *J. Virol.* **83**, 5269–5277 (2009).

88. R. L. Skalsky, B. R. Cullen, EBV Noncoding RNAs. *Curr. Top. Microbiol. Immunol.* **391**, 181–217 (2015).

89. M. G. Doyle, D. Catovsky, D. H. Crawford, Infection of leukaemic B lymphocytes by Epstein Barr virus. *Leukemia* **7**, 1858–64 (1993).

90. E. Klein, N. Nagy, A. E. Rasul, EBV genome carrying B lymphocytes that express the nuclear protein EBNA-2 but not LMP-1: Type IIb latency. *Oncoimmunology* **2** (2013).

91. A. M. Price, *et al.*, Analysis of Epstein-Barr Virus-Regulated Host Gene Expression Changes through Primary B-Cell Outgrowth Reveals Delayed Kinetics of Latent Membrane Protein 1-Mediated NF- B Activation. *J. Virol.* **86**, 11096–11106 (2012).

92. A. M. Price, M. A. Luftig, To Be or Not IIb: A Multi-Step Process for Epstein-Barr Virus Latency Establishment and Consequences for B Cell Tumorigenesis. *PLoS Pathog.* **11**, 1–7 (2015).

93. B. C. Schaefer, J. L. Strominger, S. H. Speck, Redefining the Epstein-Barr virus-encoded nuclear antigen EBNA-1 gene promoter and transcription initiation site in group I Burkitt lymphoma cell lines. *Proc. Natl. Acad. Sci. U. S. A.* **92**, 10565–10569 (1995).

94. N. C, S. J, B. A, R. A, S. J, Transcription start sites downstream of the Epstein-Barr virus (EBV) Fp promoter in early-passage Burkitt lymphoma cells define a fourth promoter for expression of the EBV EBNA-1 protein. *J. Virol.* **70**, 623–627 (1996).

95. W. Wen, *et al.*, Epstein-Barr virus BZLF1 gene, a switch from latency to lytic infection, is expressed as an immediate-early gene after primary infection of B lymphocytes. *J. Virol.* **81**, 1037–1042 (2007).

96. M. Kalla, A. Schmeinck, M. Bergbauer, D. Pich, W. Hammerschmidt, AP-1 homolog BZLF1 of Epstein-Barr virus has two essential functions dependent on the epigenetic state of the viral genome. *Proc. Natl. Acad. Sci. U. S. A.* **107**, 850–855 (2010).

97. M. Kalla, C. Göbel, W. Hammerschmidt, The lytic phase of epstein-barr virus requires a viral genome with 5-methylcytosine residues in CpG sites. *J. Virol.* **86**, 447–458 (2012).

98. S. Jochum, R. Ruiss, A. Moosmann, W. Hammerschmidt, R. Zeidler, RNAs in Epstein-Barr virions control early steps of infection. *Proc. Natl. Acad. Sci. U. S. A.* (2012) https://doi.org/10.1073/pnas.1115906109.

99. S. Jochum, A. Moosmann, S. Lang, W. Hammerschmidt, R. Zeidler, The EBV immunoevasins vIL-10 and BNLF2a protect newly infected B cells from immune recognition and elimination. *PLoS Pathog.* **8** (2012).

100. Y. Sato, *et al.*, Elimination of LMP1-expressing cells from a monolayer of gastric cancer AGS cells. *Oncotarget* **8**, 39345–39355 (2017).

101. C. Wang, *et al.*, RNA Sequencing Analyses of Gene Expression during Epstein-Barr Virus Infection of Primary B Lymphocytes. *J. Virol.* **93** (2019).

102. T. Inagaki, *et al.*, Direct Evidence of Abortive Lytic Infection-Mediated Establishment of Epstein-Barr Virus Latency During B-Cell Infection. *Front. Microbiol.* **11** (2021).

103. M. Altmann, W. Hammerschmidt, Epstein-Barr virus provides a new paradigm: a requirement for the immediate inhibition of apoptosis. *PLoS Biol.* **3**, 1–10 (2005).

104. C.-C. Wu, *et al.*, Perspective: Contribution of Epstein–Barr virus (EBV) Reactivation to the Carcinogenicity of Nasopharyngeal Cancer Cells. *Cancers (Basel).* **10**, 120 (2018).

105. C. Münz, Latency and lytic replication in Epstein–Barr virus-associated oncogenesis. *Nat. Rev. Microbiol.* **17**, 691–700 (2019).

106. M. H. Tsai, *et al.*, Spontaneous Lytic Replication and Epitheliotropism Define an Epstein-Barr Virus Strain Found in Carcinomas. *Cell Rep.* **5**, 458–470 (2013).

107. L. M. Nutter, S. P. Grill, J. S. Li, R. S. Tan, Y. C. Cheng, Induction of virus enzymes by phorbol esters and n-butyrate in Epstein-Barr virus genome-carrying Raji cells. *Cancer Res.* **47**, 4407–4412 (1987).

108. K. Takada, Cross-linking of cell surface immunoglobulins induces Epstein-Barr virus in Burkitt lymphoma lines. *Int. J. cancer* **33**, 27–32 (1984).

109. T. Murata, *et al.*, Molecular Basis of Epstein-Barr Virus Latency Establishment and Lytic Reactivation. *Viruses* **13**, 2344 (2021).

110. T. O'Grady, *et al.*, Global bidirectional transcription of the Epstein-Barr virus genome during reactivation. *J. Virol.* **88**, 1604–1616 (2014).

111. A. J. Sinclair, bZIP proteins of human gammaherpesviruses. *J. Gen. Virol.* **84**, 1941–1949 (2003).

112. M. L. Stolz, C. McCormick, The bZIP Proteins of Oncogenic Viruses. *Viruses 2020, Vol. 12, Page 757* **12**, 757 (2020).

113. P. M. Lieberman,', J. M. Hardwick, J. Sample, G. S. Hayward,' And, S. D. Haywardlt, The zta transactivator involved in induction of lytic cycle gene expression in Epstein-Barr virus-infected lymphocytes binds to both AP-1 and ZRE sites in target promoter and enhancer regions. *J. Virol.* **64**, 1143–1155 (1990).

114. G. Urier, M. Buisson, P. Chambard, A. Sergeant, The Epstein-Barr virus early protein EB1 activates transcription from different responsive elements including AP-1 binding sites. *EMBO J.* **8**, 1447–1453 (1989).

115. P. M. Bhende, W. T. Seaman, H. J. Delecluse, S. C. Kenney, The EBV lytic switch protein, Z, preferentially binds to and activates the methylated viral genome. *Nat. Genet. 2004 3610* **36**, 1099–1104 (2004).

116. S. J. Dickerson, *et al.*, Methylation-dependent binding of the epstein-barr virus BZLF1 protein to viral promoters. *PLoS Pathog.* **5** (2009).

117. A. Woellmer, J. M. Arteaga-Salas, W. Hammerschmidt, BZLF1 governs CpG-methylated chromatin of Epstein-Barr Virus reversing epigenetic repression. *PLoS Pathog.* **8** (2012).

118. T. Tsurumi, M. Fujita, A. Kudoh, Latent and lytic Epstein-Barr virus replication strategies. *Rev. Med. Virol.* **15**, 3–15 (2005).

119. G. H, *et al.*, Characterization of an R-binding site mediating the R-induced activation of the Epstein-Barr virus BMLF1 promoter. *J. Virol.* **66**, 46–52 (1992).

120. E. Manet, A. Rigolet, H. Gruffat, J. françois Giot, A. Sergeant, Domains of the Epstein-Barr virus (EBV) transcription factor R required for dimerization, DNA binding and activation. *Nucleic Acids Res.* **19**, 2661–2667 (1991).

121. L. K. Chang, *et al.*, Activation of Sp1-mediated transcription by Rta of Epstein–Barr virus via an interaction with MCAF1. *Nucleic Acids Res.* **33**, 6528–6539 (2005).

122. A. R. Robinson, S. Sen Kwek, S. R. Hagemeier, C. K. Wille, S. C. Kenney, Cellular Transcription Factor Oct-1 Interacts with the Epstein-Barr Virus BRLF1 Protein To Promote Disruption of Viral

Latency. *J. Virol.* **85**, 8940–8953 (2011).

123. E. D. Fixman, G. S. Hayward, S. Diane Hayward, Replication of Epstein-Barr virus oriLyt: lack of a dedicated virally encoded origin-binding protein and dependence on Zta in cotransfection assays. *J. Virol.* **69**, 2998–3006 (1995).

124. M.-T. Su, *et al.*, Uracil DNA glycosylase BKRF3 contributes to Epstein-Barr virus DNA replication through physical interactions with proteins in viral DNA replication complex. *J. Virol.* **88**, 8883–8899 (2014).

125. A. Schepers, D. Pich, W. Hammerschmid, Activation oforiLyt,the Lytic Origin of DNA Replication of Epstein–Barr Virus, by BZLF1. *Virology* **220**, 367–376 (1996).

126. A. Kudoh, *et al.*, Reactivation of lytic replication from B cells latently infected with Epstein-Barr virus occurs with high S-phase cyclin-dependent kinase activity while inhibiting cellular DNA replication. *J. Virol.* **77**, 851–861 (2003).

127. A. M. Makhov, D. Subramanian, E. Holley-Guthrie, S. C. Kenney, J. D. Griffith, The Epstein-Barr virus polymerase accessory factor BMRF1 adopts a ring-shaped structure as visualized by electron microscopy. *J. Biol. Chem.* **279**, 40358–40361 (2004).

128. A. Chakravorty, B. Sugden, E. C. Johannsen, An Epigenetic Journey: Epstein-Barr Virus Transcribes Chromatinized and Subsequently Unchromatinized Templates during Its Lytic Cycle. *J. Virol.* **93** (2019).

129. V. Aubry, *et al.*, Epstein-Barr Virus Late Gene Transcription Depends on the Assembly of a Virus-Specific Preinitiation Complex. *J. Virol.* **88**, 12825–12838 (2014).

130. H. Gruffat, F. Kadjouf, B. Mariamé, E. Manet, The Epstein-Barr Virus BcRF1 Gene Product Is a TBP-Like Protein with an Essential Role in Late Gene Expression. *J. Virol.* **86**, 6023–6032 (2012).

131. H. Gruffat, R. Marchione, E. Manet, Herpesvirus late gene expression: A viral-specific pre-initiation complex is key. *Front. Microbiol.* **7**, 869 (2016).

132. T. Watanabe, *et al.*, The Epstein-Barr Virus BDLF4 Gene Is Required for Efficient Expression of Viral Late Lytic Genes. *J. Virol.* **89**, 10120–10124 (2015).

133. J. Li, A. Walsh, T. K. T. Lam, H. J. Delecluse, A. El-Guindy, A single phosphoacceptor residue in BGLF3 is essential for transcription of Epstein-Barr virus late genes. *PLOS Pathog.* **15**, e1007980 (2019).

134. Y. Sato, *et al.*, S-Like-Phase Cyclin-Dependent Kinases Stabilize the Epstein-Barr Virus BDLF4 Protein To Temporally Control Late Gene Transcription. *J. Virol.* **93** (2019).

135. S.-H. Chiu, *et al.*, Epstein-Barr virus BALF3 has nuclease activity and mediates mature virion production during the lytic cycle. *J. Virol.* **88**, 4962–4975 (2014).

136. G. S. Taylor, H. M. Long, J. M. Brooks, A. B. Rickinson, A. D. Hislop, The immunology of Epstein-Barr virus-induced disease. *Annu. Rev. Immunol.* **33**, 787–821 (2015).

137. S. G. Tangye, U. Palendira, E. S. J. Edwards, Human immunity against EBV—lessons from the clinic. *J. Exp. Med.* **214**, 269–283 (2017).

138. B. Fournier, S. Latour, Immunity to EBV as revealed by immunedeficiencies. *Curr. Opin. Immunol.* **72**, 107–115 (2021).

139. S. K. Dunmire, K. A. Hogquist, H. H. Balfour, "Infectious mononucleosis" in *Current Topics in*

Microbiology and Immunology, (Springer Verlag, 2015), pp. 211–240.

140.   H. H. Balfour, S. K. Dunmire, K. A. Hogquist, Infectious mononucleosis. *Clin. Transl. Immunol.* **4**, e33 (2015).

141.   K. A. McAulay, *et al.*, HLA class I polymorphisms are associated with development of infectious mononucleosis upon primary EBV infection. *J. Clin. Invest.* **117**, 3042–3048 (2007).

142.   H. Hjalgrim, *et al.*, HLA-A alleles and infectious mononucleosis suggest a critical role for cytotoxic T-cell response in EBV-related Hodgkin lymphoma. *Proc. Natl. Acad. Sci. U. S. A.* **107**, 6400–6405 (2010).

143.   A. Jabłońska, *et al.*, TLR4 896A/G and TLR9 1174G/A polymorphisms are associated with the risk of infectious mononucleosis. *Sci. Rep.* **10** (2020).

144.   T. Azzi, *et al.*, Role for early-differentiated natural killer cells in infectious mononucleosis. *Blood* **124**, 2533–2543 (2014).

145.   S. K. Dunmire, J. M. Grimm, D. O. Schmeling, H. H. Balfour, K. A. Hogquist, The Incubation Period of Primary Epstein-Barr Virus Infection: Viral Dynamics and Immunologic Events. *PLoS Pathog.* **11** (2015).

146.   Z. Djaoud, *et al.*, Two alternate strategies for innate immunity to Epstein-Barr virus: One using NK cells and the other NK cells and γδ T cells. *J. Exp. Med.* **214**, 1827–1841 (2017).

147.   M. F. C. Callan, *et al.*, Large clonal expansions of CD8+ T cells in acute infectious mononucleosis. *Nat. Med. 1996 28* **2**, 906–911 (1996).

148.   M. F. C. Callan, *et al.*, Direct visualization of antigen-specific CD8+ T cells during the primary immune response to Epstein-Barr virus In vivo. *J. Exp. Med.* **187**, 1395–1402 (1998).

149.   M. F. C. Callan, *et al.*, CD8+ T-cell selection, function, and death in the primary immune response in vivo. *J. Clin. Invest.* **106**, 1251 (2000).

150.   a Leen, *et al.*, Differential immunogenicity of Epstein-Barr virus latent-cycle proteins for human CD4(+) T-helper 1 responses. *J. Virol.* **75**, 8649–8659 (2001).

151.   H. M. Long, *et al.*, CD4+ T-cell responses to Epstein-Barr virus (EBV) latent-cycle antigens and the recognition of EBV-transformed lymphoblastoid cell lines. *J. Virol.* **79**, 4896–4907 (2005).

152.   I. Y. Pappworth, E. C. Wang, M. Rowe, The Switch from Latent to Productive Infection in Epstein-Barr Virus-Infected B Cells Is Associated with Sensitization to NK Cell Killing. *J. Virol.* **81**, 474 (2007).

153.   B. K. Chung, *et al.*, Innate immune control of EBV-infected B cells by invariant natural killer T cells. *Blood* **122**, 2600–2608 (2013).

154.   H. Yuling, *et al.*, EBV-induced human CD8+ NKT cells suppress tumorigenesis by EBV-associated malignancies. *Cancer Res.* **69**, 7935–7944 (2009).

155.   Z. Djaoud, P. Parham, Dimorphism in the TCRγ-chain repertoire defines 2 types of human immunity to Epstein-Barr virus. *Blood Adv.* **4**, 1198–1205 (2020).

156.   C. Münz, Co-Stimulatory Molecules during Immune Control of Epstein Barr Virus Infection. *Biomolecules* **12**, 38 (2021).

157.   A. Lünemann, L. D. Vanoaica, T. Azzi, D. Nadal, C. Münz, A distinct subpopulation of human NK cells restricts B cell transformation by EBV. *J. Immunol.* **191**, 4989–4995 (2013).

158. A. Jud, *et al.*, Tonsillar CD56brightNKG2A+ NK cells restrict primary Epstein-Barr virus infection in B cells via IFN-γ. *Oncotarget* **8**, 6130–6141 (2017).

159. V. Schuster, M. Herold, H. Wachter, G. Reibnegger, Serum concentrations of interferon gamma, interleukin-6 and neopterin in patients with infectious mononucleosis and other Epstein-Barr virus-related lymphoproliferative diseases. *Infection* **21**, 210–213 (1993).

160. M. W. Hornef, H. J. Wagner, A. Kruse, H. Kirchner, Cytokine production in a whole-blood assay after Epstein-Barr virus infection in vivo. *Clin. Diagn. Lab. Immunol.* **2**, 209–213 (1995).

161. A. Biglino, *et al.*, Serum cytokine profiles in acute primary HIV-1 infection and in infectious mononucleosis. *Clin. Immunol. Immunopathol.* **78**, 61–69 (1996).

162. V. Wright-Browne, *et al.*, Serum Cytokine Levels in Infectious Mononucleosis at Diagnosis and Convalescence. *Leuk. Lymphoma* **30**, 583–589 (1998).

163. H. H. Balfour, *et al.*, Behavioral, virologic, and immunologic factors associated with acquisition and severity of primary epstein-barr virus infection in university students. *J. Infect. Dis.* **207**, 80–88 (2013).

164. O. A. Odumade, K. A. Hogquist, H. H. Balfour, Progress and problems in understanding and managing primary epstein-barr virus infections. *Clin. Microbiol. Rev.* **24**, 193–209 (2011).

165. J. M. Middeldorp, *Epstein-barr virus-specific humoral immune responses in health and disease* (2015).

166. S. J. Frank, *et al.*, Regions of the JAK2 tyrosine kinase required for coupling to the growth hormone receptor. *J. Biol. Chem.* **270**, 14776–14785 (1995).

167. L. Velazquez, *et al.*, Distinct domains of the protein tyrosine kinase tyk2 required for binding of interferon-alpha/beta and for signal transduction. *J. Biol. Chem.* **270**, 3327–3334 (1995).

168. R. Ferrao, P. J. Lupardus, The Janus Kinase (JAK) FERM and SH2 domains: Bringing specificity to JAK-receptor interactions. *Front. Endocrinol. (Lausanne).* **8**, 71 (2017).

169. D. Ungureanu, *et al.*, The pseudokinase domain of JAK2 is a dual-specificity protein kinase that negatively regulates cytokine signaling. *Nat. Struct. Mol. Biol.* **18**, 971–976 (2011).

170. P. Saharinen, K. Takaluoma, O. Silvennoinen, Regulation of the Jak2 tyrosine kinase by its pseudokinase domain. *Mol. Cell. Biol.* **20**, 3387–3395 (2000).

171. P. Saharinen, O. Silvennoinen, The pseudokinase domain is required for suppression of basal activity of Jak2 and Jak3 tyrosine kinases and for cytokine-inducible activation of signal transduction. *J. Biol. Chem.* **277**, 47954–47963 (2002).

172. X. Hu, J. Li, M. Fu, X. Zhao, W. Wang, The JAK/STAT signaling pathway: from bench to clinic. *Signal Transduct. Target. Ther.* **6**, 402 (2021).

173. E. Bousoik, H. Montazeri Aliabadi, "Do We Know Jack" About JAK? A Closer Look at JAK/STAT Signaling Pathway. *Front. Oncol.* **8**, 287 (2018).

174. A. Tesoriere, A. Dinarello, F. Argenton, The Roles of Post-Translational Modifications in STAT3 Biological Activities and Functions. *Biomedicines* **9** (2021).

175. M. Parrini, *et al.*, The C-Terminal Transactivation Domain of STAT1 Has a Gene-Specific Role in Transactivation and Cofactor Recruitment. *Front. Immunol.* **9** (2018).

176. A. Majoros, *et al.*, Canonical and Non-Canonical Aspects of JAK-STAT Signaling: Lessons from Interferons for Cytokine Responses. *Front. Immunol.* **8**, 29 (2017).

177. J. J. Babon, I. S. Lucet, J. M. Murphy, N. A. Nicola, L. N. Varghese, The molecular regulation of Janus kinase (JAK) activation. *Biochem. J.* **462**, 1–13 (2014).

178. S. Akira, *et al.*, Molecular cloning of APRF, a novel IFN-stimulated gene factor 3 p91-related transcription factor involved in the gp130-mediated signaling pathway. *Cell* **77**, 63–71 (1994).

179. Z. Zhong, Z. Wen, J. E. Darnell, Stat3: a STAT family member activated by tyrosine phosphorylation in response to epidermal growth factor and interleukin-6. *Science* **264**, 95–98 (1994).

180. T. P. Vogel, J. D. Milner, M. A. Cooper, The Ying and Yang of STAT3 in Human Disease. *J. Clin. Immunol.* **35**, 615–23 (2015).

181. T. S. Schaefer, L. K. Sanders, D. Nathans, Cooperative transcriptional activity of Jun and Stat3 beta, a short form of Stat3. *Proc. Natl. Acad. Sci. U. S. A.* **92**, 9097–9101 (1995).

182. E. Caldenhoven, *et al.*, STAT3beta, a splice variant of transcription factor STAT3, is a dominant negative regulator of transcription. *J. Biol. Chem.* **271**, 13221–13227 (1996).

183. H. Shao, A. J. Quintero, D. J. Tweardy, Identification and characterization of cis elements in the STAT3 gene regulating STAT3 alpha and STAT3 beta messenger RNA splicing. *Blood* **98**, 3853–3856 (2001).

184. A. Chakraborty, D. J. Tweardy, Granulocyte colony-stimulating factor activates a 72-kDa isoform of STAT3 in human neutrophils. *J. Leukoc. Biol.* **64**, 675–680 (1998).

185. D. L. Hevehan, W. M. Miller, E. T. Papoutsakis, Differential expression and phosphorylation of distinct STAT3 proteins during granulocytic differentiation. *Blood* **99**, 1627–1637 (2002).

186. D. Maritano, *et al.*, The STAT3 isoforms alpha and beta have unique and specific functions. *Nat. Immunol.* **5**, 401–409 (2004).

187. O. K. Park, T. S. Schaefer, D. Nathans, In vitro activation of Stat3 by epidermal growth factor receptor kinase. *Proc. Natl. Acad. Sci. U. S. A.* **93**, 13704–13708 (1996).

188. K. Takeda, *et al.*, Targeted disruption of the mouse Stat3 gene leads to early embryonic lethality. *Proc. Natl. Acad. Sci. U. S. A.* **94**, 3801–3804 (1997).

189. J. Y. Yoo, D. L. Huso, D. Nathans, S. Desiderio, Specific Ablation of Stat3β Distorts the Pattern of Stat3-Responsive Gene Expression and Impairs Recovery from Endotoxic Shock. *Cell* **108**, 331–344 (2002).

190. K. S. Chan, *et al.*, Epidermal Growth Factor Receptor-Mediated Activation of Stat3 during Multistage Skin Carcinogenesis. *Cancer Res.* **64**, 2382–2389 (2004).

191. F. M. Uckun, S. Qazi, H. Ma, L. Tuel-Ahlgren, Z. Ozer, STAT3 is a substrate of SYK tyrosine kinase in B-lineage leukemia/lymphoma cells exposed to oxidative stress. *Proc. Natl. Acad. Sci. U. S. A.* **107**, 2902 (2010).

192. T. Oellerich, *et al.*, β2 integrin–derived signals induce cell survival and proliferation of AML blasts by activating a Syk/STAT signaling axis. *Blood* **121**, 3889–3899 (2013).

193. C. Paiva, *et al.*, SYK inhibition thwarts the BAFF - B-cell receptor crosstalk and thereby antagonizes Mcl-1 in chronic lymphocytic leukemia. *Haematologica* **102**, 1890–1900 (2017).

194. G. M. Delgoffe, D. A. A. Vignali, STAT heterodimers in immunity. *JAK-STAT* **2**, e23060 (2013).

195. M. S. Wake, C. J. Watson, STAT3 the oncogene - still eluding therapy? *FEBS J.* **282**, 2600–2611 (2015).

196. V. Cimica, H. C. Chen, J. K. Iyer, N. C. Reich, Dynamics of the STAT3 transcription factor: nuclear import dependent on Ran and importin-β1. *PLoS One* **6** (2011).

197. J. Yang, *et al.*, Unphosphorylated STAT3 accumulates in response to IL-6 and activates transcription by binding to NFkappaB. *Genes Dev.* **21**, 1396–1408 (2007).

198. O. A. Timofeeva, *et al.*, Mechanisms of unphosphorylated STAT3 transcription factor binding to DNA. *J. Biol. Chem.* **287**, 14192–14200 (2012).

199. A. Nishimoto, *et al.*, JAB1 regulates unphosphorylated STAT3 DNA-binding activity through protein-protein interaction in human colon cancer cells. *Biochem. Biophys. Res. Commun.* **438**, 513–518 (2013).

200. Z. Wen, Z. Zhong, J. E. Darnell, Maximal activation of transcription by Stat1 and Stat3 requires both tyrosine and serine phosphorylation. *Cell* **82**, 241–250 (1995).

201. H. Kim, H. Baumann, The Carboxyl-terminal Region of STAT3 Controls Gene Induction by the Mouse Haptoglobin Promoter. *J. Biol. Chem.* **272**, 14571–14579 (1997).

202. J. J. Schuringa, A. T. J. Wierenga, W. Kruijer, E. Vellenga, Constitutive Stat3, Tyr705, and Ser727 phosphorylation in acute myeloid leukemia cells caused by the autocrine secretion of interleukin-6. *Blood* **95**, 3765–3770 (2000).

203. J. Chung, E. Uchida, T. C. Grammer, J. Blenis, STAT3 serine phosphorylation by ERK-dependent and -independent pathways negatively modulates its tyrosine phosphorylation. *Mol. Cell. Biol.* **17**, 6508–6516 (1997).

204. J. Wegrzyn, *et al.*, Function of mitochondrial Stat3 in cellular respiration. *Science* **323**, 793–797 (2009).

205. E. Macias, D. Rao, S. Carbajal, K. Kiguchi, J. Digiovanni, Stat3 binds to mtDNA and regulates mitochondrial gene expression in keratinocytes. *J. Invest. Dermatol.* **134**, 1971–1980 (2014).

206. J. A. Meier, A. C. Larner, Toward a new STATe: The role of STATs in mitochondrial function. *Semin. Immunol.* **26**, 20–28 (2014).

207. E. Carbognin, R. M. Betto, M. E. Soriano, A. G. Smith, G. Martello, Stat3 promotes mitochondrial transcription and oxidative respiration during maintenance and induction of naive pluripotency. *EMBO J.* **35**, 618–634 (2016).

208. D. J. Gough, L. Koetz, D. E. Levy, The MEK-ERK pathway is necessary for serine phosphorylation of mitochondrial STAT3 and Ras-mediated transformation. *PLoS One* **8** (2013).

209. M. Peron, *et al.*, Y705 and S727 are required for the mitochondrial import and transcriptional activities of STAT3, and for regulation of stem cell proliferation. *Development* **148** (2021).

210. L. Avalle, *et al.*, STAT3 localizes to the ER, acting as a gatekeeper for ER-mitochondrion Ca 2+ fluxes and apoptotic responses. *Cell Death Differ.* **26**, 932–942 (2019).

211. D. A. Frank, STAT3 as a central mediator of neoplastic cellular transformation. *Cancer Lett.* **251**, 199–210 (2007).

212. J. C. Roeser, S. D. Leach, F. McAllister, Emerging strategies for cancer immunoprevention. *Oncogene* **34**, 6029–6039 (2015).

213. P. Coppo, *et al.*, BCR-ABL activates STAT3 via JAK and MEK pathways in human cells. *Br. J. Haematol.* **134**, 171–179 (2006).

214. H. L. M. Koskela, *et al.*, Somatic STAT3 mutations in large granular lymphocytic leukemia. *N. Engl. J.*

Med. **366**, 1905–1913 (2012).

215. C. Küçük, *et al.*, Activating mutations of STAT5B and STAT3 in lymphomas derived from γδ-T or NK cells. *Nat. Commun.* **6** (2015).

216. E. Andersson, *et al.*, Activating somatic mutations outside the SH2-domain of STAT3 in LGL leukemia. *Leukemia* **30**, 1204–1208 (2016).

217. D. E. Johnson, R. A. O'Keefe, J. R. Grandis, Targeting the IL-6/JAK/STAT3 signalling axis in cancer. *Nat. Rev. Clin. Oncol.* **15**, 234–248 (2018).

218. C.-Y. Loh, *et al.*, Signal Transducer and Activator of Transcription (STATs) Proteins in Cancer and Inflammation: Functions and Therapeutic Implication. *Front. Oncol.* **9**, 48 (2019).

219. F. Zhu, K. B. Wang, L. Rui, STAT3 Activation and Oncogenesis in Lymphoma. *Cancers (Basel).* **12** (2019).

220. H.-Q. Wang, *et al.*, STAT3 pathway in cancers: Past, present, and future. *MedComm* **3**, e124 (2022).

221. P. L. Ho, E. J. Lay, W. Jian, D. Parra, K. S. Chan, Stat3 activation in urothelial stem cells leads to direct progression to invasive bladder cancer. *Cancer Res.* **72**, 3135–3142 (2012).

222. I. Kryczek, *et al.*, IL-22(+)CD4(+) T cells promote colorectal cancer stemness via STAT3 transcription factor activation and induction of the methyltransferase DOT1L. *Immunity* **40**, 772–784 (2014).

223. P. L. Leong, *et al.*, Targeted inhibition of Stat3 with a decoy oligonucleotide abrogates head and neck cancer cell growth. *Proc. Natl. Acad. Sci. U. S. A.* **100**, 4138–4143 (2003).

224. Y. Li, *et al.*, Activation of the signal transducers and activators of the transcription 3 pathway in alveolar epithelial cells induces inflammation and adenocarcinomas in mouse lung. *Cancer Res.* **67**, 8494–8503 (2007).

225. A. Fukuda, *et al.*, Stat3 and MMP7 contribute to pancreatic ductal adenocarcinoma initiation and progression. *Cancer Cell* **19**, 441–455 (2011).

226. J. Abdulghani, *et al.*, Stat3 promotes metastatic progression of prostate cancer. *Am. J. Pathol.* **172**, 1717–1728 (2008).

227. D. J. Kim, J. M. Angel, S. Sano, J. DiGiovanni, Constitutive activation and targeted disruption of signal transducer and activator of transcription 3 (Stat3) in mouse epidermis reveal its critical role in UVB-induced skin carcinogenesis. *Oncogene* **28**, 950–960 (2009).

228. M. Sen, *et al.*, Targeting Stat3 abrogates EGFR inhibitor resistance in cancer. *Clin. Cancer Res.* **18**, 4986–4996 (2012).

229. H. J. Lee, *et al.*, Drug resistance via feedback activation of Stat3 in oncogene-addicted cancer cells. *Cancer Cell* **26**, 207–221 (2014).

230. C. Rébé, F. Ghiringhelli, STAT3, a Master Regulator of Anti-Tumor Immune Response. *Cancers (Basel).* **11**, 1280 (2019).

231. L. Zhang, *et al.*, Signal transducer and activator of transcription 3 signaling in tumor immune evasion. *Pharmacol. Ther.* **230**, 107969 (2022).

232. Y. Minegishi, Hyper-IgE syndrome, 2021 update. *Allergol. Int.* **70**, 407–414 (2021).

233. C. Speckmann, *et al.*, Reduced memory B cells in patients with hyper IgE syndrome. *Clin. Immunol.*

129, 448–454 (2008).

234. A. Meyer-Bahlburg, *et al.*, Heterozygous signal transducer and activator of transcription 3 mutations in hyper-IgE syndrome result in altered B-cell maturation. *J. Allergy Clin. Immunol.* **129** (2012).

235. D. T. Avery, *et al.*, B cell-intrinsic signaling through IL-21 receptor and STAT3 is required for establishing long-lived antibody responses in humans. *J. Exp. Med.* **207**, 155–171 (2010).

236. Y. Minegishi, *et al.*, Molecular explanation for the contradiction between systemic Th17 defect and localized bacterial infection in hyper-IgE syndrome. *J. Exp. Med.* **206**, 1291 (2009).

237. B. Park, G. Y. Liu, Staphylococcus aureus and Hyper-IgE Syndrome. *Int. J. Mol. Sci.* **21**, 1–12 (2020).

238. G. F. Sonnenberg, L. A. Fouser, D. Artis, Border patrol: regulation of immunity, inflammation and tissue homeostasis at barrier surfaces by IL-22. *Nat. Immunol.* **12**, 383–390 (2011).

239. A. M. Siegel, *et al.*, A critical role for STAT3 transcription factor signaling in the development and maintenance of human T cell memory. *Immunity* **35**, 806 (2011).

240. S. E. Flanagan, *et al.*, Activating germline mutations in STAT3 cause early-onset multi-organ autoimmune disease. *Nat. Genet. 2014 468* **46**, 812–814 (2014).

241. E. M. Haapaniemi, *et al.*, Autoimmunity, hypogammaglobulinemia, lymphoproliferation, and mycobacterial disease in patients with activating mutations in STAT3. *Blood* **125**, 639–648 (2015).

242. J. D. Milner, *et al.*, Early-onset lymphoproliferation and autoimmunity caused by germline STAT3 gain-of-function mutations. *Blood* **125**, 591–599 (2015).

243. V. L. Bryant, *et al.*, Cytokine-mediated regulation of human B cell differentiation into Ig-secreting cells: predominant role of IL-21 produced by CXCR5+ T follicular helper cells. *J. Immunol.* **179**, 8180–8190 (2007).

244. E. K. Deenick, *et al.*, Naive and memory human B cells have distinct requirements for STAT3 activation to differentiate into antibody-secreting plasma cells. *J. Exp. Med.* **210**, 2739–2753 (2013).

245. C. Ding, *et al.*, STAT3 Signaling in B Cells Is Critical for Germinal Center Maintenance and Contributes to the Pathogenesis of Murine Models of Lupus. *J. Immunol.* **196**, 4477–4486 (2016).

246. A. Kane, A. Lau, R. Brink, S. G. Tangye, E. K. Deenick, B-cell–specific STAT3 deficiency: Insight into the molecular basis of autosomal-dominant hyper-IgE syndrome. *J. Allergy Clin. Immunol.* **138**, 1455-1458.e3 (2016).

247. E. K. Deenick, S. J. Pelham, A. Kane, C. S. Ma, Signal Transducer and Activator of Transcription 3 Control of Human T and B Cell Responses. *Front. Immunol.* **9**, 168 (2018).

248. M. Saito, *et al.*, Defective IL-10 signaling in hyper-IgE syndrome results in impaired generation of tolerogenic dendritic cells and induced regulatory T cells. *J. Exp. Med.* **208**, 235–249 (2011).

249. A. Cavani, *et al.*, Human CD4+ T lymphocytes with remarkable regulatory functions on dendritic cells and nickel-specific Th1 immune responses. *J. Invest. Dermatol.* **114**, 295–302 (2000).

250. K. Itoh, S. Hirohata, The role of IL-10 in human B cell activation, proliferation, and differentiation. *J. Immunol.* **154**, 4341–50 (1995).

251. S. V. Kuchipudi, The Complex Role of STAT3 in Viral Infections. *J. Immunol. Res.* **2015**, 1–9 (2015).

252. A. A. Roca Suarez, N. Van Renne, T. F. Baumert, J. Lupberger, Viral manipulation of STAT3: Evade,

exploit, and injure. *PLoS Pathog.* **14**, e1006839 (2018).

253.   Z. Chang, Y. Wang, X. Zhou, J. E. Long, STAT3 roles in viral infection: Antiviral or proviral? *Future Virol.* **13**, 557–574 (2018).

254.   E. Slinger, *et al.*, HCMV-encoded chemokine receptor US28 mediates proliferative signaling through the IL-6-STAT3 axis. *Sci. Signal.* **3** (2010).

255.   M. J. Raftery, *et al.*, Shaping phenotype, function, and survival of dendritic cells by cytomegalovirus-encoded IL-10. *J. Immunol.* **173**, 3383–3391 (2004).

256.   J. V. Spencer, The cytomegalovirus homolog of interleukin-10 requires phosphatidylinositol 3-kinase activity for inhibition of cytokine synthesis in monocytes. *J. Virol.* **81**, 2083–2086 (2007).

257.   X. Wan, H. Wang, J. Nicholas, Human herpesvirus 8 interleukin-6 (vIL-6) signals through gp130 but has structural and receptor-binding properties distinct from those of human IL-6. *J. Virol.* **73**, 8268–8278 (1999).

258.   N. Sen, *et al.*, Signal transducer and activator of transcription 3 (STAT3) and survivin induction by varicella-zoster virus promote replication and skin pathogenesis. *Proc. Natl. Acad. Sci. U. S. A.* **109**, 600–605 (2012).

259.   J. J. Docherty, T. J. Sweet, E. Bailey, S. A. Faith, T. Booth, Resveratrol inhibition of varicella-zoster virus replication in vitro. *Antiviral Res.* **72**, 171–177 (2006).

260.   S. Koganti, A. de la Paz, A. F. Freeman, S. Bhaduri-McIntosh, B lymphocytes from patients with a hypomorphic mutation in STAT3 resist Epstein-Barr virus-driven cell proliferation. *J. Virol.* **88**, 516–24 (2014).

261.   A. S. Punjabi, P. A. Carroll, L. Chen, M. Lagunoff, Persistent Activation of STAT3 by Latent Kaposi's Sarcoma-Associated Herpesvirus Infection of Endothelial Cells. *J. Virol.* **81**, 2449–2458 (2007).

262.   S. Koganti, *et al.*, STAT3 interrupts ATR-Chk1 signaling to allow oncovirus-mediated cell proliferation. *Proc. Natl. Acad. Sci. U. S. A.* **111**, 4946–51 (2014).

263.   S. Koganti, S. Burgula, S. Bhaduri-McIntosh, STAT3 activates the anti-apoptotic form of caspase 9 in oncovirus-infected B lymphocytes. *Virology* **540**, 160–164 (2020).

264.   H. Chen, L. Hutt-Fletcher, L. Cao, S. D. Hayward, A Positive Autoregulatory Loop of LMP1 Expression and STAT Activation in Epithelial Cells Latently Infected with Epstein-Barr Virus. *J. Virol.* **77**, 4139–4148 (2003).

265.   C.-P. Kung, N. Raab-Traub, Epstein-Barr virus latent membrane protein 1 induces expression of the epidermal growth factor receptor through effects on Bcl-3 and STAT3. *J. Virol.* **82**, 5486–5493 (2008).

266.   C.-P. Kung, D. G. Meckes, N. Raab-Traub, Epstein-Barr virus LMP1 activates EGFR, STAT3, and ERK through effects on PKCdelta. *J. Virol.* **85**, 4399–4408 (2011).

267.   R. Muromoto, *et al.*, Epstein-Barr virus-derived EBNA2 regulates STAT3 activation. *Biochem. Biophys. Res. Commun.* **378**, 439–443 (2009).

268.   D. Daigle, *et al.*, Upregulation of STAT3 Marks Burkitt Lymphoma Cells Refractory to Epstein-Barr Virus Lytic Cycle Induction by HDAC Inhibitors. *J. Virol.* **84**, 993–1004 (2010).

269.   E. R. Hill, *et al.*, Signal Transducer and Activator of Transcription 3 Limits Epstein-Barr Virus Lytic Activation in B Lymphocytes. *J. Virol.* **87**, 11438–11446 (2013).

270.   S. Koganti, *et al.*, Cellular STAT3 Functions via PCBP2 To Restrain Epstein-Barr Virus Lytic Activation in B Lymphocytes. *J. Virol.* **89**, 5002–5011 (2015).

271.   X. Liu, T. Sadaoka, T. Krogmann, J. I. Cohen, Epstein-Barr Virus (EBV) Tegument Protein BGLF2 Suppresses Type I Interferon Signaling To Promote EBV Reactivation. *J. Virol.* **94** (2020).

272.   J. Han, J. D. Lee, L. Bibbs, R. J. Ulevitch, A MAP kinase targeted by endotoxin and hyperosmolarity in mammalian cells. *Science* **265**, 808–811 (1994).

273.   J. Rouse, *et al.*, A novel kinase cascade triggered by stress and heat shock that stimulates MAPKAP kinase-2 and phosphorylation of the small heat shock proteins. *Cell* **78**, 1027–1037 (1994).

274.   N. W. Freshney, *et al.*, Interleukin-1 activates a novel protein kinase cascade that results in the phosphorylation of Hsp27. *Cell* **78**, 1039–1049 (1994).

275.   B. Canovas, A. R. Nebreda, Diversity and versatility of p38 kinase signalling in health and disease. *Nat. Rev. Mol. Cell Biol.* **22**, 346–366 (2021).

276.   M. Li, J. Liu, C. Zhang, Evolutionary history of the vertebrate mitogen activated protein kinases family. *PLoS One* **6** (2011).

277.   M. K. Saba-El-Leil, C. Frémin, S. Meloche, Redundancy in the world of MAP kinases: All for one. *Front. Cell Dev. Biol.* **4**, 1–9 (2016).

278.   H. Enslen, J. Raingeaud, R. J. Davis, Selective activation of p38 mitogen-activated protein (MAP) kinase isoforms by the MAP kinase kinases MKK3 and MKK6. *J. Biol. Chem.* **273**, 1741–1748 (1998).

279.   D. Brancho, *et al.*, Mechanism of p38 MAP kinase activation in vivo. *Genes Dev.* **17**, 1969–1978 (2003).

280.   R. M. Biondi, A. R. Nebreda, Signalling specificity of Ser/Thr protein kinases through docking-site-mediated interactions. *Biochem. J.* **372**, 1–13 (2003).

281.   A. Kuzmanic, *et al.*, Changes in the free-energy landscape of p38α MAP kinase through its canonical activation and binding events as studied by enhanced molecular dynamics simulations. *Elife* **6** (2017).

282.   G. S. Kumar, *et al.*, Dynamic activation and regulation of the mitogen-activated protein kinase p38. *Proc. Natl. Acad. Sci. U. S. A.* **115**, 4655–4660 (2018).

283.   B. Ge, *et al.*, MAPKK-independent activation of p38alpha mediated by TAB1-dependent autophosphorylation of p38alpha. *Science* **295**, 1291–1294 (2002).

284.   J. M. Salvador, *et al.*, Alternative p38 activation pathway mediated by T cell receptor-proximal tyrosine kinases. *Nat. Immunol.* **6**, 390–395 (2005).

285.   P. R. Mittelstadt, H. Yamaguchi, E. Appella, J. D. Ashwell, T cell receptor-mediated activation of p38{alpha} by mono-phosphorylation of the activation loop results in altered substrate specificity. *J. Biol. Chem.* **284**, 15469–15474 (2009).

286.   L. Jirmanova, D. N. Sarma, D. Jankovic, P. R. Mittelstadt, J. D.Ashwell, Genetic disruption of p38alpha Tyr323 phosphorylation prevents T-cell receptor-mediated p38alpha activation and impairs interferon-gamma production. *Blood* **113**, 2229–2237 (2009).

287.   L. Jirmanova, M. L. G. Torchia, N. D. Sarma, P. R. Mittelstadt, J. D. Ashwell, Lack of the T cell-specific alternative p38 activation pathway reduces autoimmunity and inflammation. *Blood* **118**, 3280–3289 (2011).

288.   M. S. Alam, *et al.*, Unique properties of TCR-activated p38 are necessary for NFAT-dependent T-cell activation. *PLoS Biol.* **16** (2018).

289.   T. Tomida, M. Takekawa, H. Saito, Oscillation of p38 activity controls efficient pro-inflammatory gene expression. *Nat. Commun.* **6** (2015).

290.   C. J. Staples, D. M. Owens, J. V. Maier, A. C. B. Cato, S. M. Keyse, Cross-talk between the p38alpha and JNK MAPK pathways mediated by MAP kinase phosphatase-1 determines cellular sensitivity to UV radiation. *J. Biol. Chem.* **285**, 25928–25940 (2010).

291.   H. Miura, Y. Kondo, M. Matsuda, K. Aoki, Cell-to-Cell Heterogeneity in p38-Mediated Cross-Inhibition of JNK Causes Stochastic Cell Death. *Cell Rep.* **24**, 2658–2668 (2018).

292.   V. B. Pillai, *et al.*, Acetylation of a conserved lysine residue in the ATP binding pocket of p38 augments its kinase activity during hypertrophy of cardiomyocytes. *Mol. Cell. Biol.* **31**, 2349–2363 (2011).

293.   H. J. Jeong, *et al.*, Prmt7 promotes myoblast differentiation via methylation of p38MAPK on arginine residue 70. *Cell Death Differ.* **27**, 573–586 (2020).

294.   M. Y. Liu, W. K. Hua, C. J. Chen, W. J. Lin, The MKK-Dependent Phosphorylation of p38α Is Augmented by Arginine Methylation on Arg49/Arg149 during Erythroid Differentiation. *Int. J. Mol. Sci.* **21** (2020).

295.   N. Trempolec, N. Dave-Coll, A. R. Nebreda, SnapShot: P38 MAPK substrates. *Cell* **152** (2013).

296.   J. Han, J. Wu, J. Silke, An overview of mammalian p38 mitogen-activated protein kinases, central regulators of cell stress and receptor signaling. *F1000Research* **9** (2020).

297.   N. Ronkina, M. Gaestel, MAPK-Activated Protein Kinases: Servant or Partner? *Annu. Rev. Biochem.* **91**, 505–540 (2022).

298.   T. A. Bird, *et al.*, The interleukin-1-stimulated protein kinase that phosphorylates heat shock protein hsp27 is activated by MAP kinase. *FEBS Lett.* **338**, 31–36 (1994).

299.   M. M. McLaughlin, *et al.*, Identification of mitogen-activated protein (MAP) kinase-activated protein kinase-3, a novel substrate of CSBP p38 MAP kinase. *J. Biol. Chem.* **271**, 8488–8492 (1996).

300.   L. New, *et al.*, PRAK, a novel protein kinase regulated by the p38 MAP kinase. *EMBO J.* **17**, 3372–3384 (1998).

301.   M. Deak, A. D. Clifton, J. M. Lucocq, D. R. Alessi, Mitogen- and stress-activated protein kinase-1 (MSK1) is directly activated by MAPK and SAPK2/p38, and may mediate activation of CREB. *EMBO J.* **17**, 4426–4441 (1998).

302.   B. Pierrat, J. Da Silva Correia, J. L. Mary, M. Tomás-Zuber, W. Lesslauer, RSK-B, a novel ribosomal S6 kinase family member, is a CREB kinase under dominant control of p38alpha mitogen-activated protein kinase (p38alphaMAPK). *J. Biol. Chem.* **273**, 29661–29671 (1998).

303.   A. J. Waskiewicz, A. Flynn, C. G. Proud, J. A. Cooper, Mitogen-activated protein kinases activate the serine/threonine kinases Mnk1 and Mnk2. *EMBO J.* **16**, 1909–1920 (1997).

304.   R. Fukunaga, T. Hunter, MNK1, a new MAP kinase-activated protein kinase, isolated by a novel expression screening method for identifying protein kinase substrates. *EMBO J.* **16**, 1921–1933 (1997).

305.   K. Engel, A. Kotlyarov, M. Gaestel, Leptomycin B-sensitive nuclear export of MAPKAP kinase 2 is regulated by phosphorylation. *EMBO J.* **17**, 3363–3371 (1998).

306.   P. Trulley, *et al.*, Alternative Translation Initiation Generates a Functionally Distinct Isoform of the Stress-Activated Protein Kinase MK2. *Cell Rep.* **27**, 2859-2870.e6 (2019).

307.   R. Ben-Levy, *et al.*, Identification of novel phosphorylation sites required for activation of MAPKAP kinase-2. *EMBO J.* **14**, 5920 (1995).

308.   W. Meng, *et al.*, Structure of mitogen-activated protein kinase-activated protein (MAPKAP) kinase 2 suggests a bifunctional switch that couples kinase activation with nuclear export. *J. Biol. Chem.* **277**, 37401–37405 (2002).

309.   T. Tanoue, R. Maeda, M. Adachi, E. Nishida, Identification of a docking groove on ERK and p38 MAP kinases that regulates the specificity of docking interactions. *EMBO J.* **20**, 466 (2001).

310.   R. Ben-Levy, S. Hooper, R. Wilson, H. F. Paterson, C. J. Marshall, Nuclear export of the stress-activated protein kinase p38 mediated by its substrate MAPKAP kinase-2. *Curr. Biol.* **8**, 1049–1057 (1998).

311.   N. Gutierrez-Prat, *et al.*, MK2 degradation as a sensor of signal intensity that controls stress-induced cell fate. *Proc. Natl. Acad. Sci. U. S. A.* **118**, e2024562118 (2021).

312.   S. Soni, P. Anand, Y. S. Padwad, MAPKAPK2: The master regulator of RNA-binding proteins modulates transcript stability and tumor progression. *J. Exp. Clin. Cancer Res.* **38**, 1–18 (2019).

313.   S. Akira, K. Maeda, Control of RNA Stability in Immunity. *Annu. Rev. Immunol.* **39**, 481–509 (2021).

314.   J. Han, Y. Jiang, Z. Li, V. V. Kravchenko, R. J. Ulevitch, Activation of the transcription factor MEF2C by the MAP kinase p38 in inflammation. *Nature* **386**, 296–299 (1997).

315.   Y. J. Kang, *et al.*, Macrophage deletion of p38alpha partially impairs lipopolysaccharide-induced cellular activation. *J. Immunol.* **180**, 5075–5082 (2008).

316.   K. M. S. E. Reyskens, J. S. C. Arthur, Emerging Roles of the Mitogen and Stress Activated Kinases MSK1 and MSK2. *Front. cell Dev. Biol.* **4** (2016).

317.   I. Jaco, *et al.*, MK2 Phosphorylates RIPK1 to Prevent TNF-Induced Cell Death. *Mol. Cell* **66**, 698 (2017).

318.   M. B. Menon, *et al.*, p38 MAPK/MK2-dependent phosphorylation controls cytotoxic RIPK1 signalling in inflammation and infection. *Nat. Cell Biol.* **19**, 1248–1259 (2017).

319.   Y. Dondelinger, *et al.*, MK2 phosphorylation of RIPK1 regulates TNF-mediated cell death. *Nat. Cell Biol.* **19**, 1237–1247 (2017).

320.   D. Gurusamy, *et al.*, Multi-phenotype CRISPR-Cas9 Screen Identifies p38 Kinase as a Target for Adoptive Immunotherapies. *Cancer Cell* **37**, 818-833.e9 (2020).

321.   K. V. Katlinski, *et al.*, Inactivation of Interferon Receptor Promotes the Establishment of Immune Privileged Tumor Microenvironment. *Cancer Cell* **31**, 194–207 (2017).

322.   T. M. Thornton, *et al.*, Inactivation of nuclear GSK3β by Ser(389) phosphorylation promotes lymphocyte fitness during DNA double-strand break response. *Nat. Commun.* **7** (2016).

323.   A. Craxton, *et al.*, p38 MAPK is required for CD40-induced gene expression and proliferation in B lymphocytes. *J. Immunol.* **161**, 3225–36 (1998).

324.   D. Khiem, J. G. Cyster, J. J. Schwarz, B. L. Black, A p38 MAPK-MEF2C pathway regulates B-cell proliferation. *Proc. Natl. Acad. Sci. U. S. A.* **105**, 17067–17072 (2008).

325. P. R. Wilker, *et al.*, Transcription factor Mef2c is required for B cell proliferation and survival after antigen receptor stimulation. *Nat. Immunol.* **9**, 603–612 (2008).

326. L. Wang, *et al.*, p38 activation and viral infection. *Expert Rev. Mol. Med.* **24** (2022).

327. Y. Chander, *et al.*, Role of p38 mitogen-activated protein kinase signalling in virus replication and potential for developing broad spectrum antiviral drugs. *Rev. Med. Virol.* **31**, 1–16 (2021).

328. G. Karaca, *et al.*, Inhibition of the stress-activated kinase, p38, does not affect the virus transcriptional program of herpes simplex virus type 1. *Virology* **329**, 142–156 (2004).

329. G. Zachos, B. Clements, J. Conner, Herpes simplex virus type 1 infection stimulates p38/c-Jun N-terminal mitogen-activated protein kinase pathways and activates transcription factor AP-1. *J. Biol. Chem.* **274**, 5097–5103 (1999).

330. S. Hu, W. S. Sheng, S. J. Schachtele, J. R. Lokensgard, Reactive oxygen species drive herpes simplex virus (HSV)-1-induced proinflammatory cytokine production by murine microglia. *J. Neuroinflammation* **8** (2011).

331. R. A. Johnson, S.-M. Huong, E.-S. Huang, Activation of the mitogen-activated protein kinase p38 by human cytomegalovirus infection through two distinct pathways: a novel mechanism for activation of p38. *J. Virol.* **74**, 1158–1167 (2000).

332. M. Rahaus, N. Desloges, M. H. Wolff, Replication of varicella-zoster virus is influenced by the levels of JNK/SAPK and p38/MAPK activation. *J. Gen. Virol.* **85**, 3529–3540 (2004).

333. C. McCormick, D. Ganem, The kaposin B protein of KSHV activates the p38/MK2 pathway and stabilizes cytokine mRNAs. *Science (80-.).* **307**, 739–741 (2005).

334. J. A. Corcoran, *et al.*, Kaposi's Sarcoma-Associated Herpesvirus G-Protein-Coupled Receptor Prevents AU-Rich-Element-Mediated mRNA Decay. *J. Virol.* **86**, 8859–8871 (2012).

335. J. A. Corcoran, B. P. Johnston, C. McCormick, Viral Activation of MK2-hsp27-p115RhoGEF-RhoA Signaling Axis Causes Cytoskeletal Rearrangements, P-body Disruption and ARE-mRNA Stabilization. *PLoS Pathog.* **11**, 1–23 (2015).

336. T. M. Franks, J. Lykke-Andersen, TTP and BRF proteins nucleate processing body formation to silence mRNAs with AU-rich elements. *Genes Dev.* **21**, 719–735 (2007).

337. G. Matusali, G. Arena, A. De Leo, L. Di Renzo, E. Mattia, Inhibition of p38 MAP kinase pathway induces apoptosis and prevents Epstein Barr virus reactivation in Raji cells exposed to lytic cycle inducing compounds. *Mol. Cancer* **8** (2009).

338. A. L. Adamson, *et al.*, Epstein-Barr Virus Immediate-Early Proteins BZLF1 and BRLF1 Activate the ATF2 Transcription Factor by Increasing the Levels of Phosphorylated p38 and c-Jun N-Terminal Kinases. *J. Virol.* **74**, 1224–1233 (2000).

339. R. Gonnella, *et al.*, PKC theta and p38 MAPK activate the EBV lytic cycle through autophagy induction. *Biochim. Biophys. Acta* **1853**, 1586–95 (2015).

340. A. G. Eliopoulos, N. J. Gallagher, S. M. S. Blake, C. W. Dawson, L. S. Young, Activation of the p38 mitogen-activated protein kinase pathway by Epstein-Barr virus-encoded latent membrane protein 1 coregulates interleukin-6 and interleukin-8 production. *J. Biol. Chem.* **274**, 16085–96 (1999).

341. M. Vockerodt, B. Haier, P. Buttgereit, H. Tesch, D. Kube, The Epstein-Barr virus latent membrane protein 1 induces interleukin-10 in Burkitt's lymphoma cells but not in Hodgkin's cells involving the p38/SAPK2 pathway. *Virology* **280**, 183–198 (2001).

342. U. Schultheiss, *et al.*, TRAF6 is a critical mediator of signal transduction by the viral oncogene latent membrane protein 1. *EMBO J.* **20**, 5678–5691 (2001).

343. Y. J. Song, K. Y. Jen, V. Soni, E. Kieff, E. Cahir-McFarland, IL-1 receptor-associated kinase 1 is critical for latent membrane protein 1-induced p65/RelA serine 536 phosphorylation and NF-kappaB activation. *Proc. Natl. Acad. Sci. U. S. A.* **103**, 2689–2694 (2006).

344. P. Johansson, A. Jansson, U. Rüetschi, L. Rymo, The p38 Signaling Pathway Upregulates Expression of the Epstein-Barr Virus LMP1 Oncogene. *J. Virol.* **84**, 2787–2797 (2010).

345. A. Castello, *et al.*, Insights into RNA biology from an atlas of mammalian mRNA-binding proteins. *Cell* **149**, 1393–406 (2012).

346. B. M. Lunde, C. Moore, G. Varani, RNA-binding proteins: Modular design for efficient function. *Nat. Rev. Mol. Cell Biol.* **8**, 479–490 (2007).

347. B. P. Hudson, M. A. Martinez-Yamout, H. J. Dyson, P. E. Wright, Recognition of the mRNA AU-rich element by the zinc finger domain of TIS11d. *Nat. Struct. Mol. Biol.* **11**, 257–264 (2004).

348. T. M. T. Hall, Multiple modes of RNA recognition by zinc finger proteins. *Curr. Opin. Struct. Biol.* **15**, 367–373 (2005).

349. M. L. Wells, L. Perera, P. J. Blackshear, An Ancient Family of RNA-Binding Proteins: Still Important! *Trends Biochem. Sci.* **42**, 285–296 (2017).

350. M. R. Fabian, *et al.*, Structural basis for the recruitment of the human CCR4-NOT deadenylase complex by tristetraprolin. *Nat. Struct. Mol. Biol.* **20**, 735–9 (2013).

351. H. Sandler, J. Kreth, H. T. M. Timmers, G. Stoecklin, Not1 mediates recruitment of the deadenylase Caf1 to mRNAs targeted for degradation by tristetraprolin. *Nucleic Acids Res.* **39**, 4373–4386 (2011).

352. J. Lykke-Andersen, E. Wagner, Recruitment and activation of mRNA decay enzymes by two ARE-mediated decay activation domains in the proteins TTP and BRF-1. *Genes Dev.* **19**, 351–361 (2005).

353. R. S. Phillips, S. B. V. Ramos, P. J. Blackshear, Members of the tristetraprolin family of tandem CCCH zinc finger proteins exhibit CRM1-dependent nucleocytoplasmic shuttling. *J. Biol. Chem.* **277**, 11606–11613 (2002).

354. L. Twyffels, *et al.*, A Masked PY-NLS in Drosophila TIS11 and Its Mammalian Homolog Tristetraprolin. *PLoS One* **8**, e71686 (2013).

355. K. T. Wang, *et al.*, Functional regulation of Zfp36l1 and Zfp36l2 in response to lipopolysaccharide in mouse RAW264.7 macrophages. *J. Inflamm. (United Kingdom)* **12**, 42 (2015).

356. M. Turner, M. D. Díaz-Muñoz, RNA-binding proteins control gene expression and cell fate in the immune system. *Nat. Immunol.* **19**, 120–129 (2018).

357. F. Kratochvill, *et al.*, Tristetraprolin-driven regulatory circuit controls quality and timing of mRNA decay in inflammation. *Mol. Syst. Biol.* **7** (2011).

358. N. Mukherjee, *et al.*, Global target mRNA specification and regulation by the RNA-binding protein ZFP36. *Genome Biol.* **15** (2014).

359. V. Sedlyarov, *et al.*, Tristetraprolin binding site atlas in the macrophage transcriptome reveals a switch for inflammation resolution. *Mol. Syst. Biol.* **12**, 868 (2016).

360. T. Bakheet, E. Hitti, M. Al-Saif, W. N. Moghrabi, K. S. A. Khabar, The AU-rich element landscape

across human transcriptome reveals a large proportion in introns and regulation by ELAVL1/HuR. *Biochim. Biophys. Acta - Gene Regul. Mech.* **1861**, 167–177 (2018).

361. K. Phillips, N. Kedersha, L. Shen, P. J. Blacksheart, P. Anderson, Arthritis suppressor genes TIA-1 and TTP dampen the expression of tumor necrosis factor α, cyclooxygenase 2, and inflammatory arthritis. *Proc. Natl. Acad. Sci. U. S. A.* **101**, 2011–2016 (2004).

362. P. Anderson, N. Kedersha, RNA granules: post-transcriptional and epigenetic modulators of gene expression. *Nat. Rev. Mol. Cell Biol.* **10**, 430–6 (2009).

363. D. S. W. Protter, R. Parker, Principles and Properties of Stress Granules. *Trends Cell Biol.* **26**, 668–679 (2016).

364. N. Kedersha, *et al.*, Stress granules and processing bodies are dynamically linked sites of mRNP remodeling. *J. Cell Biol.* **169**, 871–884 (2005).

365. H. Cao, F. Dzineku, P. J. Blackshear, Expression and purification of recombinant tristetraprolin that can bind to tumor necrosis factor-alpha mRNA and serve as a substrate for mitogen-activated protein kinases. *Arch. Biochem. Biophys.* **412**, 106–20 (2003).

366. H. Cao, R. Lin, Phosphorylation of recombinant tristetraprolin in vitro. *Protein J.* **27**, 163–9 (2008).

367. G. Stoecklin, *et al.*, MK2-induced tristetraprolin:14-3-3 Complexes prevent stress granule association and ARE-mRNA decay. *EMBO J.* **23**, 1313–1324 (2004).

368. S. L. Clement, C. Scheckel, G. Stoecklin, J. Lykke-Andersen, Phosphorylation of Tristetraprolin by MK2 Impairs AU-Rich Element mRNA Decay by Preventing Deadenylase Recruitment. *Mol. Cell. Biol.* **31**, 256–266 (2011).

369. C. A. Chrestensen, *et al.*, MAPKAP Kinase 2 Phosphorylates Tristetraprolin on in Vivo Sites Including Ser178, a Site Required for 14-3-3 Binding. *J. Biol. Chem.* **279**, 10176–10184 (2004).

370. R. Lang, M. Hammer, J. Mages, DUSP Meet Immunology: Dual Specificity MAPK Phosphatases in Control of the Inflammatory Response. *J. Immunol.* **177**, 7497–7504 (2006).

371. S. M. Abraham, A. R. Clark, Dual-specificity phosphatase 1: A critical regulator of innate immune responses. *Biochem. Soc. Trans.* **34**, 1018–1023 (2006).

372. T. Smallie, *et al.*, Dual-Specificity Phosphatase 1 and Tristetraprolin Cooperate To Regulate Macrophage Responses to Lipopolysaccharide. *J. Immunol.* **195**, 277–88 (2015).

373. L. Sun, *et al.*, Tristetraprolin (TTP)-14-3-3 complex formation protects TTP from dephosphorylation by protein phosphatase 2a and stabilizes tumor necrosis factor-α mRNA. *J. Biol. Chem.* **282**, 3766–3777 (2007).

374. C. Tiedje, *et al.*, The p38/MK2-Driven Exchange between Tristetraprolin and HuR Regulates AU-Rich Element-Dependent Translation. *PLoS Genet.* **8** (2012).

375. X. Tao, G. Gao, Tristetraprolin Recruits Eukaryotic Initiation Factor 4E2 To Repress Translation of AU-Rich Element-Containing mRNAs. *Mol. Cell. Biol.* **35**, 3921–32 (2015).

376. R. Fu, M. T. Olsen, K. Webb, E. J. Bennett, J. Lykke-Andersen, Recruitment of the 4EHP-GYF2 cap-binding complex to tetraproline motifs of tristetraprolin promotes repression and degradation of mRNAs with AU-rich elements. *RNA* **22**, 373–382 (2016).

377. M. Morita, *et al.*, A novel 4EHP-GIGYF2 translational repressor complex is essential for mammalian development. *Mol. Cell. Biol.* **32**, 3585–93 (2012).

378. D. Peter, *et al.*, GIGYF1/2 proteins use auxiliary sequences to selectively bind to 4EHP and repress target mRNA expression. *Genes Dev.* **31**, 1147–1161 (2017).

379. H. Otsuka, *et al.*, ARE-binding protein ZFP36L1 interacts with CNOT1 to directly repress translation via a deadenylation-independent mechanism. *Biochimie* **174**, 49–56 (2020).

380. G. A. Taylor, *et al.*, A pathogenetic role for TNFα in the syndrome of cachexia, arthritis, and autoimmunity resulting from tristetraprolin (TTP) deficiency. *Immunity* **4**, 445–454 (1996).

381. E. Carballo, W. S. Lai, P. J. Blackshear, Feedback Inhibition of Macrophage Tumor Necrosis Factor-α Production by Tristetraprolin. *Science (80-.).* **281**, 1001–1005 (1998).

382. E. Carballo, W. S. Lai, P. J. Blackshear, Evidence that tristetraprolin is a physiological regulator of granulocyte-macrophage colony-stimulating factor messenger RNA deadenylation and stability. *Blood* **95**, 1891–1899 (2000).

383. D. J. Stumpo, *et al.*, Chorioallantoic Fusion Defects and Embryonic Lethality Resulting from Disruption of Zfp36L1 , a Gene Encoding a CCCH Tandem Zinc Finger Protein of the Tristetraprolin Family. *Mol. Cell. Biol.* **24**, 6445–6455 (2004).

384. D. J. Stumpo, *et al.*, Targeted disruption of Zfp36l2, encoding a CCCH tandem zinc finger RNA-binding protein, results in defective hematopoiesis. *Blood* **114**, 2401–10 (2009).

385. L.-Q. Qiu, D. J. Stumpo, P. J. Blackshear, Myeloid-Specific Tristetraprolin Deficiency in Mice Results in Extreme Lipopolysaccharide Sensitivity in an Otherwise Minimal Phenotype. *J. Immunol.* **188**, 5150–5159 (2012).

386. L.-Q. Qiu, W. S. Lai, A. Bradbury, D. C. Zeldin, P. J. Blackshear, Tristetraprolin (TTP) coordinately regulates primary and secondary cellular responses to proinflammatory stimuli. *J. Leukoc. Biol.* **97**, 723–736 (2015).

387. M. Hammer, *et al.*, Control of dual-specificity phosphatase-1 expression in activated macrophages by IL-10. *Eur. J. Immunol.* **35**, 2991–3001 (2005).

388. B. Schaljo, *et al.*, Tristetraprolin is required for full anti-inflammatory response of murine macrophages to IL-10. *J. Immunol.* **183**, 1197–206 (2009).

389. A. Gaba, *et al.*, Cutting edge: IL-10-mediated tristetraprolin induction is part of a feedback loop that controls macrophage STAT3 activation and cytokine production. *J. Immunol.* **189**, 2089–93 (2012).

390. T. Tang, *et al.*, Macrophage responses to lipopolysaccharide are modulated by a feedback loop involving prostaglandin E2, dual specificity phosphatase 1 and tristetraprolin. *Sci. Rep.* **7** (2017).

391. R. Newman, *et al.*, Maintenance of the marginal-zone B cell compartment specifically requires the RNA-binding protein ZFP36L1. *Nat. Immunol.* **18**, 683–693 (2017).

392. E. Lu, J. G. Cyster, G-protein coupled receptors and ligands that organize humoral immune responses. *Immunol. Rev.* **289**, 158–172 (2019).

393. Y.-F. Li, S. Xu, X. Ou, K.-P. Lam, Shp1 signalling is required to establish the long-lived bone marrow plasma cell pool. *Nat. Commun.* **5**, 4273 (2014).

394. E. J. Park, *et al.*, Aberrant activation of integrin alpha4beta7 suppresses lymphocyte migration to the gut. *J. Clin. Invest.* **117**, 2526–38 (2007).

395. J. L. Murakami, *et al.*, Evidence that β7 integrin regulates hematopoietic stem cell homing and engraftment through interaction with MAdCAM-1. *Stem Cells Dev.* **25**, 18–26 (2016).

396. A. Saveliev, S. E. Bell, M. Turner, Efficient homing of antibody-secreting cells to the bone marrow requires RNA-binding protein ZFP36L1. *J. Exp. Med.* **218** (2021).

397. A. Galloway, *et al.*, RNA-binding proteins ZFP36L1 and ZFP36L2 promote cell quiescence. *Science* **352**, 453–9 (2016).

398. K. U. Vogel, L. S. Bell, A. Galloway, H. Ahlfors, M. Turner, The RNA-Binding Proteins Zfp36l1 and Zfp36l2 Enforce the Thymic β-Selection Checkpoint by Limiting DNA Damage Response Signaling and Cell Cycle Progression. *J. Immunol.* **197**, 2673–2685 (2016).

399. D. J. Hodson, *et al.*, Deletion of the RNA-binding proteins ZFP36L1 and ZFP36L2 leads to perturbed thymic development and T lymphoblastic leukemia. *Nat. Immunol.* **11**, 717–724 (2010).

400. M. J. Moore, *et al.*, ZFP36 RNA-binding proteins restrain T cell activation and anti-viral immunity. *Elife* **7** (2018).

401. F. Ebner, *et al.*, The RNA-binding protein tristetraprolin schedules apoptosis of pathogen-engaged neutrophils during bacterial infection. *J. Clin. Invest.* **127**, 2051–2065 (2017).

402. C. Ehlting, *et al.*, MAPKAP kinase 2 regulates IL-10 expression and prevents formation of intrahepatic myeloid cell aggregates during cytomegalovirus infections. *J. Hepatol.* **64**, 380–389 (2016).

403. W.-J. Jin, *et al.*, Downregulation of the AU-rich RNA-binding protein ZFP36 in chronic HBV patients: implications for anti-inflammatory therapy. *PLoS One* **7**, e33356 (2012).

404. J.-C. Twizere, *et al.*, Interaction of retroviral Tax oncoproteins with tristetraprolin and regulation of tumor necrosis factor-alpha expression. *J. Natl. Cancer Inst.* **95**, 1846–59 (2003).

405. C. M. Rosenberger, *et al.*, miR-451 regulates dendritic cell cytokine responses to influenza infection. *J. Immunol.* **189**, 5965–75 (2012).

406. S. Li, *et al.*, Activation of the MKK3-p38-MK2-ZFP36 axis by coronavirus infection restricts the upregulation of AU-rich element-containing transcripts in proinflammatory response. *J. Virol.*, jvi0208621 (2022).

407. R. J. Lin, *et al.*, Zinc finger protein ZFP36L1 inhibits influenza A virus through translational repression by targeting HA, M and NS RNA transcripts. *Nucleic Acids Res.* **48**, 7371–7384 (2020).

408. L. W. Wang, *et al.*, Epstein-Barr-Virus-Induced One-Carbon Metabolism Drives B Cell Transformation. *Cell Metab.* **30**, 539-555.e11 (2019).

409. P. Mrozek-Gorska, *et al.*, Epstein–Barr virus reprograms human B lymphocytes immediately in the prelatent phase of infection. *Proc. Natl. Acad. Sci. U. S. A.* **116**, 16046–16055 (2019).

410. R. J. Lamontagne, *et al.*, A multi-omics approach to Epstein-Barr virus immortalization of B-cells reveals EBNA1 chromatin pioneering activities targeting nucleotide metabolism. *PLOS Pathog.* **17**, e1009208 (2021).

411. D. Bhowmik, F. Zhu, Evasion of Intracellular DNA Sensing by Human Herpesviruses. *Front. Cell. Infect. Microbiol.* **11** (2021).

412. I. L. Campbell, Cytokines in viral diseases. *Curr. Opin. Immunol.* **3**, 486–491 (1991).

413. A. Alcami, Viral mimicry of cytokines, chemokines and their receptors. *Nat. Rev. Immunol. 2003 31* **3**, 36–50 (2003).

414. L. Velazquez-Salinas, A. Verdugo-Rodriguez, L. L. Rodriguez, M. V. Borca, The role of interleukin 6

during viral infections. *Front. Microbiol.* **10**, 1057 (2019).

415. S. Whittingham, *et al.*, Cytokine production in response to Epstein-Barr virus infection of peripheral blood mononuclear cells in vitro. *Immunol. Cell Biol.* **71 (Pt 4)**, 259–64 (1993).

416. A. Shumilov, *et al.*, Epstein-Barr virus particles induce centrosome amplification and chromosomal instability. *Nat. Commun.* **8**, 1–15 (2017).

417. S. P. T. Yiu, R. Guo, C. Zerbe, M. P. Weekes, B. E. Gewurz, Epstein-Barr virus BNRF1 destabilizes SMC5/6 cohesin complexes to evade its restriction of replication compartments. *Cell Rep.* **38**, 110411 (2022).

418. S. Jangra, *et al.*, Suppression of JAK-STAT Signaling by Epstein-Barr Virus Tegument Protein BGLF2 through Recruitment of SHP1 Phosphatase and Promotion of STAT2 Degradation. *J. Virol.* **95**, e0102721 (2021).

419. H. Yu, H. Lee, A. Herrmann, R. Buettner, R. Jove, Revisiting STAT3 signalling in cancer: New and unexpected biological functions. *Nat. Rev. Cancer* **14**, 736–746 (2014).

420. D. Benjamin, M. Schmidlin, L. Min, B. Gross, C. Moroni, BRF1 Protein Turnover and mRNA Decay Activity Are Regulated by Protein Kinase B at the Same Phosphorylation Sites. *Mol. Cell. Biol.* **26**, 9497–9507 (2006).

421. S. Maitra, *et al.*, The AU-rich element mRNA decay-promoting activity of BRF1 is regulated by mitogen-activated protein kinase-activated protein kinase 2. *RNA* **14**, 950–959 (2008).

422. H. Duan, N. Cherradi, J. J. Feige, C. Jefcoate, cAMP-dependent posttranscriptional regulation of steroidogenic acute regulatory (STAR) protein by the zinc finger protein ZFP36L1/TIS11b. *Mol. Endocrinol.* **23**, 497–509 (2009).

423. S. Adachi, *et al.*, ZFP36L1 and ZFP36L2 control LDLR mRNA stability via the ERK-RSK pathway. *Nucleic Acids Res.* **42**, 10037–10049 (2014).

424. F. Rataj, *et al.*, The cAMP pathway regulates mRNA decay through phosphorylation of the RNA-binding protein TIS11b/BRF1. *Mol. Biol. Cell* **27**, 3841–3854 (2016).

425. K. R. Mahtani, *et al.*, Mitogen-Activated Protein Kinase p38 Controls the Expression and Posttranslational Modification of Tristetraprolin, a Regulator of Tumor Necrosis Factor Alpha mRNA Stability. *Mol. Cell. Biol.* **21**, 6461–6469 (2001).

426. G. Stoecklin, *et al.*, Functional cloning of BRF1, a regulator of ARE-dependent mRNA turnover. *EMBO J.* **21**, 4709–4718 (2002).

427. S. A. Brooks, J. E. Connolly, W. F. C. Rigby, The role of mRNA turnover in the regulation of tristetraprolin expression: evidence for an extracellular signal-regulated kinase-specific, AU-rich element-dependent, autoregulatory pathway. *J. Immunol.* **172**, 7263–71 (2004).

428. C. R. Tchen, M. Brook, J. Saklatvala, A. R. Clark, The stability of tristetraprolin mRNA is regulated by mitogen-activated protein kinase p38 and by tristetraprolin itself. *J. Biol. Chem.* **279**, 32393–32400 (2004).

429. M. Brook, *et al.*, Posttranslational Regulation of Tristetraprolin Subcellular Localization and Protein Stability by p38 Mitogen-Activated Protein Kinase and Extracellular Signal-Regulated Kinase Pathways. *Mol. Cell. Biol.* **26**, 2408–2418 (2006).

430. N. Sugano, W. Chen, M. L. Roberts, N. R. Cooper, Epstein-Barr virus binding to CD21 activates the initial viral promoter via NF-κB induction. *J. Exp. Med.* **186**, 731–737 (1997).

431. M. D'Addario, T. A. Libermann, J. Xu, A. Ahmad, J. Menezes, Epstein-Barr virus and its glycoprotein-350 upregulate IL-6 in human B-lymphocytes via CD21, involving activation of NF-κB and different signaling pathways. *J. Mol. Biol.* **308**, 501–514 (2001).

432. P. Guha, *et al.*, STAT3 inhibition induces Bax-dependent apoptosis in liver tumor myeloid-derived suppressor cells. *Oncogene* **38**, 533–548 (2019).

433. A. Neininger, *et al.*, MK2 targets AU-rich elements and regulates biosynthesis of tumor necrosis factor and interleukin-6 independently at different post-transcriptional levels. *J. Biol. Chem.* **277**, 3065–3068 (2002).

434. W. Zhao, M. Liu, N. J. D'Silva, K. L. Kirkwood, Tristetraprolin regulates interleukin-6 expression through p38 MAPK-dependent affinity changes with mRNA 3′ untranslated region. *J. Interf. Cytokine Res.* **31**, 629–637 (2011).

435. J. E. Tanner, C. Alfieri, T. A. Chatila, F. Diaz-Mitoma, Induction of interleukin-6 after stimulation of human B-cell CD21 by Epstein-Barr virus glycoproteins gp350 and gp220. *J. Virol.* **70**, 570–575 (1996).

436. M. D'Addario, A. Ahmad, A. Morgan, J. Menezes, Binding of the Epstein-Barr virus major envelope glycoprotein gp350 results in the upregulation of the TNF-α gene expression in monocytic cells via NF-κB involving PKC, PI3-K and tyrosine kinases. *J. Mol. Biol.* (2000) https:/doi.org/10.1006/jmbi.2000.3717.

437. A. M. Campbell, C. F. De La Cruz Herrera, E. Marcon, J. Greenblatt, L. Frappier, Epstein-Barr Virus BGLF2 commandeers RISC to interfere with cellular miRNA function. *PLoS Pathog.* **18**, e1010235 (2022).

438. M. F. Stinski, J. L. Meier, *Immediate–early viral gene regulation and function* (Cambridge University Press, 2007) (June 13, 2022).

439. D. Fan, *et al.*, The Role of VP16 in the Life Cycle of Alphaherpesviruses. *Front. Microbiol.* **11**, 1910 (2020).

440. S. Schmaus, H. Wolf, F. Schwarzmann, The Reading Frame BPLF1 of Epstein-Barr Virus: A Homologue of Herpes Simplex Virus Protein VP16. *Virus Genes 2004 292* **29**, 267–277 (2004).

441. A. Cuadrado, A. R. Nebreda, Mechanisms and functions of p38 MAPK signalling. *Biochem. J.* **429**, 403–417 (2010).

442. A. Meng, X. Zhang, Y. Shi, Role of p38 MAPK and STAT3 in lipopolysaccharide-stimulated mouse alveolar macrophages. *Exp. Ther. Med.* **8**, 1772–1776 (2014).

443. S. E. Fernandes, D. K. Saini, The ERK-p38MAPK-STAT3 Signalling Axis Regulates iNOS Expression and Salmonella Infection in Senescent Cells. *Front. Cell. Infect. Microbiol.* **11**, 1041 (2021).

444. X. Liu, J. I. Cohen, Epstein-Barr Virus (EBV) Tegument Protein BGLF2 Promotes EBV Reactivation through Activation of the p38 Mitogen-Activated Protein Kinase. *J. Virol.* **90**, 1129–38 (2016).

445. H. M. A. Al Masud, *et al.*, The BOLF1 gene is necessary for effective Epstein–Barr viral infectivity. *Virology* **531**, 114–125 (2019).

446. M. Schmidlin, *et al.*, The ARE-dependent mRNA-destabilizing activity of BRF1 is regulated by protein kinase B. *EMBO J.* **23**, 4760–4769 (2004).

447. J. A. Corcoran, C. McCormick, Viral activation of stress-regulated Rho-GTPase signaling pathway disrupts sites of mRNA degradation to influence cellular gene expression. *Small GTPases* **6**, 178–185

(2015).

448.   N. Alomari, J. Totonchy, Cytokine-Targeted Therapeutics for KSHV-Associated Disease. *Viruses* **12** (2020).

449.   M. van Gent, *et al.*, Epstein-Barr Virus Large Tegument Protein BPLF1 Contributes to Innate Immune Evasion through Interference with Toll-Like Receptor Signaling. *PLOS Pathog.* **10**, e1003960 (2014).

450.   T. Chen, *et al.*, Epstein-Barr virus tegument protein BGLF2 inhibits NF-κB activity by preventing p65 Ser536 phosphorylation. *FASEB J.* **33**, 10563–10576 (2019).

451.   C. H. Ahrens, J. T. Wade, M. M. Champion, J. D. Langer, A Practical Guide to Small Protein Discovery and Characterization Using Mass Spectrometry. *J. Bacteriol.* **204** (2022).

452.   H. F. Moffett, *et al.*, B cells engineered to express pathogen-specific antibodies protect against infection. *Sci. Immunol.* **4**, 644 (2019).

453.   E. Akidil, *et al.*, Highly efficient CRISPR-Cas9-mediated gene knockout in primary human B cells for functional genetic studies of Epstein-Barr virus infection. *PLoS Pathog.* **17** (2021).

454.   A. Bell, J. Skinner, H. Kirby, A. Rickinson, Characterisation of regulatory sequences at the Epstein-Barr virus BamHI W promoter. *Virology* **252**, 149–161 (1998).

455.   H. Kirby, A. Rickinson, A. Bell, The activity of the Epstein-Barr virus BamHI W promoter in B cells is dependent on the binding of CREB/ATF factors. *J. Gen. Virol.* **81**, 1057–1066 (2000).

456.   R. J. Tierney, K.-Y. Kao, J. K. Nagra, A. B. Rickinson, Epstein-Barr Virus BamHI W Repeat Number Limits EBNA2/EBNA-LP Coexpression in Newly Infected B Cells and the Efficiency of B-Cell Transformation: a Rationale for the Multiple W Repeats in Wild-Type Virus Strains. *J. Virol.* **85**, 12362–12375 (2011).

457.   N. A. Patsopoulos, *et al.*, Multiple sclerosis genomic map implicates peripheral immune cells and microglia in susceptibility. *Science (80-.).* **365** (2019).

458.   B. Neuhierl, R. Feederle, W. Hammerschmidt, H. J. Delecluse, Glycoprotein gp110 of Epstein–Barr virus determines viral tropism and efficiency of infection. *Proc. Natl. Acad. Sci.* **99**, 15036–15041 (2002).

459.   S. Pavlova, *et al.*, An Epstein-Barr virus mutant produces immunogenic defective particles devoid of viral DNA. *J. Virol.* **87**, 2011–2022 (2013).

460.   D. G. van Zyl, *et al.*, Immunogenic particles with a broad antigenic spectrum stimulate cytolytic T cells and offer increased protection against EBV infection ex vivo and in mice. *PLoS Pathog.* **14** (2018).

461.   A. Shevchenko, H. Tomas, J. Havliš, J. V. Olsen, M. Mann, In-gel digestion for mass spectrometric characterization of proteins and proteomes. *Nat. Protoc. 2007 16* **1**, 2856–2860 (2007).

462.   S. Tyanova, T. Temu, J. Cox, The MaxQuant computational platform for mass spectrometry-based shotgun proteomics. *Nat. Protoc.* **11**, 2301–2319 (2016).

463.   J. Cox, *et al.*, Accurate Proteome-wide Label-free Quantification by Delayed Normalization and Maximal Peptide Ratio Extraction, Termed MaxLFQ. *Mol. Cell. Proteomics* **13**, 2513 (2014).

464.   S. Tyanova, J. Cox, Perseus: A bioinformatics platform for integrative analysis of proteomics data in cancer research. *Methods Mol. Biol.* **1711**, 133–148 (2018).

465.   C. M. Potel, M. H. Lin, A. J. R. Heck, S. Lemeer, Defeating Major Contaminants in Fe3+- Immobilized

Metal Ion Affinity Chromatography (IMAC) Phosphopeptide Enrichment. *Mol. Cell. Proteomics* **17**, 1028 (2018).

466. D. Wessel, U. I. Flügge, A method for the quantitative recovery of protein in dilute solution in the presence of detergents and lipids. *Anal. Biochem.* **138**, 141–143 (1984).

467. B. Ruprecht, *et al.*, Optimized Enrichment of Phosphoproteomes by Fe-IMAC Column Chromatography. *Methods Mol. Biol.* **1550**, 47–60 (2017).

468. J. Rappsilber, M. Mann, Y. Ishihama, Protocol for micro-purification, enrichment, pre-fractionation and storage of peptides for proteomics using StageTips. *Nat. Protoc. 2007 28* **2**, 1896–1906 (2007).

469. Y. C. Liao, N. T. Chen, Y. P. Shih, Y. Dong, H. Lo Su, Up-regulation of C-Terminal Tensin-like Molecule Promotes the Tumorigenicity of Colon Cancer through β-Catenin. *Cancer Res.* **69**, 4563–4566 (2009).

470. H. J. Delecluse, S. Bartnizke, W. Hammerschmidt, J. Bullerdiek, G. W. Bornkamm, Episomal and integrated copies of Epstein-Barr virus coexist in Burkitt lymphoma cell lines. *J. Virol.* **67**, 1292–1299 (1993).

471. S. Gastaldello, *et al.*, A deneddylase encoded by Epstein-Barr virus promotes viral DNA replication by regulating the activity of cullin-RING ligases. *Nat. Cell Biol.* **12**, 351–361 (2010).

472. C. B. Whitehurst, C. Vaziri, J. Shackelford, J. S. Pagano, Epstein-Barr virus BPLF1 deubiquitinates PCNA and attenuates polymerase η recruitment to DNA damage sites. *J. Virol.* **86**, 8097–8106 (2012).

473. R. Kumar, C. B. Whitehurst, J. S. Pagano, The Rad6/18 Ubiquitin Complex Interacts with the Epstein-Barr Virus Deubiquitinating Enzyme, BPLF1, and Contributes to Virus Infectivity. *J. Virol.* **88**, 6411 (2014).

474. O. F. Dyson, J. S. Pagano, C. B. Whitehurst, The Translesion Polymerase Pol η Is Required for Efficient Epstein-Barr Virus Infectivity and Is Regulated by the Viral Deubiquitinating Enzyme BPLF1. *J. Virol.* **91** (2017).

475. S. Saito, *et al.*, Epstein-Barr virus deubiquitinase downregulates TRAF6-mediated NF-κB signaling during productive replication. *J. Virol.* **87**, 4060–4070 (2013).

476. M. van Gent, *et al.*, Epstein-Barr virus large tegument protein BPLF1 contributes to innate immune evasion through interference with toll-like receptor signaling. *PLoS Pathog.* **10** (2014).

477. S. Gupta, *et al.*, 14-3-3 scaffold proteins mediate the inactivation of trim25 and inhibition of the type I interferon response by herpesvirus deconjugases. *PLoS Pathog.* **15** (2019).

478. P. Ylä-Anttila, S. Gupta, M. G. Masucci, The Epstein-Barr virus deubiquitinase BPLF1 targets SQSTM1/p62 to inhibit selective autophagy. *Autophagy* **17**, 3461–3474 (2021).

479. Y.-F. Chiu, *et al.*, Characterization and Intracellular Trafficking of Epstein-Barr Virus BBLF1, a Protein Involved in Virion Maturation. *J. Virol.* **86**, 9647–9655 (2012).

480. C. P. Lee, M. R. Chen, Conquering the nuclear envelope barriers by ebv lytic replication. *Viruses* **13**, 702 (2021).

481. Y. Yanagi, *et al.*, Initial Characterization of the Epstein‾Barr Virus BSRF1 Gene Product. *Viruses* **11** (2019).

482. H. P. He, *et al.*, Structure of Epstein-Barr virus tegument protein complex BBRF2-BSRF1 reveals its potential role in viral envelopment. *Nat. Commun.* **11** (2020).

483. H. M. A. Al Masud, *et al.*, Epstein-Barr Virus BKRF4 Gene Product Is Required for Efficient Progeny Production. *J. Virol.* **91** (2017).

484. T.-H. Ho, *et al.*, A Screen for Epstein-Barr Virus Proteins That Inhibit the DNA Damage Response Reveals a Novel Histone Binding Protein. *J. Virol.* **92** (2018).

485. Y. Liu, *et al.*, Epstein-Barr Virus Tegument Protein BKRF4 is a Histone Chaperone. *J. Mol. Biol.* **434** (2022).

486. J. Chen, *et al.*, Epstein-Barr virus protein BKRF4 restricts nucleosome assembly to suppress host antiviral responses. *Proc. Natl. Acad. Sci. U. S. A.* **119** (2022).

487. N. Konishi, *et al.*, BGLF2 Increases Infectivity of Epstein-Barr Virus by Activating AP-1 upon De Novo Infection. *mSphere* **3** (2018).

488. T. Watanabe, *et al.*, The Epstein-Barr virus BRRF2 gene product is involved in viral progeny production. *Virology* **484**, 33–40 (2015).

489. T. Watanabe, *et al.*, The C-Terminus of Epstein-Barr Virus BRRF2 Is Required for its Proper Localization and Efficient Virus Production. *Front. Microbiol.* **8** (2017).

490. M. Duarte, *et al.*, An RS motif within the Epstein-Barr virus BLRF2 tegument protein is phosphorylated by SRPK2 and is important for viral replication. *PLoS One* **8** (2013).

491. Y. Hara, *et al.*, Comprehensive Analyses of Intraviral Epstein-Barr Virus Protein-Protein Interactions Hint Central Role of BLRF2 in the Tegument Network. *J. Virol.* **96** (2022).

492. C. Münz, Ed., *Epstein Barr Virus Volume 2* (Springer International Publishing, 2015).

493. Y. Kawaguchi, Y. Mori, H. Kimura, Eds., *Human Herpesviruses* (Springer Singapore, 2018).

494. R. Rahman, D. Gopinath, W. Buajeeb, S. Poomsawat, N. W. Johnson, Potential Role of Epstein-Barr Virus in Oral Potentially Malignant Disorders and Oral Squamous Cell Carcinoma: A Scoping Review. *Viruses* **14** (2022).

495. C. Münz, Immune Escape by Non-coding RNAs of the Epstein Barr Virus. *Front. Microbiol.* **12**, 657387 (2021).

496. B. F. R. Caetano, B. A. S. Jorge, B. G. Müller-Coan, D. Elgui de Oliveira, Epstein-Barr virus microRNAs in the pathogenesis of human cancers. *Cancer Lett.* **499**, 14–23 (2021).

Acknowledgements

First, I would like to thank my Supervisor Prof. H.-J. Delecluse for the mentoring, supervision, and support over these years of work. You gave me the opportunity and the freedom to grow as a scientist and as a critical thinker, nevertheless making yourself always available and never lacking in guidance. I consider this an invaluable gift.

I would also like to thank Prof. Dr Martin Muller and Dr Florence Baudin for being members of my Thesis Advisory Committee. Your supervision allowed me to focus on what was relevant and important to address the biological questions at the core of my Ph.D project.

A Ph.D is hardly only the result of one person´s work, because so many contribute, directly or indirectly, to its successful completion. For this reason, a special thank has to go to many people.

To my fellow lab members, both present and past. I have cherished and always considered invaluable our conversations, scientific and non-scientific. Your support, suggestions, and ideas have always been for me a source of growth and improvement. To Zhe, my bench neighbour, with whom I exchanged so many ideas and thoughts, and from whom I had learnt so much. You are an example of dedication and hard work. I am sure you will be able to pass it on to the next generations of scientists.

To Angelika, the smiling face that welcomed me when I arrived and that has always had a nice word of support to go through even the hardest moment of my Ph.D. You have always done more than your job as a secretary, and I have always appreciated you deeply for that. To Helge and Daniel, whose invaluable work and support are one of the reasons I have reached this milestone. To Rèmy, for the incommensurable amount of sharing of ideas, especially late in the evening, that often helped solve problems and reshape the way I addressed my research.

To Anatoliy. You took me under your wing as I arrived in the lab, and you showed me the way around. Not just a lab mate, or a post-doc, but a mentor and a friend.

To Dwain. We began as colleagues, but we grew into close friends very quickly. I am so deeply grateful that I had the occasion to work with you during these years and, even more, that I became your friend.

To Nicola. I can´t even imagine what my life in Heidelberg, my life as a Ph.D. student, would have been (and was) without you. The many, many hours we spent talking, in person and on the phone, the laughs, the sadness, the moments of anger and tears, the moments of joy, maybe out dancing (you were the first who managed to bring me dancing at a club!). All this makes our friendship special to me.

To Alice. Never, never I would have imagined that providing you with negative fractions would have turned into such a beautiful and deep friendship. The many nights we spent in the building, working till late at night, checking on each other, and eating junk food were probably one of the best parts of these years.

To all the great people I met while living in Heidelberg. Thank you. Spending my free time with you has often been the best way to recharge and get through even the most extenuating periods. A particular mention goes to Jing and Felix. We haven't seen each other as much as I would have liked since the pandemic has begun but getting to know you has been a great and immense pleasure.

To my friends back home, whose friendship I could always count on, despite the distance. To Eleonora, Beatrice, Davide, Guido, and Giulia, that I often felt so close in their friendship that sometimes I mistakenly thought that we were still living in the same city. To Michela, who kept mentoring me for all these years, whose true and honest friendship I was always able to rely on.

To Luca, Vanessa, and the beautiful Chloe. Luca and Vanessa, who saw me growing (literally) for more than half of my age, have always been a pillar in my life. The relationship that bonds us is so far-reaching that I am always amazed by the luck I had meeting you. To the beautiful Chloe, who was born and grew so much during this PhD. Your smile, your laugh, and your smart questions have always been the best medicine for any of my sorrows.

To Preston. It is still incredible to me that, despite all our differences, we managed to navigate so much and be connected by this beautiful friendship. In your very special ways, you have supported me a lot during these years.

To all of those I didn´t mention directly, but whose love, friendship and closeness meant a lot to me. I will always be grateful for having a chance to meet and share a part of my life with you. In many different ways, you all helped me grow and reach this result.

To my amazing family, which is the very exact reason why I am who I am and managed to get to this point. Your love, your presence, and your kindness are without boundaries and don´t know the distance. Mamma, Babbo, vi voglio bene. Claudio, you are not just a brother, you are one of my closest friends and you mean a lot to me. You taught me so much over the years, and knowing that I could always count on you, no matter what, made every problem a lot easier to solve. The many hours we spent, on the phone, talking about anything from politics to dogs, sharing stupid gifs and memes or Twitter posts, have been often able to put a smile on my face, even during the most stressful and grim of times. I am looking forward to seeing you growing as you approach this new stage of your life together with Anika!

To all of you I say

Thank you.